DEVELOPMENT OF SHORT-COLUMN GC/MS AND GC/MS/MS STRATEGIES: FUNDAMENTALS AND APPLICATIONS TO ANABOLIC STEROID ANALYSIS

By

STACY-ANN ROSSI

A DISSERTATION PRESENTED TO THE GRADUATE SCHOOL
OF THE UNIVERSITY OF FLORIDA IN PARTIAL FULFILLMENT
OF THE REQUIREMENTS FOR THE DEGREE OF
DOCTOR OF PHILOSOPHY

UNIVERSITY OF FLORIDA

1991

With love and gratitude, to Mom and Dad.

ACKNOWLEDGEMENTS

I would like to express my gratitude to Dr. Richard A. Yost for his guidance and direction and for allowing me to become an independent researcher. I would also like to acknowledge Dr. Jodie Johnson for his continued assistance in solving instrumental and experimental problems, as well as his editorial help with papers. I would like to acknowledge the members of my research committee, Drs. Willard Harrison, Jim Winefordner, David Micha, and Charles Thomas.

I would like to thank Drs. David Powell and Kitty Williams for their part in helping me earn this degree. I want to acknowledge Dr. Williams for her tireless work in setting up informative labs for the undergraduates, as well as teaching her TAs something in the process. I would like to thank Dr. Powell for his support; I enjoyed working with him and value his friendship. I would also like to acknowledge the many support people that I have worked with these past few years. My thanks go out to the many people in the business office and analytical division offices and the electronics, glass, and machine shops.

I would like to thank ex-group members Jody Freeman and Brian Beato for their friendship and help in getting me started. These four or so years would not have been as much fun without the support of and discussions with my friends and co-workers in the Yost research group. In particular, I would like to thank Brent

Kleintop and Don Eades for helping me become computer literate and for always having an extra smile for me when mine was missing. I also want to thank Uli Bernier and Tony Annachino for their help and friendship along the way.

This work would not have been possible without the encouragement and support of my family. Linda, Scott, Rick, as brothers and sisters go, you all are the best. Most of all, I want to thank my parents for always being there for me. I know this wasn't easy at times for any of us, but thanks for keeping me on the right track; I love you both. I also want to thank the newest member of my family, Chris Barshick, who is, indeed, my best friend, colleague and better half; I love you and on September 19 you will know how much.

TABLE OF CONTENTS

Abstract of Dissertation Presented to the Graduate School
of the University of Florida in Partial Fulfillment of the
Requirements for the Degree of Doctor of Philosophy

DEVELOPMENT OF SHORT-COLUMN GC/MS AND GC/MS/MS STRATEGIES: FUNDAMENTALS AND APPLICATIONS TO ANABOLIC STEROID ANALYSIS

By

Stacy-Ann Rossi

December 1991

Chairperson: Richard A. Yost
Major Department: Chemistry

This dissertation focuses on two aspects of short-column gas chromatography/mass spectrometry (GC/MS): characterizing the parameters that affect short-column strategies and exploring the advantages of short GC columns for trace analysis of underivatized anabolic steroids. Anabolic steroids were chosen as the targeted class of compounds because, without derivatization, these thermally-labile compounds typically would not be amenable to conventional-length column GC/MS.

A number of parameters were characterized with respect to their effect on the sensitivity, input bandwidth and chromatographic resolution obtained with short GC columns. The most important was the carrier gas velocity which is controlled by the applied column inlet pressure. At a column inlet pressure of 2 psi and assuming an

outlet pressure of less than 1 torr, the carrier gas velocity exiting the end of the GC column was at least 750 m/s. At this high velocity, a reduction in sensitivity was observed as a result of decreasing ionization efficiency. Use of subambient column inlet pressures (on the order of -15 in Hg) increases sensitivity by as much as 20% by reducing the carrier gas flow rate. In addition at these high gas velocities, an increase in the input bandwidth was observed. A method of decreasing this extracolumn variance was investigated using Curie-point thermal desorption; however, due to design limitations narrower input bandwidths were not obtained. This method, however, was found to overcome high solvent backgrounds that are problematic for short column methods. The limited chromatographic resolution inherent in short column strategies was overcome using tandem mass spectrometry (MS/MS); characteristic mass spectra were obtained even for chromatographically unresolved peaks.

The combination of short GC columns and MS/MS strategies was shown to enhance both selectivity and sensitivity for trace analysis of underivatized anabolic steroids in complex or biological samples. It was demonstrated that these criteria essentially are controlled by the analytical method and instrumental conditions. Selected reaction monitoring using positive ion chemical ionization was shown to be the most selective and sensitive method with collisionally activated dissociation efficiencies from 2 to 25%. This method resulted in detection limits from 2 to 40 ng/mL for spiked urine samples, required reduced sample preparation and analysis times and showed potential as a rapid screening/confirmation technique.

CHAPTER 1

INTRODUCTION

The focus of this dissertation is two-part. In the first part, certain practical limitations inherent to short-column GC/MS strategies are presented. To overcome these limitations, the study of fundamental gas chromatographic and mass spectrometric theories, concepts, and experimental parameters was required. In the second part, the advantages of short GC columns in combination with tandem mass spectrometry are explored for trace analysis of underivatized anabolic steroids. The feasibility of a selective screening method requiring minimal sample preparation is discussed. An introduction to the concepts to be examined in this dissertation is presented in the following sections.

Anabolic Steroids

Anabolic steroids are a class of drugs that are among the list of substances banned by the International Olympic Committee (1-3). These steroids have been used in athletics to improve performance since the 1950s. Since that time, professional sports organizations such as the National Collegiate Athletic Association, National Football League, Womens International Tennis Association,

and United States Powerlifting Federation have tested athletes for anabolic steroid use (4). Due to the concerns of adverse health effects and sports ethics, considerable research effort has been devoted to determining the biological action of these compounds and to developing rapid and sensitive analytical methodologies for detecting their use.

Biological Significance of Anabolic Steroids

Anabolic steroids are a class of steroids that are structurally related to the male sex hormone testosterone. Six representative steroids have been chosen for this study, including the endogenous steroid, testosterone; their structures are shown in Figure 1-1. Abuse of these synthetic derivatives of testosterone results in pharmacological and toxicological effects which are both anabolic (muscle-building) and androgenic (masculinizing) (4-6). These steroids were designed to maintain the anabolic effect of testosterone while reducing the androgenic effect. Athletes who use these drugs believe that they increase lean body mass (muscle), strength, and endurance, and reduce recovery time between workouts (4, 7-13). However, despite their popularity among athletes, there is disagreement as to whether use of these steroids actually improves athletic performance. A review of the literature was performed in 1984 which concluded that steroids could increase muscle mass and strength if the athlete had trained intensively before and after steroid use and consumed a high caloric diet (6). Several mechanisms have been suggested for how anabolic steroids increase strength; a few of these include enhanced protein synthesis

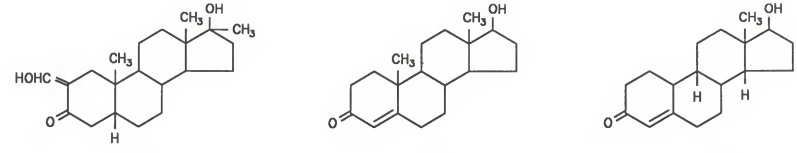

Figure 1-1: Structures of the six anabolic steroids used in these studies: (a) oxymetholone (oxym), (b) testosterone (test), (c) nortestosterone (nort), (d) stanozolol (stan), (e) methyltestosterone (met), and (f) dehydrotestosterone (dehyt). ( ) indicate abbreviation of steroid names used in subsequent chapters.

stimulated by anabolic receptors located in muscle cells (14), improvement of protein utilization by promoting a positive nitrogen balance (14), a physiological effect of euphoria and decreased fatigue which allows the athlete to increase the intensity and duration of their workout (15,16), and a placebo effect (17).

The primary concerns of the medical profession with the use of these drugs are the risks of complications and the lack of information on their long-term effects. The side effects of anabolic steroids reported in the literature range from acne to cancerous liver tumors (4-6, 18-22). Potential complications related to anabolic steroid use are summarized in Table 1-1. An assessment of the hazards of anabolic steroid use is further complicated by athletes tending to take 10 or more times the recommended dose and often taking more than one form of the drug at a time. Although anabolic steroids have been prescribed by physicians in the treatment of certain types of anemia (6), large dosages and long-term unsupervised use of these drugs have resulted in death for otherwise healthy athletes.

Techniques for the Analysis of Anabolic Steroids

A number of analytical methods have been developed for the detection of anabolic steroids (23,24). These techniques, including radioimmunoassay, high pressure liquid chromatography, gas chromatography and methods involving mass spectrometry, have been used in steroid metabolism research, veterinary science, in the pharmaceutical industry, and for screening purposes. Among these techniques, GC/MS is the most widely used for screening of anabolic steroids in humans (25-27).

Table 1-1: Side effects of anabolic steroid use

Liver:	hepatoxicity
Reproductive:	testicular atrophy menstrual irregularity virilization/feminization
Musculoskeletal:	increased susceptibility to injury of ligaments/cartilage in joints premature epiphyseal closure resulting in stunted growth
Cardiovascular and Cerebrovascular:	elevated blood pressure increased risk of atherosclerotic heart disease myocardial infarction, stroke, or left ventricular hypertrophy
Endocrine:	acne altered glucose metabolism altered thyroid profile
Other:	aggressiveness, depression, headache, nausea, altered appetite, increased cholesterol

Radioimmunoassay. Radioimmunoassays (RIA) for the detection of anabolic steroids in urine were developed initially by Brooks in the late 1970s (28). Radioimmunoassay kits have been developed for the detection of three groups of steroids: 19-nortestosterone analogs, norethandrolone analogs (17-ethyl substituted steroids), and 17α-methyl substituted analogs (28-30). These RIA kits require an initial organic extraction of the steroids from urine and subsequent preparation of the oxime derivative, followed by the immunoassay procedure using antibodies developed for the detection of a specific steroid or group of steroids. Separation is performed by charcoal adsorption and the bound fraction is counted using iodine-125 or hydrogen-3 as the tracer.

It was found, however, that these methods suffer from insufficient cross-reactivity for several of the steroids of interest, including methenelone and stanozolol (31), while cross-reactivity with normal urinary steroids or components of birth control medications can result in false positive results. The cross reaction for testosterone can be eliminated by acetylation prior to performing the assay (28). Other problems associated with RIA methods, besides insufficient cross-reactivity, are the broad specificity range of the antibodies and poor overall sensitivity. Because RIA procedures offer high sample throughput, RIA screening is still used; however, any samples which are found to contain anabolic steroids are then examined by GC/MS to avoid false positive results and to identify the anabolic steroids present.

High pressure liquid chromatography. High pressure liquid chromatography (HPLC) has been used mainly for the separation and identification of anabolic steroids in the veterinary and pharmaceutical fields, while only a few reports have discussed the use of HPLC for screening purposes (32-34). Reverse-phase bonded (C_{18}) columns and a methanol:water mobile phase have been the predominant systems used with UV detection. An advantage of HPLC is that steroids can be analyzed after extraction from urine samples and without derivatization. Prepurification of urinary samples using a diol phase HPLC column has also been reported (32); this is an advantage since urinary matrix components are retarded on normal-phase columns.

One limitation of HPLC is the relatively poor sensitivity as compared to other methods; for example, the detection limit for methandienone in urine was reported as 1 ng on-column by Frischkorn (32). This makes HPLC unsuitable for a routine screening or doping control method. Improved sensitivity and selectivity have been reported for fluorescence detection of the dansyl derivative (35), as well as chemiluminescence detection (36). To date, HPLC is not used as a routine urine screening method; however, LC/MS procedures may improve the sensitivity of this method and may be developed in the future as an alternative screening method.

Mass spectrometric methods. Mass spectrometric techniques for the determination of anabolic steroids have included gas chromatography/mass spectrometry, liquid chromatography/mass spectrometry (LC/MS), fast atom

bombardment (FAB) mass spectrometry, secondary ion mass spectrometry (SIMS), and laser desorption Fourier transform mass spectrometry (LD/FTMS) (37). At present, GC/MS is the method of choice, although extensive derivatization or chemical modification procedures are required because of the polarity, low volatility, and thermal instability of these compounds.

GC/MS procedures require extraction of the urine sample using C_{18} sep-pak cartridges and hydrolysis of the dried extract with a β-glucuronidase enzyme solution, followed by selective derivatization of the anabolic steroids (23, 25-27). In order to have adequate sensitivity for screening, it is necessary to use selected ion monitoring (SIM). With SIM, 2 to 5 ions per compound can be monitored and discrete ion groups can be set up on the basis of retention time. Each ion group can then be monitored over the corresponding elution range (25). Electron ionization (EI) is typically used and is considered the most sensitive method for screening (23). However, because ions produced by EI are generally of low abundance, chemical ionization methods have been investigated as an alternative method (38,39).

Analysis of Underivatized Steroids

The potential advantage of mass spectrometric techniques that do not employ chromatographic separation is the ability to determine underivatized steroids directly. Desorption ionization methods such as FAB, SIMS and laser desorption allow for the determination of steroids with minimal thermal degradation resulting in simpler mass spectra with fewer fragment ions. It should also be noted that these desorption

ionization techniques are capable of the analysis of higher molecular weight compounds such as the steroidal oligoglycosides which would not be amenable to direct GC/MS methods (37), while another advantage is the reduction of sample preparation time since derivatization, extraction and hydrolysis procedures may not be necessary. A limitation of these methods, however, is the lack of separation capabilities; this can be a problem when a high chemical background results from the sample or desorption matrices.

The underivatized steroids that have been analyzed by these techniques include carbonyl steroids (32,40,41) (such as anabolic and corticosteroids), steroidal oligoglycosides (42), sulfate salts and glucuronides (43,44). It is evident that development of an analytical assay for the determination of underivatized anabolic steroids using the separation capabilities of GC/MS, but with minimal sample preparation, would be an advance in anabolic steroid screening methodologies; a potential method based on short-column GC/MS/MS will be explored in Chapters 4-6.

Short-Column GC/MS

Short-column GC/MS has been shown previously to provide minimal peak broadening, higher sample concentrations at the detector, enhanced sensitivity, and extremely rapid analyses (45). The use of short capillary columns also allows for the analysis of compounds too involatile or thermally labile to be amenable to

conventional-length column GC methods, as well as compounds too volatile for direct insertion probe methods (45,46). Short-column GC/MS strategies have been applied to a wide range of compounds, including tryptolines (47), chlorinated compounds (45), carbamate pesticides (46), trichothecene toxins and diglycerides (48,49). Minimal sample preparation, short analysis times, and the potential for reduced thermal degradation since short columns can be operated at lower temperatures, are some of the potential advantages of short-column GC/MS for the analysis of thermally-labile compounds, such as underivatized anabolic steroids.

Advantages and Limitations of Short-Column GC/MS

Short GC columns have been shown to be advantageous for use in GC/MS (50-52); in particular, Giddings demonstrated that minimum analysis times in GC could be obtained when the column outlet is connected to a vacuum (53). The advantages of vacuum outlet operation (52, 54-56) are more pronounced if wide-bore columns (50) or short columns (52) are used. Short-column GC/MS strategies are subject, however, to certain limitations, including: loss of resolution (45,46,50,57,58), decreased sensitivity (51,57,59), and extracolumn band broadening (51, 59-61). These limitations become severe especially at high carrier gas velocities.

Sensitivity. If short GC columns are operated at their optimum gas velocity, narrow chromatographic bands and higher sample concentrations (compared to conventional-length columns) at the detector will result (62). In theory, short

columns should, therefore, provide the best detection limits for GC/MS. However, it was shown that the advantage of low detection limits with short columns in GC/MS may be lost if high carrier gas flow rates are used (51,57). When electron ionization is used, the sensitivity decreases dramatically with increasing flow rate; this is likely due to disruption of the ionization process in the ion source.

The use of short GC columns at conventional inlet pressures is limited by the gas load imposed on the mass spectrometer. It was found that operating the inlet at subambient pressures would reduce the flow rate of the carrier gas entering the mass spectrometer and decrease the gas load on the vacuum system (63). Subambient inlet also allows short columns to be operated at their optimum gas velocities. The effects of carrier gas flow rate on sensitivity and the use of subambient inlet pressures will be discussed in detail in Chapter 2.

Chromatographic resolution and band broadening. In theory, a reduction in column length by a factor of ten will result in an increase in optimum gas velocity by a factor of three. This increase in optimum gas velocity for the shorter column is accompanied by a decrease in analysis time by a factor of thirty with only a minimal loss of resolution of approximately the square root of ten. This is illustrated in Figure 1-2, which shows a Golay plot of plate height versus average velocity for both a 30 m and a 3 m column (note: these results were calculated by Mark Hail using a BASIC program designed to calculate theoretical GC parameters; original documentation can be found in reference 51 and his dissertation). These curves are

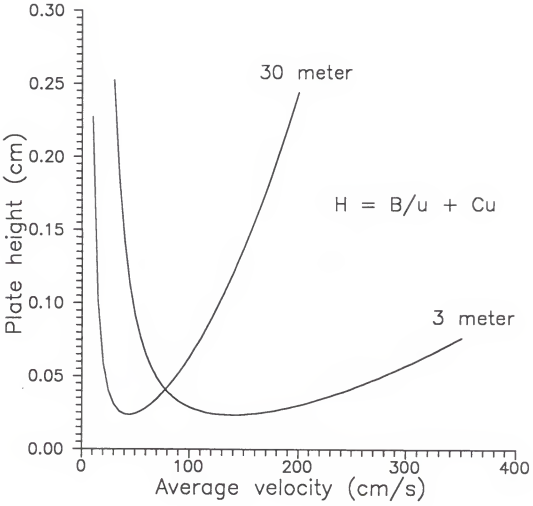

Figure 1-2: Theoretical relationship between optimum gas velocity and plate height for both 30 m and 3m columns (51).

described by the Golay equation given in 1-1 (64),

$$H = B/u + Cu \qquad (1\text{-}1)$$

where H is the plate height, B is a term relating to the longitudinal diffusion of the solute zone, C is a term relating to mass transfer in the gas and liquid stationary phases, and u is the average gas velocity. This equation describes the theoretical dependence of plate height on the average gas velocity. Modifications of this equation will become important to account for extracolumn effects at high average gas velocities.

Guiochon has discussed the role of extracolumn effects and their importance in high-speed GC applications using short and/or wide-bore columns (60). An additional term can be added to the Golay equation to account for these variances and is shown in equation 1-2 (60),

$$H_{app} = B/u + Cu + Du^2 \qquad (1\text{-}2)$$

with

$$D = \sigma_{ec}^2 / (1 + k)^2 L \qquad (1\text{-}3)$$

where H_{app} is the apparent plate height, D is a term used to describe the

extracolumn variance (σ_{ec}^2), k is the capacity factor, and L is the column length. The extracolumn contributions are the result of band broadening due to instrumental time constants. As shown in equations 1-2 and 1-3, the extracolumn variance becomes more significant as shorter columns or higher average velocities are used.

The variance for a total chromatographic system can summarized by equation 1-4 (59,62,65,66)

$$\sigma_t^2 = \sigma_c^2 + \sigma_{ec}^2 \qquad (1\text{-}4)$$

with

$$\sigma_{ec}^2 = \sigma_d^2 + \sigma_i^2 \qquad (1\text{-}5)$$

where σ_t is the total variance, σ_c is the variance due to chromatographic peak broadening, σ_d is the variance associated with the detector, and σ_i is the variance associated with the injector design and injection method. Due to these extracolumn effects, the use of short columns necessitates careful consideration of the injection technique if maximum performance is to be obtained.

Alternative injection methods that have been developed for high-speed GC applications include a miniaturized gas chromatograph with a solenoid actuated diaphragm valve and an automated pneumatically actuated high pressure valve (66). This work stresses the need for extremely small input bandwidths to minimize

extracolumn effects due to the injection technique. Another injection method that has been used with short GC columns is Curie-point thermal desorption (48,49,67). Evaluation of this injection method with respect to extracolumn variance will be presented in Chapter 3.

MS/MS Strategies for Trace Analysis of Complex Mixtures

Tandem mass spectrometry (MS/MS) has, since its development in the 1970s, been gaining acceptance as a rapid, sensitive, and selective analytical method for the analysis of complex biological samples (68-71). The advantages gained by MS/MS often complement those gained by extensive sample cleanup procedures or chromatographic separation (72-74). In fact, MS/MS has been used in place of separation or sample preparation schemes.

In MS/MS strategies, separation of the analyte and matrix components is achieved by mass selection of the analyte ion of interest in the first quadrupole (Q1) region. In the second quadrupole region (Q2), or collision cell, the selected ion undergoes collisionally activated dissociation (CAD) with neutral gas molecules. The fragment or daughter ions are then mass analyzed in the third quadrupole (Q3). This MS/MS scan mode and other scan modes used in these studies are shown in Figure 1-3. The daughter operational mode is analogous to a normal Q1 or Q3 MS. For normal MS, either Q1 or Q3 is operated in an rf/DC mode while the other two quadrupoles are operated in an rf-only mode. Normal full scan MS and MS/MS

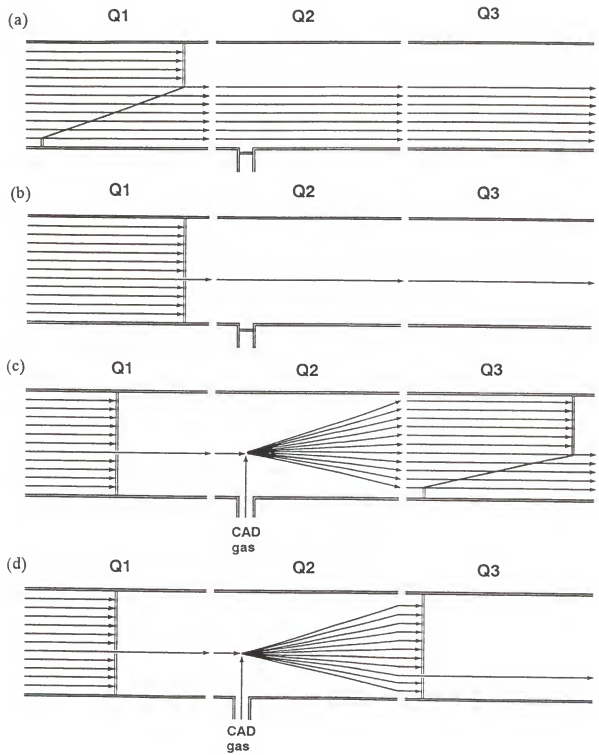

Figure 1-3: Mass spectrometric operational modes: (a) normal Q1 full scan mode, (b) selected ion monitoring mode, (c) full scan (daughter) MS/MS mode, and (d) selected reaction monitoring mode.

modes, although highly informative, usually lack the sensitivity for determining trace components. An enhancement in sensitivity can be gained by using selected ion monitoring (SIM) or selected reaction monitoring (SRM). In these modes, only selected ions are monitored for each analyte, thus maximizing the analyte signal; this occurs, however, at the expense of some selectivity.

In comparison to GC/MS, MS/MS appears to have several distinct advantages (75). First, complex mixtures can be analyzed by MS/MS with little or no sample cleanup. Second, the primary separation of sample components is analogous to GC/MS but, is a much more rapid process and is not constrained to a limited time. Lastly, MS/MS strategies may have a wider range of applicability since a greater number of compounds are amenable to analysis by MS than by GC. Tandem mass spectrometry in conjunction with short GC columns offers the advantages of both techniques: rapid sample introduction with some chromatographic separation and additional selectivity and sensitivity using an appropriate MS/MS scan mode. The advantages of short-column GC/MS/MS will be discussed in Chapter 6.

Considerations in Trace Analysis by MS/MS

Trace analysis by MS/MS can be performed successfully if care is taken to optimize the analytical method based on sensitivity, selectivity, and speed of analysis (76). These criteria are essentially controlled by the analytical method and instrumental conditions. Four basic steps are involved in any analytical MS/MS strategy for trace mixture analysis. These steps include the following: sample

preparation, sample introduction, ionization, and detection. Gaskell has summarized previously the selectivity of a trace analysis method determined by each stage of the analytical procedure (77). This is shown in Table 1-2. Also noted in the table are the places where sensitivity may be compromised.

In choosing a sample preparation scheme, both speed and selectivity are desired. Selectivity can be achieved by extraction and derivatization procedures. However, these procedures are performed at the expense of time. Selectivity can also be achieved by using chromatographic separation. Separation of the analyte and remaining matrix components can even be accomplished on short (< 5 m) capillary columns. The type of analysis required and the type of compounds being analyzed will determine the choice of ionization method. In trace analysis, chemical ionization is often used as it typically yields an intense molecular ion with few fragment ions. Electron ionization tends to be a harder ionization method, but yields more structural information. For detection, MS/MS operational modes can be used to enhance selectivity, but occurs at the expense of some sensitivity. For quantitation, SRM can be used to improve the limit of detection.

In order to take advantage of the capabilities of MS/MS strategies, optimization of the instrumental parameters is critical. Selection of the ionization method will essentially control the sensitivity of the analysis. Optimization of collision gas pressure and collision energy is necessary to achieve maximum collisionally activated dissociation (CAD) efficiency. Nitrogen or argon collision gases are typically used, with the choice depending on the stability of the parent ion,

Table 1-2: Selectivity and sensitivity of trace analysis procedures (77)

stage of procedure	basis of selectivity	potential sensitivity loss
sample extraction	polarity, acid/base chemistry, molecular size, stereochemistry	loss of sample
chromatographic separation	partition properties	loss of sample
MS ionization	proton affinity electron affinity	ionization efficiency
MS detection	molecular weight fragmentation	transmission efficiency detection efficiency

while the collision gas pressure can be adjusted to affect the number of collisions that the parent ion undergoes. Collision energy will determine the kinetic energy for the dissociation reaction and the extent of fragmentation. Control of these parameters is critical to produce characteristic and reproducible daughter mass spectra. This will be demonstrated in Chapter 5.

Overview of Dissertation Content

This dissertation is organized into 7 chapters. Chapter 1 has served as an introduction into the concepts that will be presented in the body of the dissertation (Chapters 2-6). Fundamental studies investigating the factors that affect sensitivity in short column GC/MS are presented in Chapter 2. The use of subambient inlet pressures to overcome these sensitivity-limiting factors is also described. An evaluation of an alternative injection method for short column GC/MS is given in Chapter 3. Both theoretical and practical aspects of standard syringe injection and Curie-point thermal desorption are compared. In Chapter 4, rapid short-column gas chromatographic/mass spectrometric strategies are investigated and optimized for the direct determination of underivatized anabolic steroids. The feasibility of this method as an alternative to current screening methods is suggested. Extending the work done in Chapter 4, the use of tandem mass spectrometric strategies and alternative ionization methods is described in Chapter 5. Tandem mass spectrometric conditions and ionization methods are optimized and chosen with

respect to maximizing sensitivity and selectivity. Chapter 6 evaluates the GC/MS/MS strategies developed in Chapters 4 & 5 for the determination of underivatized anabolic steroids in urine. The advantages and limitations are discussed, as well as the results of quantitation studies. The final chapter, Chapter 7, reviews the major conclusions presented in this work. This chapter stresses the potential of short-column GC/MS/MS screening of underivatized anabolic steroids in real samples. In addition, suggestions for future work in this area are made.

CHAPTER 2

INVESTIGATION OF SENSITIVITY-LIMITING FACTORS IN SHORT-COLUMN GC/MS

Introduction

Gas chromatography (GC) and direct insertion probes are common sample introduction methods for mass spectrometry. There are, however, many issues that govern the decision of which introduction technique to use. Separation requirements and speed of analysis must be considered, as well as compound-dependent factors such as sample volatility and thermal stability. Other issues that enter into the decision include sample transfer efficiency, ionization efficiency, and background chemical interferences. These latter issues effectively control the sensitivity and selectivity and, therefore, the limit of detection of an analysis.

It was found that under typical experimental conditions, short-column GC introduction methods yield dramatically poorer (lower) sensitivities than probe introduction methods for a series of underivatized anabolic steroids and aromatic hydrocarbons. In this chapter, the fundamental differences between probe and short-column GC introduction have been investigated with respect to the level of sensitivity obtainable by these methods. Detailed studies of the parameters affecting sample transfer efficiency and ionization efficiency are presented. Consideration is also

given to separation capabilities, speed of analysis, and compound-dependent factors such as sample volatility and thermal stability. In addition, studies investigating ion source-related phenomena are presented to elucidate the sensitivity-limiting factors associated with short-column GC and their effect on direct insertion probe sample introduction methods.

Experimental

Samples and Reagents

Preliminary studies were performed on a series of anabolic steroids including 19-nortestosterone, 1-dehydrotestosterone, testosterone, 17α-methyltestosterone, and stanozolol (Sigma Chemical Co., St. Louis, MO). The aromatic hydrocarbons benzene (MW 78, b.p. 79.7 °C) (Mallinckrodt, Inc., Paris, KY) and pyrene (MW 202, b.p. 404 °C) (EPA, Research Triangle Park, NC), were used for the remaining studies. Reagent grade methylene chloride (Fisher Scientific, Fair Lawn, NJ) was used as the solvent. Commercial grade helium (Liquid Air Corp., Walnut Creek, CA) was used as GC carrier and make-up gases; methane (Liquid Air Corp.) was used as the chemical ionization reagent gas.

Gas Chromatography

Gas chromatography was carried out on a Finnigan MAT 9610 gas chromatograph (San Jose, CA). A comparative study employed a Varian model 3400

gas chromatograph (Sunnyvale, CA). Gas chromatographic sample introduction was carried out on J&W Scientific (Rancho Cordova, CA) SE-54 capillary columns. Both 3.25 m and 30 m long (0.25 mm i.d., 0.25 μm film thickness) capillary columns were used. For most studies, column temperatures were isothermal at 150 °C (pyrene studies) or 50 °C (benzene studies). For some studies, a temperature program was used in which the initial temperature was held at 50 °C for 30 s, then increased at a rate of 25 °C/min. to 250 °C. The injection port and interface temperatures were 250 °C. Injections were typically made in the splitless injection mode (split closed between 0.2 and 1.0 min.) using 1 μL injections of a 250 ng/μL solution.

For subambient inlet pressure experiments the GC was modified to allow for either normal pressure-regulated operation or flow-controlled operation (51). To obtain subambient inlet pressures a mechanical pump was connected to the outlet of the GC split and a pressure gauge capable of reading positive and negative pressures was connected to the sweep outlet. Flow control was achieved using an MKS Model 1159A mass flow controller with a type 246 power supply/digital readout (MKS Instruments, Inc., Andover, MA).

Mass Spectrometry

A Finnigan MAT TSQ45 gas chromatograph/triple quadrupole mass spectrometer was used in these studies. A comparative study was performed on a Finnigan MAT TSQ70 triple quadrupole mass spectrometer. Electron energies of 70 eV for electron ionization (EI) and 100 eV for chemical ionization (CI) were employed. Electron ionization and chemical ionization spectra were obtained with

the appropriate interchangeable ion volumes. Experimental conditions for the mass spectrometer were GC/MS interface and transfer line temperatures of 250 °C, ionizer temperature of 190 °C for EI and 150 °C for CI, emission current of 0.3 mA, and preamplifier gain of 10^8 V/A. Chemical ionization was performed at an ionizer pressure of 0.2 torr methane as measured by a thermocouple gauge connected to the ion source.

A schematic of the instrumental set-up showing both probe and GC sample introduction inlets and the location of a secondary ion gauge used to measure the ion source manifold pressure is shown in Figure 2-1. The normal glass viewport of the ion source was replaced with a flange-mounted secondary ion gauge for monitoring the ion source manifold pressure directly. All ion source manifold pressures reported are the indicated pressures obtained from this ion gauge and model 280 external ion gauge controller (Granville-Phillips Co., Boulder, CO).

Gas chromatographic sample introduction was performed both with the conventional 9610 GC/MS transfer line and with a laboratory-constructed GC/MS interface probe (note that the GC/MS interface probe was designed and constructed by Brent Kleintop in our laboratory). The GC/MS interface probe consisted of a modified solids probe and probe tip that consisted of a swagelok and ferrule connection to maintain the vacuum seal. The portion of the GC column that was contained within the solids probe was extended until the end of the column was just visible at the probe tip. The GC probe was used under ambient conditions so that it could be used in conjunction with the 9610 GC injection port providing the oven

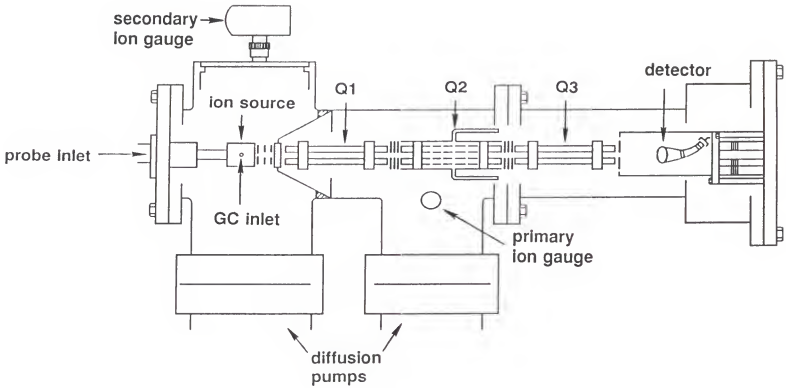

Figure 2-1: Schematic diagram of a triple quadrupole mass spectrometer showing both GC and probe sample introduction inlets and the location of the secondary ion gauge.

door was left open. The GC probe was then introduced into the ion source through the conventional probe lock. Probe sample introduction was performed with both a direct exposure probe (DEP) and a solids probe. The DEP was initially held at a current of 0 mA, then programmed at a rate of 20 mA/s to 750 mA (note: 1 mA corresponds to approximately 1 °C). The solids probe was operated at an initial temperature of 50 °C, then increased to a final temperature of 400 °C at a rate of 99 °C/min. A solids probe, operated isothermally, was also used for constant introduction of samples within capped aluminum vials.

Scan rates, mass range, and multiplier settings were kept constant for studies that compared two or more variables. Full scan mass spectra were acquired by scanning the first quadrupole from 33 - 225 u in 0.32 s (for pyrene studies) or 33 - 100 u in 0.44 s (for benzene studies). Peak areas were determined by integrating the ion current over the peak profile after visually choosing the baseline.

Results and Discussion

Short-column GC, solids probe, and direct exposure probe sample introduction methods have been compared under the same experimental conditions with respect to sample transfer efficiency, ionization efficiency, limit of detection and linear dynamic range. Initial studies on underivatized anabolic steroids and aromatic hydrocarbons have shown that short-column GC injection methods yield dramatically lower sensitivities than probe introduction methods. Investigations into the

fundamental differences between probe and short-column GC were undertaken to determine the effect of different parameters (e.g. ionization mode, direction of sample introduction, column length, injection method, and column inlet pressure) on sensitivity. The results of these studies and of further investigations into ion source-related phenomena are presented below.

Initial GC/Probe Comparison

Initial assays for the determination of underivatized anabolic steroids by short-column GC/MS with splitless injection resulted in poorer sensitivities than anticipated. It was hypothesized that the low sensitivity obtained for short-column GC introduction of these thermally-labile analytes may have been a result of thermal decomposition or incomplete sample transfer from the GC into the mass spectrometer. To test this hypothesis, probe introduction was used to estimate the relative sensitivity that should be obtained for a given amount of sample and a given set of experimental conditions. In this regard, sensitivities obtained by probe introduction could serve as benchmarks for measuring the relative sensitivities for GC introduction under similar experimental conditions. A study of short-column GC, DEP, and solids probe sample introduction methods was performed under the same experimental conditions and the relative sensitivities compared. In these studies, as shown in Figure 2-2, probe introduction methods were observed to have higher sensitivities (peak area of the molecular ion per microgram of steroid injected) than short-column GC methods by a factor of approximately 5 to 10,

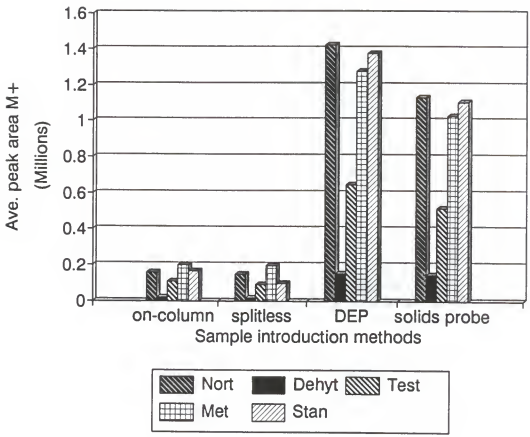

Figure 2-2: Comparison of GC and probe sample introduction method sensitivities for a series of underivatized anabolic steroids.

depending on the compound. The low GC sensitivities suggested that incomplete sample transfer from the GC to the mass spectrometer was occurring. This loss could occur either in the injection port or from the column.

On-column GC injection was compared to splitless injection to indicate whether complete sample transfer onto the column was occurring. Since similar results were obtained by both injection methods, it was concluded that minimal sample was being lost in the injection port. In order to rule out the possibility of thermal decomposition and loss of compound on the column, experiments were also performed on a thermally stable test compound, pyrene. For this compound, probe introduction resulted in sensitivities higher by a factor of 7 compared to short-column GC. Since thermal decomposition of pyrene along the column can be ruled out, loss of sensitivity along the GC column is not likely.

Overall these preliminary studies indicate that certain fundamental differences exist between probe and short-column GC sample introduction methods that do not allow for comparable sensitivities to be obtained by these two methods under similar experimental conditions. Therefore, further investigations into the different parameters that may affect GC and probe introduction were undertaken.

Investigation of Gas Chromatographic Parameters

The effects of gas chromatographic parameters on sensitivity were determined in order to elucidate the reason for the lower apparent sample transfer efficiency of GC compared with probe. GC parameters such as the GC injection method, column

length, and column inlet pressure (flow rate of the carrier gas) were studied. Of these parameters, the flow rate of the GC carrier gas appears to have the most dramatic effect on loss of sensitivity. The results of investigations into these parameters, as well as into other GC variables, are discussed below. These studies were carried out on benzene and pyrene in order to minimize any effects due to thermal decomposition.

Gas chromatographic injection methods. A method for estimating sample transfer efficiency for GC injection methods has been described using on-column injection (78). This test was performed in order to determine the efficiency of sample transfer for the splitless injection method. As previously discussed in the initial GC/probe comparison section above, on-column injections were performed to get a measure of complete sample transfer onto the column. For the underivatized steroids, as shown in Figure 2-2, comparable results were obtained for on-column and splitless injection methods. This indicated that essentially complete sample transfer onto the column was occurring and little or no sample was being lost in the injection port using the splitless injection method.

To confirm these results and also to determine the effect of column inlet pressure on sample injection, a constant rate of benzene was introduced through the column using a fine-metering valve. In this set-up, the fine-metering valve was connected via a tee between the outlet of the injection port and the capillary column; the column inlet pressure was varied from 2 to 15 psi. The results of this study

showed a decrease of 96% for the reconstructed ion current when the inlet pressure was increased from 2 to 15 psi. The molecular ion current also decreased by 92%. Based on these results, it can be concluded that minimal sample loss is caused by the injection technique. Sample loss as a function of increasing column inlet pressure, however, does occur and will be discussed further in the following sections.

GC column length. Short-column GC/MS sensitivity has previously been shown to be affected by column inlet pressure (51). It was shown that, for short GC columns, sensitivity decreased as a function of higher carrier gas flow rates. The effect of column inlet pressure/carrier gas flow rate was studied with respect to column length to determine if this problem is limited to short columns. Based on previous work, it was shown that, for concentration-sensitive detectors such as mass spectrometers, the signal (peak height) is directly proportional to the maximum concentration of the chromatographic peak flowing through the detector (50). This is summarized in equation 2-1 (62),

$$h_p \propto C_{max,det} = q_{inj} N^{1/2} / V_R 2^{1/2} \qquad (2\text{-}1)$$

where h_p is peak height, $C_{max,det}$ is maximum concentration at the detector, q_{inj} is amount of analyte injected, N is the number of theoretical plates, and V_R is the retention volume. Therefore, as the length of the column is decreased, both N and V_R also decrease, which results in an increase in signal, h_p; this can be seen in Table

2-1. Comparing the results for each column operating close to its optimum gas velocity for chromatographic resolution, the signal for the 3 m column (at 207 cm/s) is greater than that for the 30 m column (at 35 cm/s). Optimum gas velocity (corresponding to the minimum plate height) is calculated to be approximately 40 cm/s for the 30 m column and 125 cm/s for the 3 m column; note that the optimum gas velocity for the 3 m column cannot be obtained by pressure regulation. Comparing the effect of column inlet pressure, the overall loss in sensitivity from 2 to 15 psi is comparable for the 3 m short-column (95%) and the 30 m long column (97%). This suggests that sensitivity loss in GC/MS is not limited to short columns, but is a function of the column inlet pressure.

In addition, Table 2-1 lists the retention times at various column inlet pressures for both columns. It is evident that the same analysis could be performed in 1/5 the time using the short GC column. This increased speed of analysis is also accompanied by operation at a column temperature 100 °C cooler. Therefore, with short-column GC/MS, more analyses can be performed in a given amount of time since column temperature re-equilibration time is decreased and speed of analysis increased.

Column inlet pressure and flow rate. Two major processes may be occurring in the ion source which could result in a decrease in signal with increasing helium carrier gas flow. These processes, disruptive gas dynamics and helium charge exchange, may decrease the intensity of the molecular ion, $M^{+\cdot}$, as a function of high

Table 2-1: Effects of different GC columns on sensitivity for pyrene

column	peak height M^{+} [a]	ion gauge pressure [b]	column inlet pressure (psi)	ave. linear velocity (cm/s)[c]	retention time (min.)
3 m [d]	1,360	6.3	2	210	1.6
	310	8.1	6	260	1.3
	50	17.	15	370	1.0
30 m [e]	240	0.9	2	20	8.0
	70	1.2	6	24	7.2
	20	2.7	15	35	5.0

[a] counts divided by 1,000
[b] ion source manifold pressure reading x 10^{-6} torr, uncorrected for helium
[c] linear velocity calculated using the Poiseuille equation and measured column inlet and outlet pressures
[d] column isothermal at 150 °C, multiplier setting at 875 V
[e] column isothermal at 250 °C, multiplier setting at 1,000 V

helium flow rates within the ion source. The effect of column inlet pressure (carrier gas flow rate) on sensitivity for pyrene introduced using both short-column GC and solids probe is shown in Figures 2-3a and b, respectively. The GC data in Figure 2-3a (solid line) show that maximum GC sensitivity is obtained at the lowest possible column inlet pressure that can be accurately measured by pressure regulation. It is also evident from these data that the overall loss in sensitivity by increasing the column inlet pressure from 2 psi to 15 psi is a factor of 20. In addition, increasing column inlet pressures are accompanied by increasing ion source manifold pressures as indicated by an ion gauge mounted on the flange directly above the ion source region. This suggests that loss in GC sensitivity could be due to the carrier gas causing disruption of the ionization process, scattering of ions within the ion source or an increase in the probability of charge exchange.

The possibility of disruptive gas dynamics was investigated further by adding additional helium as make-up gas in the ion source through the chemical ionization reagent gas lines located within the GC transfer line, coaxial with the capillary column. An illustration of the ion source region showing GC and probe sample introduction inlets and the approximate location of the make-up gas inlet line is shown in Figure 2-4. In this study, for each column inlet pressure, the helium make-up gas flow was adjusted to give a constant ion source manifold pressure equivalent to that at a column inlet pressure of 15 psi. It is apparent from the data (Figure 2-3a, dashed line) that the peak area drops by a factor of 4 upon addition of make-up gas at the lowest column inlet pressure; however, the addition of make-up gas does

Figure 2-3: Comparison of the effects of column inlet pressure on sensitivity for pyrene for (a) short-column GC and (b) direct insertion probe. Solid lines indicate no additional helium in the ion source, while dashed lines indicate make-up gas added coaxially around the column to bring the ion source manifold pressure up to that observed at the maximum column inlet pressure of 15 psi.

(a)

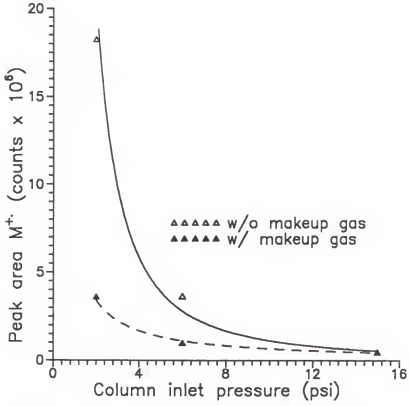
Peak area M+· (counts x 10^6)
20
15
10
5
0
0
4
8
12
16
Column inlet pressure (psi)
△△△△△ w/o makeup gas
▲▲▲▲▲ w/ makeup gas

(b)

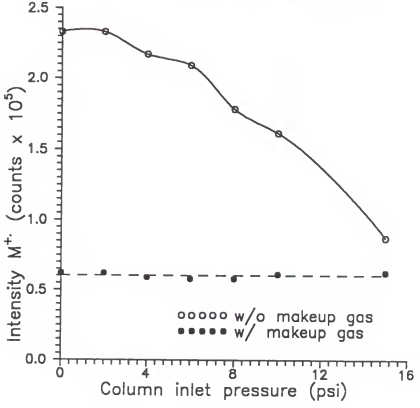
Intensity M+· (counts x 10^5)
2.5
2.0
1.5
1.0
0.5
0.0
0
4
8
12
16
Column inlet pressure (psi)
ooooo w/o makeup gas
●●●●● w/ makeup gas

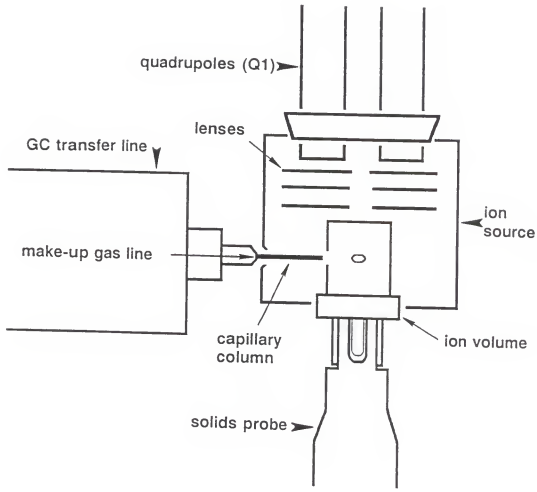

Figure 2-4: Top view of the TSQ45 ion source. GC and probe sample introduction entrances are indicated in relation to the ion volume, ion source, lenses, and quadrupoles. An arrow indicates where helium make-up gas is added coaxially around the capillary column.

not reduce the sensitivity to the level observed at high column inlet pressures (15 psi) as would be expected if only the total helium flow entering the ion source were significant. It is, therefore, clear that the helium added coaxially around the capillary column as make-up gas has less of an effect on sensitivity than the helium exiting the column itself.

To further investigate the possibility of disruptive gas dynamics pyrene, placed within a capped aluminum vial, was introduced into the ion source at a constant rate using a solids probe. The inlet pressure on the GC column also introduced into the ion source was varied as in the GC column inlet pressure studies. The results of this study (Figure 2-3b, solid line) show a threefold decrease in sensitivity as the column inlet pressure was increased from 2 to 15 psi. When make-up gas is added to raise the ion source manifold pressure to that observed at a column inlet pressure of 15 psi (dashed line of Figure 2-3b), the overall sensitivity is reduced, but remains constant with increasing column inlet pressure. Therefore, for probe introduction, it is not important whether the helium flow in the ion source is introduced through the GC column or coaxially around the column as make-up gas; rather, it is the total helium flow into the ion source that determines the sensitivity. This is in contrast to the make-up gas study with GC sample introduction, where the sensitivity decreased with increasing column inlet pressure (this distinction is clear if the make-up gas data in Figures 2-3a and b (dashed lines) are compared). This difference may be due to the velocity and residence time of the sample molecules within the ion source.

The linear velocity of the carrier gas molecules at the outlet of the column can be calculated (using a BASIC program written by Mark Hail) by modifying the Poiseuille equation (54) and using the James-Martin and Giddings gas compressibility correction factors (79,80). With an inlet pressure of 2 psi and an outlet pressure of less than 1 torr, the calculated linear velocity at the exit of a 3 m long GC column is at least 750 m/s. With an increase in inlet pressure to 15 psi, the linear velocity of the molecules as they exit the GC column increases to 1,500 m/s and their residence time in the ion source is significantly reduced; this is presumably the cause of the reduction in sensitivity seen in the make-up gas study of Figure 2-3a. However, when vaporized off a solids probe, the sample molecules should have a much lower velocity (close to thermal) and therefore a longer residence time in the ion source. Although increasing total helium flows in the ion source reduced the overall sensitivity for probe introduction, it is not a function of whether the helium is introduced within or coaxial to the GC column. Therefore, it appears that the major loss of GC sensitivity may be due to disruptive gas dynamics which is dependent upon the velocity of the carrier gas exiting the GC column into the ion source.

Another possible explanation for the loss in sensitivity of the $M^{+\cdot}$ ion at high helium flow rates is the extensive fragmentation due to helium charge exchange (CE). Helium charge exchange has been shown to result in more extensive fragmentation than 70 eV electron ionization (81). Charge exchange can occur if the ionization energy (IE) of the sample is less than the recombination energy (RE) of

the reactant species (e.g. $He^{+\cdot}$, with RE 24.6 eV) (82); if the energy difference between the two is large, reduced sensitivity with regard to the molecular ion could occur due to extensive fragmentation (83). It was shown that for the anabolic steroid methyltestosterone, the percentage of the reconstructed ion current from m/z 33 to 350 (% RIC) carried by the molecular ion, $M^{+\cdot}$ (m/z 302), was reduced by 25% upon increasing the column inlet pressure from 2 psi to 10 psi. The results for a similar study using pyrene (IE 7.4 eV) (84) can be seen in Table 2-2, which lists the degree of fragmentation, expressed as the % RIC carried by the molecular ion, versus the column inlet pressure for short-column GC and probe introduction methods with and without make-up gas. Table 2-2 also includes the %RIC of the ion at m/z 101 which previous work (85) has shown to be due to a doubly charged molecular ion, M^{2+} (appearance energy 24.0 eV), rather than a fragment ion. It is evident in Table 2-2 that the % RIC $M^{+\cdot}$ for pyrene does not decrease at higher column inlet pressures, but increases; although both the RIC and intensity of the $M^{+\cdot}$ ion decrease as the column inlet pressure increases. This suggests that at high helium flow rates, the $M^{+\cdot}$ ion of pyrene is being formed not only by EI, but also by CE, thus the % RIC of the $M^{+\cdot}$ ion increases with increasing helium flow rates. Despite the closeness of the appearance potential of the doubly charged molecular ion (24.0 eV) and the ionization energy of $He^{+\cdot}$ (24.6 eV), it is doubtful that charge exchange with $He^{+\cdot}$ could form an M^{2+} ion; therefore, the % RIC M^{2+} remains relatively constant with respect to helium inlet pressure for this compound. In contrast, the decrease in the %RIC $M^{+\cdot}$ with increasing helium pressure observed for the anabolic steroid,

Table 2-2: Extent of charge exchange versus sample introduction method for pyrene

sample introduction	column inlet pressure (psi)	w/o make-up[a] % RIC $M^{+\cdot}$[c]	w/o make-up[a] % RIC m/z 101[d]	w/ make-up[b] % RIC $M^{+\cdot}$[c]	w/ make-up[b] % RIC m/z 101[d]
GC	2	46	11	48	15
	6	50	13	56	15
	15	63	13	63	13
Probe	--[e]	44	8	--	--
	2	38	11	47	14
	6	39	12	40	14
	15	40	14	40	14

[a] no additional helium in the ion source
[b] additional helium make-up gas in the ion source, added coaxially around the GC column
[c] percent reconstructed ion current for the molecular ion of pyrene, m/z 202
[d] percent reconstructed ion current for m/z 101, M^{2+} ion, of pyrene
[e] no helium in the ion source, injection port end of column is capped

methyltestosterone, is the result of an easily fragmented molecular ion as compared to pyrene whose molecular ion is resonance stabilized through its fused aromatic ring structure. The more extensive fragmentation due to charge exchange for the anabolic steroid as compared to pyrene indicates the compound-dependency of the charge exchange process.

Charge exchange, although a possible factor, appears to play little role in the overall loss of sensitivity of the molecular ion for short-column GC/MS. Based on the above results, it is clear that disruptive gas dynamics must account for the loss of GC sensitivity as a function of high helium flow rates, possibly by reducing the residence times of the neutrals within the ion source. It is also clear that helium added around the column does not affect sensitivity as much as helium flow out of the column.

Compound-dependent factors. GC and probe column inlet pressure studies were also performed on benzene, as well as pyrene which was previously discussed, in order to determine if sample volatility influences sample transfer efficiency. Figures 2-5a and b show the effect of column inlet pressure on sensitivity for short-column GC and probe introduction (both with and without make-up gas added) for benzene. The equivalent studies for pyrene were shown in Figures 2-3a and b. Similar to the results of the experiments with pyrene, the benzene data show a decrease in sensitivity of 98% for GC and 68% for probe with an increase in column inlet pressure from 2 to 15 psi. As in the pyrene study, the total helium flow for

Figure 2-5: Comparison of the effects of column inlet pressure on sensitivity for benzene for (a) short-column GC and (b) direct insertion probe. Solid lines indicate no additional helium in the ion source, while dashed lines indicate make-up gas added coaxially around the column to bring the ion source manifold pressure up to that observed at the maximum column inlet pressure of 15 psi.

(a)

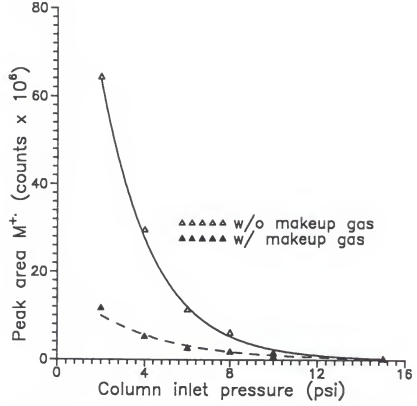
Peak area M+· (counts x 10^6)
80
60
40
20
0
4
8
12
16
Column inlet pressure (psi)
w/o makeup gas
w/ makeup gas

(b)

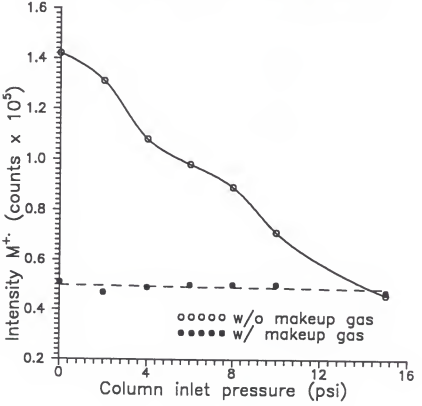
Intensity M+· (counts x 10^5)
1.6
1.4
1.2
1.0
0.8
0.6
0.4
0.2
0
4
8
12
16
Column inlet pressure (psi)
w/o makeup gas
w/ makeup gas

probe introduction with make-up gas added (dashed line, Figure 2-5b) lowers the sensitivity to the level obtained at high helium flow rates. GC introduction with make-up gas added (Figure 2-5a, dashed line) also shows a reduction in sensitivity, but, again does not decrease to the level of sensitivity at high column inlet pressures. Since pyrene and benzene have different vapor pressures, the similarity of the results for these two compounds shows that sample volatility has little or no effect on GC sample transfer efficiency or sensitivity.

Investigation of Mass Spectrometric Parameters

From the investigations of the GC parameters it is apparent that with increasing column inlet pressure the linear velocities of the neutral molecules exiting the GC column into the ion source increase and may be disrupting the electron beam, ionization efficiency, extraction efficiency, ion focussing, or neutral residence time in the ion source. Therefore, the effects of various MS parameters were investigated with respect to these processes and as a function of column inlet pressure. Several parameters including direction of sample introduction and ionization method, as well as the variability of different mass spectrometers, were studied and are discussed below.

Direction of sample introduction. A major difference between GC and probe introduction methods is the direction in which the sample molecules enter the ion source. As can be seen in the ion source illustration, Figure 2-4, direct insertion

probes are introduced into the ion source such that the sample is vaporized just outside the ion volume and is introduced on-axis with the quadrupoles at a relatively low velocity. GC sample introduction into the ion source occurs from the side (perpendicular to the probe) and the column ends immediately outside the ion volume. Samples eluting from the GC are introduced off-axis in relation to the quadrupole rods with relatively high linear velocities. Based on these differences, it was thought that the direction of sample introduction may influence the sample transfer efficiency or ionization efficiency of these sample introduction methods.

To investigate this, a GC/MS interface probe introduced on-axis through the conventional probe lock was employed and used as a comparison to normal (off-axis) GC/MS transfer line introduction. Table 2-3 shows the results of a column inlet pressure study for both the GC probe and GC transfer line using benzene. It is evident from these data that without make-up gas, the sensitivity for both GC probe and GC transfer line introduction is the same. The reduction in sensitivity for an increase in column inlet pressure from 2 to 15 psi is approximately 99% in both cases. The sensitivity with make-up gas added is slightly higher for the GC probe than for the GC transfer line, but only at the lower inlet pressures. This is probably due to the fact that the make-up gas flow (again added through the GC transfer line) is perpendicular to the flow of helium through the GC column within the probe, whereas for the GC transfer line the helium flow through the GC column and make-up gas are coaxial. Therefore, for GC transfer line introduction the total helium

Table 2-3: Comparison of the direction of sample introduction for benzene

column inlet	column inlet pressure (psi)	without make-up gas [a] peak area $M^{+\cdot}$ [c]	without make-up gas [a] ion gauge pressure [d]	with make-up gas [b] peak area $M^{+\cdot}$ [c]	with make-up gas [b] ion gauge pressure [d]
Transfer Line [e]	2	64,430	3.6	11,820	7.6
	4	29,660	3.9	5,330	7.5
	6	11,430	4.1	2,710	7.6
	8	6,190	4.7	1,840	7.4
	10	1,620	5.4	840	7.5
	15	320	7.5	250	7.1
probe [f]	2	68,840	3.5	17,090	8.3
	4	30,810	4.3	11,710	8.1
	6	13,610	4.7	4,670	8.1
	8	6,540	5.2	2,450	8.3
	10	1,360	5.8	510	8.4
	15	310	8.1	160	8.0

[a] no additional helium in the ion source
[b] additional helium make-up gas in the ion source, added coaxially around the GC column
[c] counts divided by 1,000
[d] ion source manifold pressure reading x 10^{-5} torr, uncorrected for helium
[e] GC entering ion source through GC/MS transfer line, off-axis to quadrupoles
[f] GC entering ion source through GC/MS interface probe and probe lock, on-axis with quadrupoles

flow is in the same direction, resulting in a greater disturbance of the ionization process.

Based on these results, it can be concluded that the direction of sample introduction does not affect sample transfer efficiency or ionization efficiency. It is also evident that the total helium flow in the ion source reduces the sensitivity of an analysis, but it is the helium flow exiting the column itself that is the dominant factor.

Ionization methods. High ion source pressures have been shown to decrease the sensitivity for GC and probe introduction methods under EI conditions. However, since high ion source pressures are typical for CI conditions, it was unclear whether or not loss of sensitivity for GC introduction would occur for CI. Therefore, a comparison of short-column GC and probe sensitivities for EI and CI was performed at various column inlet pressures.

A comparison of sample introduction methods for EI and CI at different column inlet pressures can be seen in Figures 2-6a and b, respectively. For an increase in column inlet pressure from 2 to 15 psi, the sensitivity of GC sample introduction for EI decreased by 95% compared to CI which was reduced by 93%. For probe introduction, the sensitivity for EI decreased by 57% compared to 41% for CI. Contrary to previous findings (51), in these studies decreasing sensitivity occurs with increasing column inlet pressure for CI, as well as for EI. These results

Figure 2-6: Comparison of (a) EI and (b) CI ionization efficiencies at different column inlet pressures. Triangles represent GC introduction and circles represent DEP.

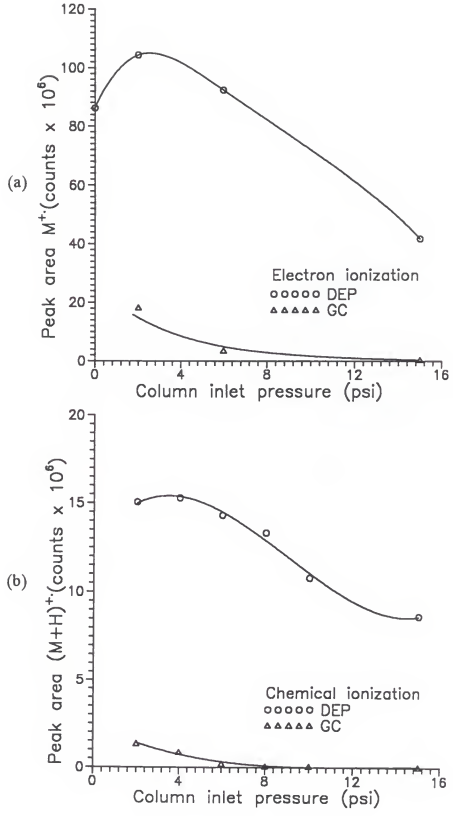
(a)
Peak area M+·(counts x 10^6)
120
100
80
60
40
20
0
Electron ionization
ooooo DEP
ΔΔΔΔΔ GC
0
4
8
12
16
Column inlet pressure (psi)
(b)
Peak area (M+H)+·(counts x 10^6)
20
15
10
5
0
Chemical ionization
ooooo DEP
ΔΔΔΔΔ GC
0
4
8
12
16
Column inlet pressure (psi)

again support the hypothesis that it is the helium flow exiting the column, not the total ion source pressure, that ultimately controls the sensitivity of GC/MS analyses.

Comparison of mass spectrometers. Column inlet pressure studies were also carried out on a Finnigan MAT TSQ70 triple quadrupole mass spectrometer and compared to the results obtained on the TSQ45 triple quadrupole mass spectrometer. These studies were performed to rule out the possibility that the observed phenomenon is instrument specific. Both solids probe and GC experiments were performed on the TSQ70 using the same GC column as in the TSQ45 experiments and maintaining approximately the same experimental conditions. It should be noted that the ion sources in these two instruments are identical, as are the relative introduction positions of the probe and GC column. Column inlet pressure studies were also performed on the TSQ45 comparing mass spectra obtained with both the first quadrupole (Q1) and the third quadrupole (Q3) in order to rule out transmission efficiency effects.

The results of the column inlet pressure study for GC introduction on the TSQ70 showed the same trend as observed for the TSQ45. The overall decrease in sensitivity for an increase in column inlet pressure from 2 to 15 psi was 93% (TSQ70) compared to 95% (TSQ45) for short-column GC introduction. Probe and GC introduction methods were also compared for the two instruments. For the TSQ70, the sensitivity of probe introduction was 2.4 times greater than GC, compared to 5.7 times for the TSQ45. These results show that the lower sensitivity

for GC compared to probe sample introduction is a fundamental problem of short-column GC/MS for both mass spectrometers. However, the extent to which this is a problem may be somewhat instrument-dependent.

With triple quadrupoles, normal mass spectrometry can be accomplished with either Q1 or Q3 in the mass filter mode (rf and DC voltages); in either case, the other two quadrupoles operate in an rf-only mode. As seen in Figure 2-1, the ion source region and mass analyzer region of the TSQ45 are differentially-pumped; thus, the pressure in Q3 should be lower than in Q1 which is adjacent to the high pressure region of the ion source. To investigate the effect of ion source manifold pressure on quadrupole transmission efficiency, a comparison was performed of Q1 and Q3 acquired mass spectra. One would anticipate that high helium pressures would have less impact on transmission through an rf-only quadrupole than on transmission through a quadrupole in the mass-filter mode, based upon the much smaller positional and angular acceptance of the mass-filter (86). Therefore, it would be expected that transmission with Q1 in the mass filter mode would be affected more by ion source helium pressure than it would with Q3 in the mass-filter mode.

In this experiment, a constant amount of FC43 (perfluorotributylamine) was admitted into the ion source, the instrument was tuned to yield approximately equal sensitivity for the m/z 219 fragment ion for both quadrupoles, and Q1 and Q3 mass spectra were acquired from m/z 33 to 700 at various column inlet pressures. The results of this experiment showed a decrease in the intensity of the m/z 219 ion, as well as the RIC, as a function of column inlet pressure for both quadrupoles;

however, the sensitivity of Q3 was, consistently, slightly lower than Q1. Since transmission efficiency through the quadrupoles for Q1 did not decrease more dramatically than for Q3, as expected, loss of quadrupole transmission efficiency as a function of high ion source pressures was shown not to be a major cause of the low GC/MS sensitivity.

Optimization using Subambient Inlet Pressures

Based on the data presented above, it is evident that high helium flows into the ion source are the cause of the low sensitivity for short-column GC introduction. Under normal short-column GC operating conditions, it is not possible to obtain flow rates low enough to prevent disruption of the ionization process, and thus comparable sensitivities for GC and probe methods cannot be achieved. It has been shown previously that optimum linear velocity (corresponding to the minimum plate height and maximum chromatographic resolution) is inversely proportional to column length and that the inlet pressure required to achieve this optimum velocity is directly proportional to the square root of the column length (54). For the short small diameter GC columns used here, it was demonstrated that subambient inlet pressures are required to achieve the optimum linear velocity (51). Under conventional pressure-regulated operation, it is difficult to attain these low injection port pressures such that low stable flow rates can be maintained. Thus, the Finnigan 9610 GC was modified to obtain subambient inlet conditions by connecting the GC

split outlet to a vacuum pump and using a mass flow controller to adjust the carrier gas flow rate into the injection port.

A study comparing subambient and normal GC inlet conditions was performed at various helium flow rates, as shown in Figure 2-7. In this figure, sensitivity for the $M^{+\cdot}$ ion of pyrene is plotted against the uncorrected pressure reading of an ion gauge mounted directly above the ion source region. This pressure is used as a measure of the total helium flow in the ion source. The use of subambient column inlet pressures (squares) permits operation at lower flow rates (and hence lower ion source pressures) than for column inlet pressures above atmospheric (triangles). At similar ion gauge pressures (and presumably similar helium flows) the sensitivity is within experimental error, unaffected by whether the column inlet pressure is above or below atmospheric pressure. This occurs for ion gauge pressures between 1.5 and 3 x 10^{-5} torr. It should be noted that the two subambient inlet data points that fall well off the GC curve (shown as solid squares) are the result of uncorrected ion gauge response at the two lowest column inlet pressures and hence very low helium flow rates. At such low helium flow rates, a significant fraction of the column flow becomes air, which has an ion gauge response approximately 7 times higher than that of helium. Note that the ion gauge is calibrated for nitrogen (air). As the helium flow increases, it will begin to dominate the ion gauge response, yielding a lower response than air, and the pressure initially appears to go down. With further increases in helium flow, helium becomes the dominant gas and the ion source pressure reading increases.

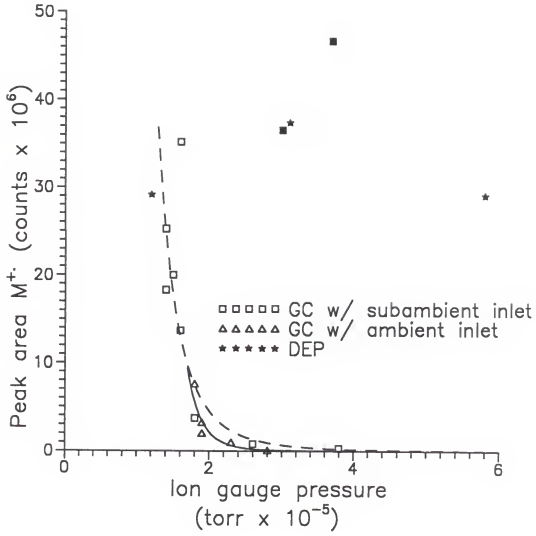

Figure 2-7: Comparison of the effect of column flow rate, as indicated by uncorrected ion source manifold pressure, on GC and probe sensitivity for pyrene using subambient GC inlet pressures. Stars indicate DEP introduction at various flow rates. Squares represent GC introduction under subambient inlet conditions. Triangles indicate GC introduction under normal GC conditions.

It is also clear from this figure that at low enough helium flow rates (under subambient inlet conditions), short-column GC sensitivity is comparable to DEP sensitivity (stars). The differences in the peak areas for the DEP data points arise from the different helium flows used for each of the three runs. The rightmost DEP data point, showing the lowest sensitivity, was taken with a helium flow into the injection port of 2.5 mL/min. from the flow controller under subambient inlet conditions (negative column inlet pressure). Under these conditions, the low flow of helium through the column results in a significant amount of air entering the ion source and hence a high ion gauge pressure reading. The leftmost DEP data point, with similarly low sensitivity, was taken with no helium flow into the ion source. This was accomplished by capping off the injection port end of the GC column. The important point to note, however, is the middle DEP data point, yielding the highest sensitivity. This DEP run was taken with a helium flow rate of 2.5 mL/min. from the flow controller under normal GC conditions (positive column inlet pressure). The fact that this DEP run gave the highest sensitivity indicates that low flows of helium into the ion source may be beneficial in enhancing the sensitivity of probe introduction. However, if helium flows are increased much further, disruption of the ionization process will occur, as previously shown.

Evaluation of Sample Introduction Methods

Based upon the information gained in the experiments described above, evaluation of short-column GC and probe introduction methods was performed

under similar operating conditions. Short-column GC and probe sample introduction methods were compared with respect to limit of detection and linear dynamic range. A calibration curve study for short-column GC introduction was performed under subambient inlet conditions using a helium flow into the injection port of 3.5 mL/minute. The corresponding study for probe introduction was performed with a DEP and with no helium present in the ion source. These results are summarized in Table 2-4. As seen in this table, both methods result in a linear calibration curve (log-log slopes between 0.99 and 1.04); however, short-column GC introduction results in a lower limit of detection and a larger linear dynamic range. In addition, it should be pointed out that the risk of chemical interference increases under subambient inlet conditions. When vacuum is pulled on the split line, air leaks in the GC carrier gas lines or through the septa become more problematic and can cause column decomposition. Siloxanes resulting from column bleed can cause increased background or result in GC peaks if contamination of the injection port occurs. Therefore, although low flow rates are crucial to short-column GC/MS sensitivity, care must be taken to minimize air leaks within carrier gas lines and the injection port.

Conclusions

Based on these studies, it is clear that comparable sensitivity for sample introduction by short-column GC and direct exposure probes is possible if critical

Table 2-4: Comparison of sample introduction methods with pyrene

sample introduction	LOD	linear range	background interferences
GC[a]	5pg[b]	5pg to 50ng[c]	siloxanes stationary-phase background
DEP	100pg[d]	100pg to 100ng[e]	phthalate and hydrocarbon background

[a] splitless injection, split closed 0.2 min.
[b] lowest detectable amount with a S/N ratio of 5:1
[c] linear range with a log-log slope = 0.99
[d] lowest detectable amount with a S/N ratio of 9:1
[e] linear range with a log-log slope = 1.04

parameters are controlled. It was determined that high flow rates of helium (or presumably any carrier gas) into the ion source will disrupt the ionization process and limit the level of sensitivity obtainable by both GC and probe sample introduction methods. High helium pressures in the ion source are believed to either reduce the residence time of the neutral sample molecules or cause scattering within the ion source thus disrupting the ionization process. Charge exchange and loss of quadrupole transmission efficiency as a function of high helium flows and high ion source pressures appear to have little overall role in the loss of sensitivity for short-column GC/MS. It was shown that low flow rates of carrier gas are required for maximum short-column GC sensitivity and may also enhance the sensitivity for probe introduction. Subambient column inlet operation is required to achieve the low carrier gas flows needed for short-column GC/MS. Under subambient inlet operation, short-column GC/MS offers the advantages of lower limits of detection, minimal analysis times, a large linear range, and, most importantly, separation capabilities.

CHAPTER 3

EVALUATION OF CURIE-POINT THERMAL DESORPTION AS A RAPID INJECTION METHOD FOR SHORT-COLUMN GC/MS

Introduction

It has been shown previously that for short columns (< 5 m), the experimental chromatographic resolution at high carrier gas velocities is not as good as that predicted by theory (51). The differences between experimental and theoretical values can be attributed to extracolumn variances from the sample injection method. This is believed to occur due to the finite time required for vaporization of the sample and solvent before being loaded on to the head of the column. If optimum short-column GC/MS performance is to be obtained, development of a high-speed injection method is necessary to eliminate this extracolumn band broadening.

Curie-point thermal desorption (CPTD) has been investigated as a potential alternative injection method for short-column GC/MS. Because CPTD is a solventless injection method and works on the basis of thermal desorption of the analyte from a rapidly heated wire, rather than vaporization of the analyte and an excess of injection solvent, it was believed that it would be a faster injection method. Initially, it was hypothesized that the variance due to thermal desorption, $\sigma_{desorp.}$,

would be less than the variance from vaporization, $\sigma_{vapor.}$ since the desorption process occurs on the order of 0.1 to 2 s depending on the power output of the rf generator (87,88). If this hypothesis were correct, then a narrow input bandwidth should be achieved using CPTD injection even at high linear velocities.

In this chapter, the use of Curie-point thermal desorption as a high-speed injection method for short-column GC/MS has been investigated. Studies have been performed to compare CPTD to traditional syringe injection methods. Experimental results were compared to predicted theoretical data to determine the extent of extracolumn band broadening associated with these injection methods. An evaluation of these injection methods with respect to the practical aspects of a GC injection technique will be presented. Finally, suggested requirements for an ideal injection method for short-column GC/MS will be discussed.

Experimental

Samples and Reagents

The majority of the studies were performed using the anabolic steroid, methyltestosterone (Sigma Chemical Co.), as a test compound. Separation capabilities were evaluated for a mixture of six anabolic steroids (shown in Figure 1-1). Reagent grade methylene chloride (Fisher Scientific) was used as the solvent. A study of solvents was also performed using the following: methylene chloride,

methanol, pyridine, pentane, dimethylformamide (Fisher Scientific), and acetonitrile (Kodak). Commercial grade helium (Liquid Air Corp.) was used as the GC carrier gas.

Sample Injection Methods

Both traditional splitless syringe injection and Curie-point thermal desorption injection techniques were studied. Syringe injection was performed using a Hamilton 10 μL syringe equipped with a teflon-tipped plunger (Scientific Instrument Services). Curie-point thermal desorption injection was performed using a homebuilt Curie-point unit provided by Dr. Henk Meuzelaar at the University of Utah. A schematic of this system is shown in Figure 3-1 (67). Filament wires having Curie-points of 358, 610, and 980 °C were also provided by the University of Utah. Glass reaction tubes were designed at the University of Utah and duplicated by the glass shop at the University of Florida. The Curie-point unit body was heated with a 0-135 V variac operated at 5V. An additional ceramic heater was also used to heat the glass reaction tube within the Curie-point unit and had its own external heating control (Omega Engineering, Inc.). An rf power supply (Univ. of Utah) was used to heat the wire inductively to its Curie point.

Gas Chromatography

Gas chromatography was carried out on J&W Scientific SE-54 capillary columns (4.0 m or 3.8 m, 0.25 mm i.d., 0.25 μm film thickness). For splitless injections, the split was left closed for 0.1 to 0.5 min. and then opened for the

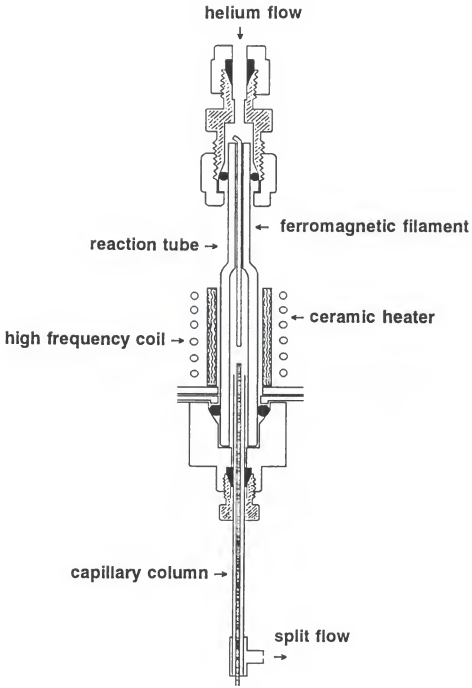

Figure 3-1: Illustration of the Curie-point unit showing the glass reaction tube, the Curie-point wire, and the rf coil.

remainder of the GC run. A column temperature of 200 °C was used for most of the studies. A temperature program from 150 to 250 °C at a rate of 20 °C/min. was used for the mixture separation studies. Standard syringe injection was performed through the capillary injection port using a splitless quartz injection port liner. The 9610 GC packed column injection port was modified for interfacing the Curie-point unit. The injection port was kept at 250 °C and the Curie-point unit maintained at a temperature of 150 °F. Carrier gas flow rate was adjusted by both pressure regulation (2 to 20 psi) and by flow control (-15 in. Hg vac to 20 psi). Typically, 1 μL injections of a 250 ng/μL solution were made for syringe injection. Curie-point experiments were typically performed using 2-4 μL of a 500 to 1,000 ng/μL solution and a total wire heating time of 20 s.

Mass spectrometry

A Finnigan MAT TSQ45 gas chromatograph/triple quadrupole mass spectrometer was used in these studies. Conditions for the mass spectrometer were GC/MS interface and transfer line temperatures of 250 °C, ionizer temperature of 190 °C, electron energy of 70 eV, and emission current of 0.3 mA. Full mass spectra were acquired for the mixture separation, total heating time, and solvent studies. In these studies, the first quadrupole was scanned from 33 - 350 u in 0.5 s. For the peak width studies, the first quadrupole was scanned only over the mass of interest (301.5 - 302.5 u in 0.05 s) to eliminate any extracolumn variance due to the detector response time. Peak widths were measured by visually manipulating cross-hairs to determine the number of scans across the peak at half-height. Peak widths were

then calculated by multiplying the number of scans a peak was wide by the total scan time (s/scan). Average velocities were calculated using the Poiseuille equation and the measured column inlet and outlet pressures (54). Plate heights were calculated using the Foley-Dorsey equation to correct for non-Gaussian peak shapes (89).

Results and Discussion

The hypothesis that $\sigma_{desorp.} < \sigma_{vapor.}$ was investigated, as were the instrumental parameters that affect the peak width, sensitivity, and reproducibility, of syringe and CPTD injection methods. In addition, the practical aspects of these injection methods, such as speed of analysis, chromatographic resolution, and the extent of thermal decomposition will also be presented. All studies were performed using the underivatized anabolic steroid, methyltestosterone, to observe the extent of thermal decomposition and to determine the ability of these two injection methods to handle thermally-labile and involatile compounds.

Curie-point Thermal Desorption

Curie-point units are most commonly used for performing pyrolysis rather than thermal desorption. Pyrolysis is the thermal degradation of molecules to produce substances of lower molecular weight and higher volatility (90). This process, however, tends to produce many lower molecular weight molecules with few remaining intact parent molecules. Alternatively, the Curie-point unit can be used

for thermal desorption of intact molecules which can then be fragmented by electron ionization. This results in less complicated spectra since the degree of fragmentation can be controlled by varying the electron energy (91).

The Curie-point unit used in these studies is a pulse-mode unit that is based on radio frequency inductive heating of ferromagnetic wires. When placed in an rf field, these wires heat almost instantaneously to their Curie point. The Curie point of a wire is the temperature at which the wire becomes paramagnetic and its energy intake drops, thus holding the temperature of the wire at this point; this temperature is determined by the metal or alloy of which the wire is composed. The temperature rise time (TRT) is the time required for the wire to reach its Curie point equilibrium temperature (T_c). Wire composition, geometry, and the available rf power will affect the TRT. The TRT, T_c temperature-time profile (TTP), and total heating time (THT) are the critical parameters to control for CPTD, since they affect the thermal desorption/decomposition process (91,92).

Curie point temperature. The effect of Curie point temperature (T_c) on peak width and retention time as a function of average carrier gas velocity was studied using 610 and 980 °C wires. A comparison of peak widths at half height was used to determine the effect of T_c on the input bandwidth for CPTD as a function of average velocity. Retention time data was used to determine if T_c affects the TTP of the thermal desorption process. These data are summarized in Table 3-1.

Table 3-1: Effects of T_e and THT

T_e (°C)[a]	average velocity (cm/s)	retention time (s)	peak width (s)[b]
610	158	95.3	3.4
	186	88.3	3.4
	234	70.8	3.4
	281	59.6	3.1
	328	52.6	2.8
980	158	94.4	3.1
	234	68.2	2.9
	328	49.4	2.7

THT (s)[c]	peak width (s)[b]	peak height[d]	peak area $M^{+\cdot}$[e]	% RIC $M^{+\cdot}$[f]
5	4.2	51.0	52.7	2.90
10	4.6	69.4	78.6	2.77
15	4.0	72.9	69.8	2.86
20	4.2	73.5	91.7	2.74
25	4.2	118.1	133.6	2.64

[a] data for a 3.8 m column using a THT of 20 s and scanning 301.5 - 303.5 u at a scan rate of 0.05 s/scan; data for triplicate injections

[b] data for peak widths taken at half height

[c] data for a 4.1 m column using a 610 °C wire, an average velocity of 172 cm/s and scanning 33 - 325 u in 0.55 s; data for 5 replicate injections

[d] counts divided by 10^3

[e] counts divided by 10^4

[f] percent reconstructed ion current for the molecular ion of methyltestosterone at m/z 302

As can be seen in Table 3-1, at an average velocity of 158 cm/s, the peak widths obtained for both Curie-point wires were similar, with a difference of only 0.3 s. This is also true for the highest average velocity studied; at 328 cm/s the difference in peak widths was 0.1 s. Based on these results it can be inferred that input bandwidth for CPTD injection is not a function of the Curie point of the wire since the peak width data is within the experimental reproducibility for both wires. The reproducibility of the peak width data, calculated as the percent relative standard deviation (%RSD), is between 2 and 4 % for the 610 °C wire and for the 980 °C wire was between 1 and 7%; note that for best reproducibility, previous work has recommended using wires with temperatures between 510 and 610 °C (91,93).

Previous work has also shown that thermal decomposition/desorption may be complete before the final T_c is reached (91,94). This is a function of the TRT of the Curie-point wire and the stability/volatility of the analyte. If the TRTs of the 610 and 980 °C wires were the same, then a compound desorbed from these wires should exhibit approximately the same retention time. Retention time as a function of Curie point temperature is shown in Table 3-1. At low velocities, the difference in the retention times (0.9 min) for the desorption of methyltestosterone from the two wires suggests that the temperature-time profiles of these two wires are very similar. However, the differences in retention times (2.6 to 3.2 min) observed at the higher average carrier gas velocities suggest that the 980 °C wire may have a slightly faster TRT than the 610 °C since the retention times are shorter. Desorption prior to

reaching T_c or a faster TRT for the 980 °C wire could explain the differences in the retention times observed in these studies.

Total heating time. The time during which the wire remains at its Curie point is referred to as the total heating time. This time is triggered by the rf power supply. In the present system, this time can be varied from 1 to 99 s. Total heating time was varied from 5 s to 25 s to determine its effect on the input band width, the extent of fragmentation, and sensitivity. These data are shown in Table 3-1. Peak widths (used as an indication of input band width) were relatively unaffected by the total heating time. Since the peak widths are all less than the shortest THT (5 s), it seems likely that the compound has been completely desorbed within this time and longer THTs are not necessary. Note that even though total heating times as high as 1000 s have been reported in the literature, suggested values are still typically less than 2 s (91,93). The extent of fragmentation, as reflected in the % RIC of the $M^{+\cdot}$ ion, also appears to be unaffected by THT. The % RIC of the $M^{+\cdot}$ ion would be expected to decrease significantly the longer the wire remained heated if thermal decomposition were occurring, but this was not observed. This again suggests that the steroid has been desorbed completely in a relatively short time.

Peak areas (sensitivity), in contrast, increased by a factor of approximately 2.5 by changing the THT from 5 to 25 s. Since peak widths (measured at half height) remained relatively constant, this increase in area was accompanied by an increase in peak height; note that peak height also increased 2.3 times by increasing the THT

from 5 s to 25 s. Although not supported by the data shown, it is hypothesized that the increase in sensitivity observed with an increase in THT from 5 to 25 s is a result of desorption of sample off the glass reaction tube. It is possible that desorption from the wire occurs very rapidly (within 5 s) where part of the sample goes on to the cooler surrounding glass reaction tube. With longer THT (25 s or greater) sample may be re-desorbing from the glass reaction tube as well. If this hypothesis were correct then an increase in peak width and retention time of the sample would be expected for the slower desorption process (at THT > 25 s). Although a possible explanation, this hypothesis is not supported by the data in that peak widths (as measured at the baseline) remained relatively constant with respect to THT and the retention time of the sample did not increase significantly from a THT of 5 s (retention time 117.2 s) to a THT of 25 s (retention time 118.7 s). Another possible explanation is simply irreproduciblity in the data which is a common problem for the CPTD injection method.

Solvent. A comparison of suspending solvents has been shown previously (93). In this study, methanol, water, and carbon disulfide were compared with respect to the reproducibility of the resulting mass spectra. From this study, it was concluded that the variations caused by the different solvents exceed the variations observed when using the same solvent. This study was performed with the present Curie-point system in an attempt to increase injection reproducibility. In this study the following solvents were used: methylene chloride, methanol, pyridine,

acetonitrile, pentane, and dimethylformamide. In all cases, the test compound dissolved in all of the solvents studied except pentane. Solvents were compared with the ability to load the sample onto the wire evenly, ease of solvent evaporation (drying time), injection reproducibility, and sample transfer/desorption efficiency (sensitivity). In all cases, a 1 mg/mL solution of methyltestosterone was used; 3 μL of the solution was loaded onto the wire and the solvent was evaporated at room temperature or air dried using a heat gun operated on a cool setting.

Reproducibilities were estimated from calculated RSDs based on average peak widths at half height and peak areas of the molecular ion. These data are summarized in Table 3-2. It was observed that using methylene chloride, methanol, or acetonitrile as the solvent resulted in uneven sample loading and clumping on the wire. This can be problematic in that the wire is inserted into the glass reaction tube from the top and the wire diameter and the inside diameter of the glass reaction tube are very similar. Thus when inserting a wire into a glass reaction tube, sample that has clumped onto the wire may be scraped off and lost. Pentane and dimethylformamide, in contrast, produced a finely dispersed coating of sample on the wire, while pyridine resulted in no visible sample on the wire. Unfortunately, the data shown in Table 3-2 is inconclusive; however, the data is useful in pointing out the criteria of a good solvent for Curie-point desorption studies. These criteria include drying time, the ability to load the sample onto the wire (wetting ability), and the ability to produce a fine dispersion (even coating) of sample on the wire. The recommended solvent as reported in the literature (91,93) is methanol; however, of

Table 3-2: Comparison of solvents

solvent	b.p. °C	solvent removal	peak width (s)	%RSD[a]	peak area $M^{+\cdot}$	%RSD[b]
methylene chloride	40	evaporated[c]	4.7	7	303,000	20
methanol	64.6	dried[d]	5.3	6	16,200	27
pyridine	115.5	dried	5.0	11	516,500	147
acetonitrile	81.6	evaporated	4.4	12	477,700	15
dimethylformamide	149	dried	3.8	14	850,000	45
pentane	36	evaporated	5.1	6	71,200	37

[a] percent relative standard deviations for average peak widths at half height for triplicate injections
[b] percent relative standard deviations for average peak areas of the molecular ion for triplicate injections
[c] solvent dried at room temperature by evaporation
[d] solvent dried by use of a heat gun operated at a cool setting

the solvents studied here, methylene chloride or acetonitrile appear to be the better choices as the reproducibility, sensitivity, and peak width data are more acceptable than those of the other solvents investigated.

Theoretical Aspects

As described in Chapter 1, the total variance in a chromatographic system is the sum of the variances associated with the column and the extracolumn variances; the extracolumn variances can be subdivided into the variances associated with the detector and the injector (66). In these studies, the detector variance was minimized by scanning over a 1-2 u window at a scan rate of 0.05 s/scan, yielding 20 to 40 data points per second. This allows the study of extracolumn contributions due solely to the injection technique.

Figure 3-2a is a plot of peak width as a function of average velocity for both syringe injection and CPTD injection. From this plot it is evident that the experimental performance is not as good as that predicted by theory. The extracolumn band broadening resulted in an additional 0.4 s to the theoretical bandwidth at half-height for syringe injection. The same degree of band broadening was reported previously for syringe injection (51). The extracolumn band broadening for the CPTD injection, however, was 3 times greater than that of the syringe injection. It should be noted that subambient data (ave. velocities less than 150 cm/s) for the CPTD injection method were not acquired as the design of the Curie-point unit was incompatible with subambient inlet operation. It was suspected that

Figure 3-2: Theoretical and experimental performance of syringe injection and Curie-point thermal desorption injection for (a) peak width and (b) plate height as a function of average velocity.

(a)

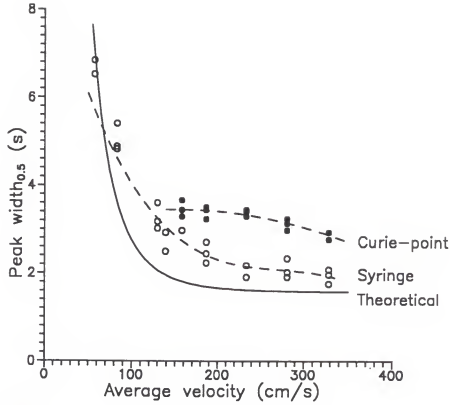
Peak width$_{0.5}$ (s)
Average velocity (cm/s)
Curie–point
Syringe
Theoretical

(b)

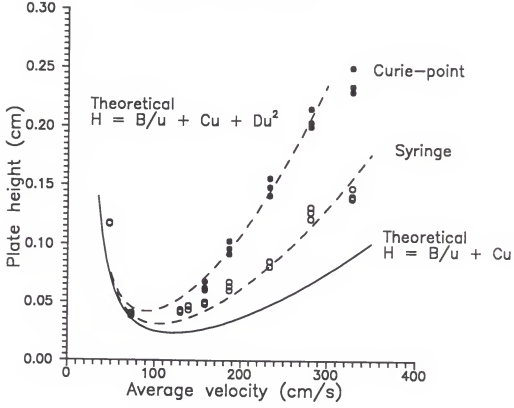
Plate height (cm)
Average velocity (cm/s)
Theoretical
H = B/u + Cu + Du^2
Curie–point
Syringe
Theoretical
H = B/u + Cu

significant air leaks in the Curie-point unit made subambient operation impossible as a positive head pressure on the column was unable to be obtained using flow control of the carrier gas. Thus, the relation between peak width and low average velocities (less than or equal to the optimum gas velocity) for Curie-point thermal desorption was not ascertained.

A plot of plate height as a function of average velocity for these two injection methods is shown in Figure 3-2b. It is clear that CPTD injection results in greater extracolumn band broadening than syringe injection. The variance associated with the desorption method was 5 s^2 compared to 2.5 s^2 for the syringe injection method. In addition, plate heights had to be corrected for non-Gaussian peak shapes. The number of theoretical plates could be corrected for peak skew using the Foley-Dorsey equation (89). This equation takes into account a B/A term which corrects for peak skew. Plate heights could then be calculated using the corrected number of theoretical plates.

Figure 3-3 is a plot of peak width as a function of average velocity for both injection methods using pressure regulation of the carrier gas. This figure can be compared to Figure 3-2a which was run using flow control of the carrier gas. There are two points to note in Figure 3-3 that were not evident in Figure 3-2a. The first is that, at the lowest average velocity that could be achieved under pressure regulation, the peak width for CPTD injection is less than that for syringe injection. This was not observed in Figure 3-2a since subambient inlet operation of the Curie-point unit (and therefore less than optimum gas velocities) could not be achieved.

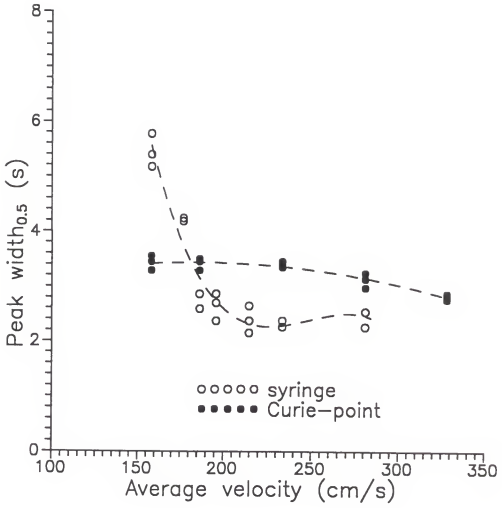

Figure 3-3: Peak width as a function of average velocity for syringe injection and Curie-point thermal desorption injection using pressure regulation of the carrier gas flow.

Secondly, it appears that CPTD injection is not as much a function of average velocity as syringe injection. The overall change in peak width from increasing the average velocity from 157 cm/s to 328 cm/s was 3 s for syringe injection compared to 0.6 s for Curie-point thermal desorption. The effect of carrier gas velocity has been reported in the literature for pyrolysis experiments (95). In the pyrolysis experiments, it was found that the reproducibility of spectra from pulsed filament pyrolyzers were insensitive to variations in pressure or flow. In the study shown here, reproducibility of peak widths were shown to be insensitive to changes in average carrier gas velocity as well.

Practical Aspects

In practical terms, the advantages of using short GC columns are the rapid analysis times, the ability to operate at cooler column temperatures, and the ability to analyze involatile and thermally-labile compounds. These advantages can only be attained, however, if an appropriate injection method is used. Both syringe and CPTD injection methods were tested, using a mixture of six anabolic steroids, with respect to separation capabilities, chemical interferences, speed of analysis, the ability to operate under isothermal column conditions, sensitivity, and the extent of thermal decomposition.

Comparison of syringe and Curie-point thermal desorption chromatograms. The chromatograms, Figure 3-4, were acquired using a temperature program and splitless injection. The column initially was held at 150 °C for 0.5 min., then ramped at 20 °C/min. to 250 °C. The top chromatogram was for syringe injection and shows a high level of solvent tailing; mass spectra for these compounds must be background subtracted. This chromatogram also shows peaks due to siloxane (column) contamination. Peaks due to siloxanes arise when these compounds are washed out of a contaminated injection port by the solvent. The bottom chromatogram in Figure 3-4b was taken using CPTD as the injection method. Since CPTD is a solventless injection method, minimal background is observed; also, note the absence of the siloxane peaks. In addition, the separation capabilities and speed of analysis for these two injection methods appear to be comparable.

The advantage of Curie-point thermal desorption can be seen in Figure 3-5. These two chromatograms were taken at a column temperature of 200 °C isothermal using splitless injection. Under these conditions, the chromatogram for the CPTD injection suffers only from a slight loss in chromatographic resolution and peak shape while the chromatogram for syringe injection is severely compromised by the solvent front. Although separation capabilities are decreased under isothermal column conditions, analysis time decreases for the first five compounds. It is also evident from these chromatograms that the syringe method using splitless injection under isothermal conditions is not a feasible option for short-column GC/MS.

Figure 3-4: Mass chromatograms for (a) syringe injection and (b) Curie-point thermal desorption injection. Chromatograms were acquired using a temperature program. Peaks can be identified by the following numbers, 1: nortestosterone, 2: testosterone, 3: methyltestosterone, 4: dehydrotestosterone, 5: oxymetholone, 6: stanozolol.

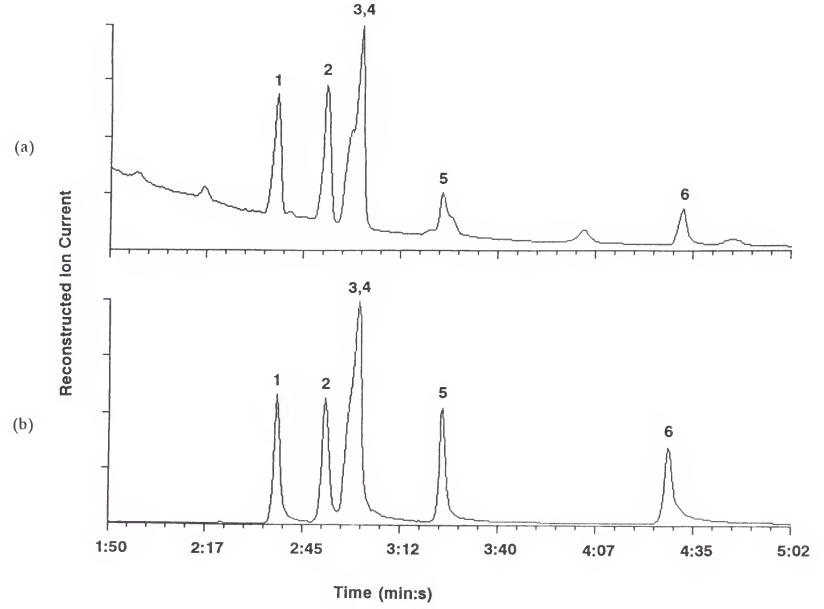
(a)
(b)
Reconstructed Ion Current
1
2
3,4
5
6
1:50
2:17
2:45
3:12
3:40
4:07
4:35
5:02
Time (min:s)

Figure 3-5: Mass chromatograms for (a) syringe injection and (b) Curie-point thermal desorption injection. Chromatograms were acquired under isothermal column conditions (200 °C). Peak numbers refer to the following compounds, 1: nortestosterone, 2: testosterone, 3: methyltestosterone, 4: dehydrotestosterone, 5: oxymetholone, 6: stanozolol.

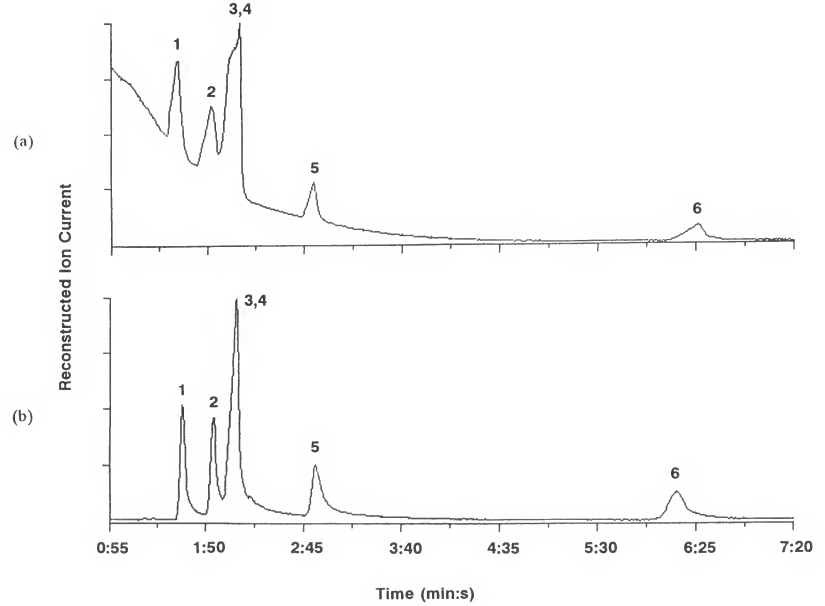
(a)
(b)
Reconstructed Ion Current
1
2
3,4
5
6
0:55
1:50
2:45
3:40
4:35
5:30
6:25
7:20
Time (min:s)

Sensitivity. An estimate of the level of sensitivity obtainable by these two injection methods can be seen in Table 3-3. In this table, sensitivity is determined as the average peak area of the molecular ion per microgram of steroid injected. For all the steroids analyzed, the sensitivity of syringe injection is slightly greater than CPTD injection; note that the sensitivity ratio (CPTD/syringe) for all of the compounds is slightly less than one. In addition, CPTD injection requires μg (typically 2) of sample compared to ng (typically 250) for syringe injection. The necessity of using μg sample quantities, presumably because of secondary reactions, catalytic effects, or heat transfer problems, has been reported in the pyrolysis literature (93). In the present Curie-point design, it was noted that a white film was left on the inside of the glass reaction tube after a CPTD injection was made. It is believed that this film was the result of sample desorbing from the wire onto the cooler glass reaction tube surface. Attempts to heat or desorb more sample from the reaction tube at that point were unsuccessful.

In addition, if sample sizes less than a μg were used (e.g. ng amounts), typically no GC peak was observed. A possible explanation as to why more sample is required for CPTD injection compared to syringe has to due with sample loading onto the wire. It is possible that multiple layers of sample molecules are loaded onto a wire such that the outside layers desorb intact while the inside monolayer decomposes prior to desorption due to the intense heat of the wire. If small amounts of sample are loaded onto the wire such that only a monolayer of sample is produced then no intact sample would be desorbed. To test this hypothesis, additional data is required to study the concentration (amount of sample loaded onto

Table 3-3: Sensitivity and thermal decomposition for syringe and Curie-point thermal desorption injection methods

	sensitivity[a]			thermal decomposition[b]		
steroid	syringe	Curie-point	ratio CPTD/syringe	syringe	Curie-point	ratio CPTD/syringe
Nort	32,000	17,000	0.54	0.50	0.33	0.66
Dehyt	3,000	2,000	0.67	0.14	0.17	1.2
Test	10,000	6,000	0.60	0.33	0.25	0.76
Met	21,000	12,000	0.57	0.25	0.20	0.80
Stan	6,000	4,000	0.67	0.045	0.033	0.73

[a] average peak area of the molecular ion per microgram of steroid injected
[b] percent reconstructed ion current the $(M-H_2O)^+$ divided by the percent reconstructed ion current for M^+

the wire) dependence of the desorption process. Further study of the desorption process would be required to determine conclusively the reason for the lower sensitivity of CPTD compared to syringe injection. Determination of the composition of the white film would also be a necessary step in this investigation.

Extent of thermal decomposition. The relative abundance of the $(M-H_2O)^+$ ion has been used previously as an indication of the extent of thermal decomposition/dehydration of steroids (96). The extent of thermal decomposition has been estimated by dividing the peak area of the molecular ion minus water by the peak area of the molecular ion. The higher the ratio, the greater the degree of thermal decomposition by loss of water. These data are shown in Table 3-3. For all of the steroids, CPTD injection exhibits approximately the same results as syringe injection. Except for dehydrotestosterone, the results for CPTD are slightly lower than for syringe injection (note: the ratio of thermal decomposition values, CPTD to syringe, are slightly less than 1). This shows that minimal thermal decomposition (pyrolysis) occurs for the CPTD injection method. These data also show that the thermal desorption injection method yields comparable results to solvent vaporization injection methods.

Preliminary on-wire derivatization study. Another practical advantage of Curie-point thermal desorption injection is the potential to perform on-wire derivatization. In this method the derivatization process occurs on the wire or in the

gas-phase. An example of on-wire derivatization is shown in Figure 3-6. In this experiment, a sample of testosterone and methyltestosterone was loaded onto a 610 °C wire. A solution of derivatizing reagent, trisilyl reagent, was then applied by syringe to the wire. The wire was then inserted into the Curie-point unit and run as a normal CPTD experiment. A THT of 20 s and a column temperature of 200 °C were used. As shown in Figure 3-6, GC peaks were produced for both underivatized testosterone and methyltestosterone, as well as a peak for the TMS derivative of testosterone at m/z 360. Further study in this area will be required to determine the correct ratio of amounts of reagent-to-steroid, the appropriate choice of derivatizing reagent, and to characterize the derivatization and desorption processes.

Conclusions

Based on the studies performed here, a list of the requirements of an ideal injection method for short-column GC/MS was formulated. This list is presented in Table 3-4; an X in the table indicates that the method meets the listed requirement while a - means that the requirement has not yet been achieved.

The ideal injection method should produce a narrow input bandwidth to minimize σ_{ec} and to maximize the concentration of the analyte at the detector (i.e. maximize sensitivity). Controlled flow paths and low dead volume are essential so that accurate measurement and control of the average carrier gas velocity can be achieved. The effects of solvent overload in short column GC/MS was demonstrated

Figure 3-6: Preliminary investigation into the process of on-wire derivatization Curie-point thermal desorption GC/MS. Chromatogram shows peaks corresponding to (a) underivatized testosterone, (b) underivatized methyltestosterone, (c) the TMS derivative of testosterone, and (d) the RIC.

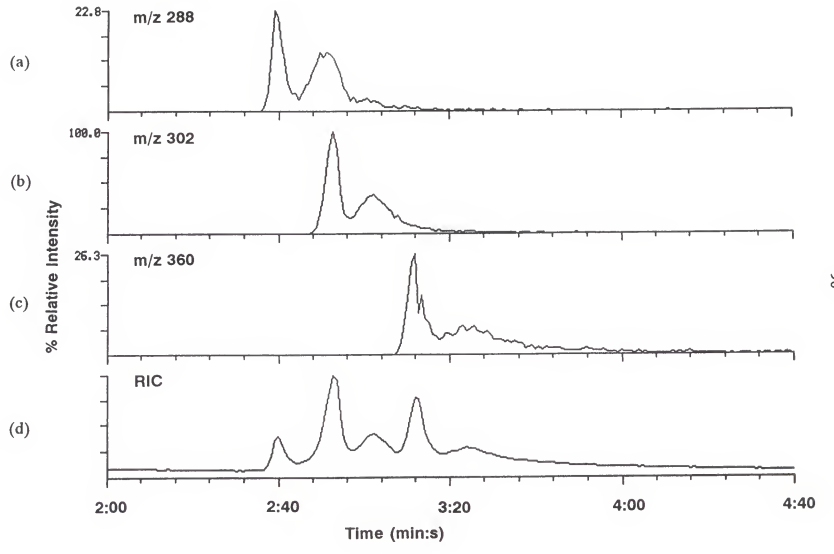
(a)
22.8
m/z 288
(b)
100.0
m/z 302
(c)
26.3
m/z 360
(d)
RIC
% Relative Intensity
2:00
2:40
3:20
4:00
4:40
Time (min:s)

Table 3-4: Requirements of an ideal injection method for short-column GC/MS

requirement	syringe	Curie-point
controlled flow paths/low dead volume	X	-
optimum input bandwidth at low velocities[a]		
- flow control operation	X	-
- pressure regulation	-	X
optimum input bandwidths at high velocities[a]		
- flow control	-	-
- pressure regulation	-	-
minimal interference from solvent		X
applicable to a wide range of compounds		
- volatile compounds	X	-
- highly involatile compounds	-	X
minimal sample loss	X	-
minimal background	-	X

[a] optimum refers to the input bandwidth as determined by theoretical calculations
X indicates that the injection method meets the requirement
- indicates that the injection method does not meet the requirement

and indicates the utility of a solventless injection method. An ideal injection method should also be applicable to a wide range of compounds. The ability to handle highly volatile, relatively involatile, and thermally-labile compounds is desired. Lastly, minimal sample loss due to the injection technique is critical in order to achieve reproducibility and maximum sample transfer efficiency.

In these studies, Curie-point thermal desorption has been shown to meet some of the requirements of an ideal injection method. However, certain design changes in the Curie-point unit will be required if this method is to become an ideal injection method for short-column GC/MS. These include the following: incorporation of the unit inside a normal injection port, changes in present split design, and design of a more powerful rf supply. These modifications of the present design to overcome some of the current limitations will be discussed in more detail in Chapter 7. Standard syringe injection is still the method of choice for short column GC/MS. Care must be taken, however, to minimize solvent overloading with short GC columns. This can be done by choosing an appropriate solvent and column temperature conditions.

CHAPTER 4

DETERMINATION OF UNDERIVATIZED ANABOLIC STEROIDS BY SHORT-COLUMN GAS CHROMATOGRAPHY/MASS SPECTROMETRY

Introduction

In this chapter, the feasibility of determining underivatized anabolic steroids by short-column gas chromatography/mass spectrometry is investigated. Short column GC/MS has been shown previously to be advantageous for the analysis of compounds too involatile or thermally labile to be amenable to conventional-length column GC methods (50,45). The advantages that may be gained by developing a short-column GC/MS strategy for the direct determination of underivatized anabolic steroids include minimal sample preparation, short analysis time, and the potential for reduced thermal degradation since short columns can be operated at lower temperatures.

In the determination of thermally unstable and involatile compounds, however, optimization of chromatographic and mass spectrometric conditions is critical to maintain chromatographic integrity, to minimize thermal degradation, and to maximize sensitivity. GC parameters including column temperature, injection method, and column inlet pressure need to be optimized with respect to sensitivity, speed of analysis, chromatographic selectivity and resolution. Mass spectrometric

parameters such as electron energy, ionizer temperature, and ionization method can also be varied to maximize the intensity of the molecular ion and limit the degree of fragmentation.

An intensive study of the above variables has been performed in order to optimize short-column GC/MS conditions for the determination of underivatized anabolic steroids. The results of these studies have shown that certain critical parameters must be controlled, necessitating that compromises be made in the operating conditions. These studies have also shown that the direct determination of underivatized anabolic steroids based on short-column GC/MS is a feasible alternative to current methods (as discussed in Chapter 1).

Experimental

Steroids and Reagents

The anabolic steroids shown in Figure 4-1, 19-nortestosterone, 1-dehydrotestosterone, testosterone, 17α-methyltestosterone, stanozolol, and oxymetholone, were all purchased from Sigma Chemical Company. Reagent grade methylene chloride (Fisher Scientific) was used as the solvent. Helium (Liquid Air Corp.), used as the GC carrier gas, was commercial grade. Derivatization reagents including methoxamine hydrochloride, N,O-bis(trimethylsilyl)acetamide, and trimethylchlorosilane were all purchased from Sigma Chemical Co. Pyridine (Fisher

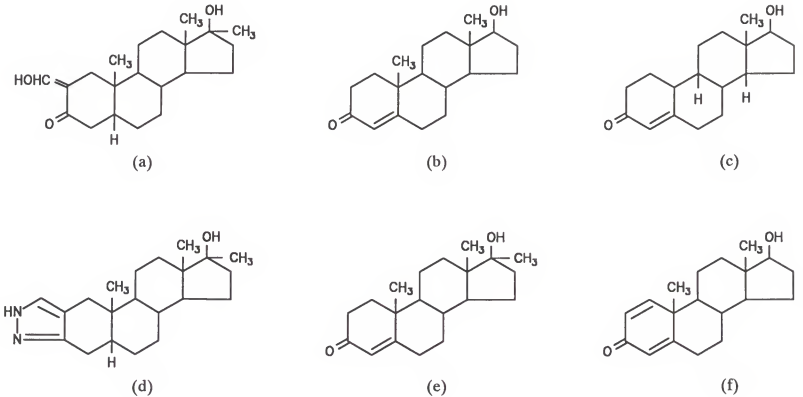

Figure 4-1: Structures of the six anabolic steroids studied: (a) oxymetholone (oxym), (b) testosterone (test), (c) nortestosterone (nort), (d) stanozolol (stan), (e) methyltestosterone (met), (f) dehydrotestosterone (dehyt). ( ) indicate abbreviation of steroid names used.

Scientific) was used as the solvent for preparation of the derivatives. Derivatization procedures were standard according to a handbook on derivatization reactions (97).

Gas Chromatography

Gas chromatography was performed on a Finnigan MAT (San Jose, CA) 9610 gas chromatograph. Gas chromatographic sample introduction was carried out on a short J&W Scientific SE-54 capillary column (3.5 m long, 0.25 mm i.d., 0.25 μm film thickness). In the GC parameter studies, column inlet pressure was varied from 2 to 20 psi, injection method from split injection (0 s splitless period) to splitless injection (0.1 to 1.5 s splitless period), injection volume from 1 to 5 μL, and column temperature (isothermal operation) from 175 to 215 °C. Typically, injections were made in the splitless injection mode with a column inlet pressure of approximately 2 psi. For studies employing a temperature program, the column temperature was initially held at 150 °C for 0.5 to 1 min., then increased at 20 °C/min. to a final temperature of 250 °C. The injector temperature was 250 °C. Unless otherwise stated, 1 μL injections of a 250 ng/μL solution were made in triplicate at each of the conditions for the GC/MS studies.

Mass Spectrometry

A Finnigan MAT TSQ45 gas chromatograph/triple quadrupole mass spectrometer was used in these studies. Conditions for the mass spectrometer were GC/MS interface and transfer line temperatures of 250 °C, ionizer temperature of 190 °C, electron energy of 70 eV, and emission current of 0.3 mA. In the study of

electron energy, the energy was varied from 25 to 100 eV. Constant sample introduction into the ion source was performed by using a solids probe (for solid samples within capped aluminum vials) or a Granville-Phillips variable leak valve (for volatile liquids). Full scan mass spectra were acquired, scanning the first quadrupole from 33-500 u in 0.75 s. The peak areas from mass chromatograms of selected ions were calculated by integrating the ion current over the peak profile after visually choosing the baseline for each GC sample.

Results and Discussion

Gas chromatographic/mass spectrometric conditions were optimized for maximum sensitivity, precision, chromatographic selectivity, and speed of analysis. As discussed below, for short-column GC/MS strategies, these four criteria do not necessarily optimize under the same conditions as for conventional-length column GC/MS techniques that utilize derivatization. The effects of selected experimental parameters, including column inlet pressure, injection method, sample injection volume, column temperature, electron energy, ionization method and ionizer temperature have been investigated to elucidate the critical parameters to control for short-column GC/MS of thermally-labile compounds. The results of these studies are shown in Table 4-1. A discussion of how these values were arrived at follows.

Table 4-1: Recommended conditions for EI short-column[a] GC/MS of underivatized anabolic steroids

electron energy	40 eV
ionizer temperature	190 °C
column inlet pressure	subambient to low pressure regulation
column temperature	temperature program (150 °C to 250 °C)
injection method	splitless (0.5 min. split closed)

[a] for column lengths between 3 and 5 meters

Gas Chromatographic Parameters

Optimization of short-column GC conditions was undertaken in order to maximize the sample transfer efficiency (sensitivity) from the GC into the ion source of the mass spectrometer, while maintaining chromatographic integrity (peak shape, peak width, and chromatographic resolution) and minimizing thermal decomposition. Experiments were performed using only methyltestosterone, as a test compound, for simplicity and to minimize the analysis times.

Column temperature. The temperature (isothermal and temperature-programmed) of the column was optimized and the results are summarized in Table 4-2. Retention times on the short GC column ranged from 6 min. at 175 °C isothermal to 1.5 min. at 205 °C to 3 min. using a temperature program from 150 to 250 °C at 20 °C/minute. Separation of the sample and solvent front at the higher column temperatures, however, was not possible. At a constant column inlet pressure of 2 psi, temperature programming also resulted in significantly sharper

Table 4-2: Effects of column temperature on chromatographic performance

column temperature	retention time (min)	peak width (s)	%RIC $(M\text{-}H_2O)^{+}$ [a]	peak area $M^{+\cdot}$
175 °C	6.0	10.8	2.14	55,500
185 °C	3.8	8.5	2.12	60,100
195 °C	2.5	6.8	2.01	67,000
205 °C	1.8	5.5	1.62	85,800
215 °C	1.2	6.5	0.09	53,300
TP[b]	3.0	2.0	1.55	115,000

[a] percent reconstructed ion current of the molecular ion minus water; used as indication of the degree of thermal decomposition

[b] temperature program from 150 to 250 °C

peaks as compared to isothermal operation (over the range of 175 - 215 °C). The minimum peak width at half height for temperature-programmed operation was approximately 2 s, compared to approximately 5.5 s at 205 °C isothermal. This is governed by the thermal properties of the compound and the loss of thermal focussing effects with higher initial column temperatures.

The maximum sensitivity (largest peak area) under isothermal conditions was obtained at a temperature of 205 °C. Even higher sensitivity was obtained by using the temperature program. The higher sensitivity obtained with temperature program operation and splitless injection is due to a solvent effect, where a cooler initial column temperature allows solvent focussing of the injected sample. Rapid elution time, coupled with the ability to separate the compound from the solvent front, makes temperature programming more appealing. A temperature ramp can be chosen such that the compound elutes quickly, but is still chromatographically resolved from the solvent front. However, the necessity for multiple injections favors isothermal operation since no column temperature re-equilibration time is needed. Therefore, in choosing temperature program or isothermal conditions, a trade-off between sensitivity and chromatographic resolution must be weighed against an increase in speed of analysis.

Table 4-2 also lists an estimate of the degree of thermal decomposition as a function of column temperature. From these data, it appears that the longer the compound remains on the column (longer retention times), the greater the extent of thermal decomposition (higher % RIC M-H_2O). Thermal decomposition has been

estimated as the percentage of the reconstructed ion current (% RIC) carried by the molecular ion minus water $(M-H_2O)^{+\cdot}$. Previous researchers have indicated that $(M-H_2O)^{+\cdot}$ ions are formed in the ion source both from gas-phase fragmentation of the molecular ion and from thermal dehydration of the steroid prior to ionization (96). If thermal decomposition occurs in the injection port or on the head of the GC column, then a separate GC peak for the decomposition product should be observed in the mass chromatogram. If decomposition occurs along the GC column, peak tailing/fronting may be observed. Separation of the dehydration/decomposition product from the intact steroid may not be possible, however, because of the short retention times. Overall, temperature programming yields the best results since the compound elutes quickly at its optimum temperature (211 °C for methyltestosterone) with a sharp peak profile, separated from the solvent front.

Injection method and volume. Another parameter that affects sensitivity, as well as the degree of solvent tailing, is the injection method (62). Split injections tend to reduce solvent tailing, but result in reduced signal, as compared to splitless injections. For splitless injections, when the split valve was opened after less than 0.5 min., a decrease in peak area of approximately 30% was observed. Alternatively, splitless times greater than 1 min. resulted in a decrease in sensitivity of only 10%, but produced a higher solvent background and increased solvent tailing. Therefore, a splitless time of 0.5 min. appears to be the best choice for obtaining maximum sensitivity with minimal solvent interference.

In addition, an investigation into the relationship between the GC injection technique and sample transfer efficiency was performed using methyltestosterone with methylene chloride as the solvent. Figure 4-2a and b show the results of varying the amount and volume of sample injected. As expected, if the same volume (1μL) is injected of solutions with increasing amounts of sample, as in generating a calibration curve, linear results are obtained (Figure 4-2a, circles). However, when different injection volumes are used (Figure 4-2a, squares), linear results are not obtained. When the same amount (500 ng) of sample is injected but in different sample volumes (Figure 4-2b, triangles), the resulting responses are not constant as one would expect; rather, the response is higher when a larger volume is injected. The non-linearity of these results suggest that increased sample transfer onto the column is occurring with increasing injection volume.

Column inlet pressure. The effects of column inlet pressure on peak width and retention time were determined, since this will affect the chromatographic resolution and speed of analysis. Retention times using a temperature program from 150 to 250 °C were between 3 min. (at a column inlet pressure of 2 psi) and 2.25 min. (at 20 psi). Under isothermal conditions, little variation in retention times were observed between an inlet pressure of 2 psi, yielding a retention time of 1.5 min., and 10 psi with a retention time of 1 minute. The minimum peak width was determined to be 1.75 s at a column inlet pressure of 5 psi using temperature-programmed column operation. Although there was not a significant difference in

Figure 4-2: Comparison of the effects of injection volume on GC transfer efficiency. Triangles represent 500 ng of steroid injected corresponding to 1 μL of 500 ng/μL, 2 μL of 250 ng/μL, and 5 μL of 100 ng/μL. Squares represent results for injections of a 100 ng/μL solution (1, 2, and 5 μL injections corresponding to 100, 200 and 500 ng steroid injected). Circles represent results for 1 μL injections of 3 different concentrations of methyltestosterone (100, 250, and 500 ng/μL). GC transfer efficiency is compared with respect to (a) amount injected and (b) injection volume.

(a)

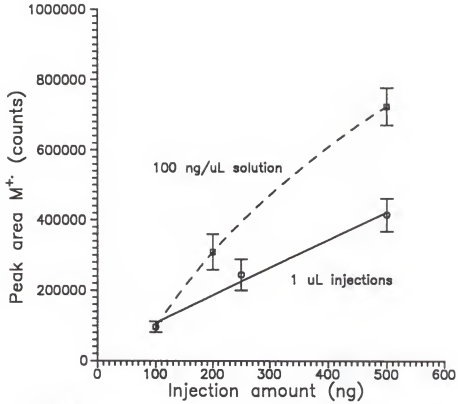
1000000
800000
600000
400000
200000
0
Peak area M+· (counts)
100 ng/uL solution
1 uL injections
0
100
200
300
400
500
600
Injection amount (ng)

(b)

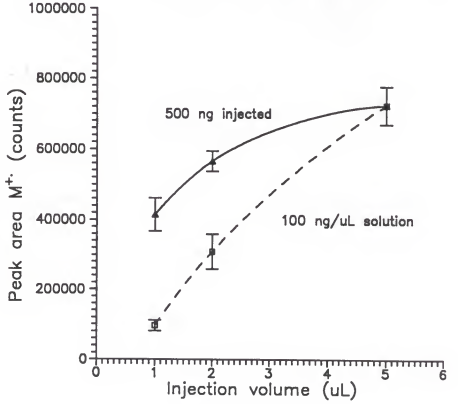
1000000
800000
600000
400000
200000
0
Peak area M+· (counts)
500 ng injected
100 ng/uL solution
0
1
2
3
4
5
6
Injection volume (uL)

peak width at higher inlet pressures, the difference in peak width at low inlet pressures was between 1 and 2.5 s, depending on the column temperature. It is also important to note that at low inlet pressures (and therefore short retention times), solvent overloading of the ion source becomes a problem, since the peak of interest elutes within the solvent tail.

Column inlet pressure was also found to affect sensitivity. The loss of short-column sensitivity as a function of column inlet pressure was discussed at length in Chapter 2 and is shown in Table 4-3 for the compound methyltestosterone; note that both the RIC and molecular ion sensitivities decrease with increasing column inlet pressure. In Chapter 2, it was concluded that very low column inlet pressures (subambient) were necessary to obtain maximum short-column GC/MS sensitivity. For these studies, however, the possibility of air leaks causing column decomposition and creating active sites on the column makes this option less useful for the determination of underivatized polar steroids.

Helium charge exchange at high helium pressures in the ion source was suggested as another possible explanation for the loss of sensitivity for the $M^{+\cdot}$ ion, since helium charge exchange is typically much more energetic than 70 eV electron ionization (81). Table 4-3 lists the degree of fragmentation, expressed as the percentage of the reconstructed ion current carried by the molecular ion, versus column inlet pressure. If helium charge exchange were a major process occurring within the ion source, then the % RIC should decrease at high column inlet pressures due to extensive fragmentation. It is evident in Table 4-3, however, that

Table 4-3: Sensitivity and the extent of fragmentation of $M^{+\cdot}$ as a function of column inlet pressure for the compound methyltestosterone

	fragmentation		sensitivity	
inlet pressure	ion source pressure [a]	ave. % RIC $M^{+\cdot}$ [b]	ave. peak area RIC [c]	ave. peak area $M^{+\cdot}$ [d]
1 psi	4.5	3.66	98.6	12.8
2	5.4	4.26	33.0	5.1
4	5.8	4.56	16.8	2.7
6	7.3	4.65	18.4	2.8
10	10.2	3.11	3.2	0.5

[a] indication of ion source pressure as indicated by the high vacuum pressure in the analyzer region of the vacuum manifold (in torr x 10^{-6})
[b] intensity of the molecular ion as a percentage of the reconstructed ion current from m/z 33 to 500
[c] average peak area of the reconstructed ion current (counts x 10^4)
[d] average peak area of the molecular ion (counts x 10^4)

the % RIC data for the $M^{+\cdot}$ ion are not significantly different and no apparent trend is observed when the column inlet pressure is increased from 1 psi to 10 psi. Less fragmentation (less abundant lower mass ions), however, was observed in the EI mass spectra taken at 1 psi compared to that at 10 psi, suggesting that the role of charge exchange may be minor.

Mass Spectrometric Parameters

Mass spectrometric conditions were optimized in order to maximize ionization efficiency with respect to the intensity of the $M^{+\cdot}$ ion and the degree of fragmentation, as reflected in the % RIC of the $M^{+\cdot}$ ion. Electron energy, ionization method, and ionizer temperature were studied, although only electron energy and ionization method had an effect on short-column GC/MS sensitivity.

Electron energy. A study of electron energy for the test compound methyltestosterone was performed at a column inlet pressure of 2 psi using temperature-programmed conditions. The results show that a compromise between % RIC (degree of fragmentation) and absolute intensity of the $M^{+\cdot}$ ion must be made, since optima occur at different electron energies. The maximum intensity observed for the $M^{+\cdot}$ ion occurred at an electron energy of 40 eV. The % RIC $M^{+\cdot}$ at this electron energy was 6%. When the % RIC was at a maximum of 36%, and therefore minimal fragmentation is observed, the intensity of the molecular ion was only 40% of the maximum intensity observed. As one would expect, at higher

electron energies ionization efficiency increases, but there is also increased fragmentation; at lower electron energies the absolute intensity of the $M^{+\cdot}$ ion is significantly reduced and the degree of fragmentation is large (98). A compromise is achieved at an intermediate electron energy of 40 eV where the absolute intensity of $M^{+\cdot}$ is maximized and total ionization efficiency and the degree of fragmentation are acceptable.

Ionization method. Ionization methods such as electron ionization (EI), positive ion chemical ionization (PCI), and negative ion chemical ionization (NCI) can be used to affect the sensitivity and selectivity of an analysis. A comparison of ionization methods was performed on a mixture of six anabolic steroids (identified in Figure 4-1). Figure 4-3 shows representative spectra of methyltestosterone for each of the three ionization methods. The most selective ionization method was determined to be NCI, as it typically formed only an $(M-H)^-$ ion, followed by PCI which produced few fragment ions and its $(M+H)^+$ ion was also the most abundant ion in the spectrum. Electron ionization, in contrast, produced many abundant fragment ions and therefore is better suited for structural information studies rather than for trace detection. Sensitivity as a function of ionization method was also studied and will be discussed in Chapter 5.

Figure 4-3: Comparison of three mass spectra of methyltestosterone using three different ionization methods: (a) electron ionization, (b) positive ion chemical ionization, and (c) negative ion chemical ionization.

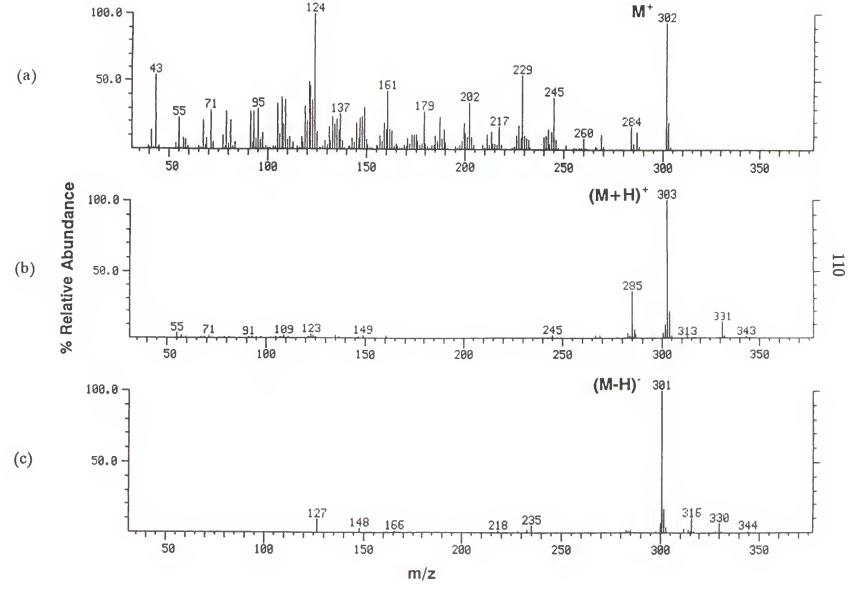
(a)
(b)
(c)
% Relative Abundance
m/z
M+
(M+H)+
(M-H)-
100.0
50.0
50
100
150
200
250
300
350
43
55
71
95
124
137
161
179
202
217
229
245
260
284
302
285
303
313
331
343
301
316
330
344
127
148
166
218
235
110

Evaluation of Optimized Short-Column GC/MS Conditions

Comparison to conventional methods. In order to determine the feasibility of short-column GC/MS of underivatized steroids, results were compared to those obtained for three different derivatives (methoxamine (MO), trimethylsilyl (TMS), and a mixed TMS/MO derivative), as shown in Figure 4-4. Based on these preliminary results (before optimization), the response factors (average peak area of the molecular ion per microgram of compound injected) for the ratio of derivatized-to-underivatized steroid under the same GC/MS conditions on the average is close to 1 (equivalent sensitivity for the derivatized and underivatized steroid). However, this ratio ranges as high as 13 and as low as 0.02 depending on the percent completion of the derivatization reaction and the degree of fragmentation of the molecular ion. In the case of dehydrotestosterone, for instance, the formation of the methoxime derivative dramatically enhances the sensitivity for the molecular ion, presumably by decreasing the degree of fragmentation (note the low % RIC for the $M^{+\cdot}$ ion of underivatized dehydrotestosterone in Table 4-4). Also, the low ratio for the TMS derivative of methyltestosterone occurred because very little TMS derivative (< 20%) was formed for this compound. The mixed TMS/MO ratios were also all slightly lower because the peak areas for the partial derivative (i.e. only TMS or MO group, but not both) were not accounted for in the ratio. The response ratio for stanozolol was especially low since approximately 50% of this compound remained underivatized. The percent derivatization was estimated by comparing the GC peak

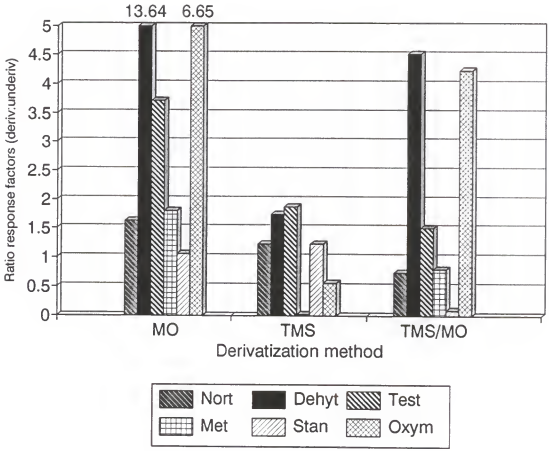

Figure 4-4: Comparison of the relative sensitivities for the $M^{+\cdot}$ ions of three derivatized steroid mixtures (methoxamine, MO; trimethylsilyl, TMS; and mixed TMS/MO) to those for an underivatized steroid mixture. Response factors for the ratio of derivatized-to-underivatized steroid were calculated as the average peak areas of the molecular ions per microgram of compound injected. Note the abbreviations in the legend stand for nortestosterone (nort), dehydrotestosterone (dehyt), testosterone (test), methyltestosterone (met), stanozolol (stan), and oxymetholone (oxym).

Table 4-4: Comparison of preliminary short-column GC/MS results for derivatized and underivatized anabolic steroids

peak #/ steroid	derivative	retention time (min)	response per ng [a]	ave. % RIC M^{+} [b]
1 NorT	none	4.7	180	3.43
	MO	5.0	290	4.45
	TMS	4.9	220	2.30
	TMS/MO	5.0	130	2.67
4 DehyT	none	5.2	20	0.51
	MO	5.3	290	1.91
	TMS	5.3	40	0.37
	TMS/MO	5.3	100	2.37
2 TesT	none	5.0	120	1.49
	MO	5.2	440	2.91
	TMS	5.2	220	2.04
	TMS/MO	5.3	180	2.04
3 MeT	none	5.1	220	3.23
	MO	5.3	390	3.29
	TMS	5.5	5	0.12
	TMS/MO	5.6	170	1.89
5 Oxym	none	5.6	4	1.27
	MO	6.5	20	1.59
	TMS	6.6	2	0.42
	TMS/MO	6.8	20	4.04
6 Stan	none	6.7	70	3.85
	MO	6.9	60	2.49
	TMS	6.7	70	4.69
	TMS/MO	7.2	5	0.94

[a] "response factor", average peak area of the molecular ion per nanogram of original steroid

[b] average percent reconstructed ion current for the molecular ion

area of the derivative to that of the remaining underivatized compound, since the retention times of the two were different.

A comparison of chromatograms acquired before and after optimization of GC/MS parameters is shown in Figure 4-5. It is evident that optimization is essential to control peak shape, chromatographic resolution, and sensitivity. Figure 4-5 also compares chromatograms acquired for both underivatized and TMS derivatized steroids. Although chromatographic resolution is improved by derivatization, the data interpretation can be more complicated. The potential for incomplete derivatization resulting in partially derivatized products and complicated chromatograms, as well as lengthy derivatization procedures, makes these techniques tedious as compared to underivatized methods.

Overall, from these preliminary results, the choice of derivatization method would be to form the methoxime derivative since it generally yields the best response factors and the least fragmentation. However, based on chromatographic resolution and percent derivatization, the TMS derivative would be the better choice. The TMS derivative is the derivatization method most commonly reported in the literature. The possible gain in sensitivity and chromatographic resolution for derivatization, however, must be weighed against the overall sample preparation times.

Separation capabilities and chromatographic resolution. In order to evaluate the optimized short-column GC/MS method, six standard underivatized steroids were analyzed individually and as a single mixture. These data are summarized in

Figure 4-5: Chromatograms comparing separation capabilities of short-column GC/MS for (a) unoptimized conditions for underivatized steroids, (b) optimized conditions for underivatized steroids, and (c) unoptimized conditions for the analysis of TMS derivatives. Note that peak numbers are in reference to 1: nortestosterone, 2: testosterone, 3: methyltestosterone, 4: dehydrotestosterone, 5: oxymetholone, 6: stanozolol.

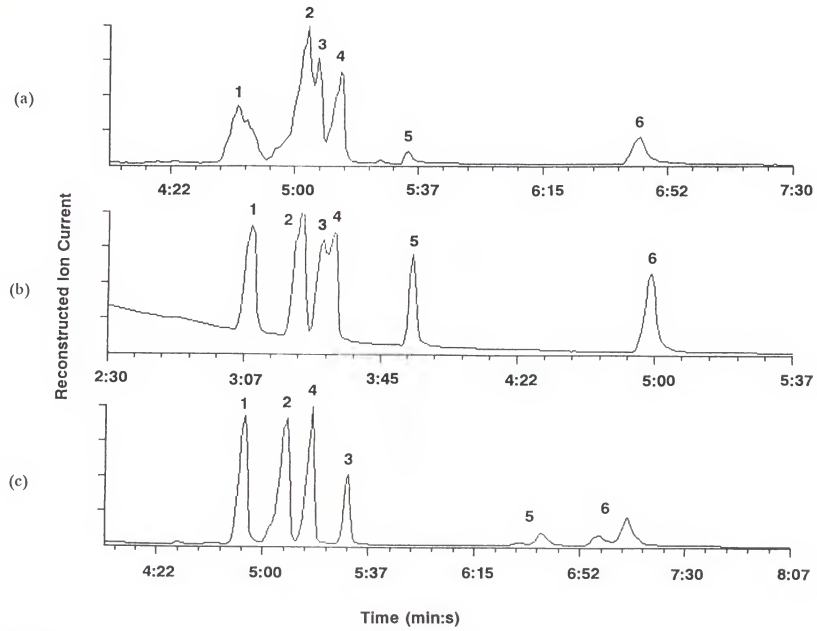
(a)
(b)
(c)
1
2
3
4
5
6
4:22
5:00
5:37
6:15
6:52
7:30
2:30
3:07
3:45
4:22
5:00
5:37
4:22
5:00
5:37
6:15
6:52
7:30
8:07
Reconstructed Ion Current
Time (min:s)

Table 4-5 and Figure 4-5b. Chromatographic performance (retention time, peak width and peak shape), as well as sensitivity, for the underivatized steroid mixture are improved over the preliminary underivatized steroid results (Table 4-4 and Figure 4-5a). Under optimized conditions, retention times were between 3 and 5 minutes, such that the overall analysis time was shorter by 2 minutes over the preliminary chromatogram.

From the chromatogram in Figure 4-5b, it is evident that in some cases chromatographic resolution is limited (e.g., between dehydrotestosterone, testosterone, and methyltestosterone). Each of the steroids, however, can be mass chromatographically resolved. A comparison of separation capabilities for 30 m and 4 m columns is shown in Figure 4-6. It is evident in these chromatograms that chromatographic resolution for the 30 m column is improved (although not to baseline) over the results for the 4 m column. However, an increase in analysis time of 14 min. must be compared to the small gain in resolution. Although not evident in these chromatograms, the sensitivity for the long column is reduced as compared to the short column. Figures 4-7 and 4-8 compare the mass spectra of the three least resolved compounds from the chromatogram in Figure 4-6a. It is evident that even with limited chromatographic resolution little interference from adjacent overlapping peaks is seen in the mass spectra. Only in the case of dehydrotestosterone does any significant overlap in the spectra occur (notice the $M^{+\cdot}$ ion of methyltestosterone present at m/z 302) as seen in Figure 4-7. This ion does not interfere in the identification of dehydrotestosterone, however, since the lower m/z fragment ion

Table 4-5: Reproducibility of short-column GC/MS analysis of underivatized anabolic steroids

individual steroids [a]	column inlet pressure 2 psi: % RSD peak area [b]	response per ng [c]	ave. %RIC $M^{+\cdot}$ [d]	column inlet pressure 6 psi: % RSD peak area [b]	response per ng [c]	ave. %RIC $M^{+\cdot}$ [d]
NorT	18	790	5.96	3	300	6.28
TesT	11	500	3.07	9	190	3.23
MeT	21	350	4.75	11	140	4.34
DehyT	8	120	1.18	20	60	1.15
Oxym	33	120	1.87	24	50	1.92
Stan	29	350	5.36	14	160	4.98
Steroid Mixture [a]						
NorT	12	1,070	6.22	12	320	6.43
TesT	12	870	3.33	7	230	3.28
MeT	12	720	4.88	10	180	3.97
DehyT	13	180	1.20	10	50	1.03
Oxym	22	210	2.16	21	40	1.81
Stan	25	680	6.39	14	140	5.05

[a] compounds listed in order of elution
[b] reproducibility, expressed as the relative standard deviation of five injections
[c] "response factor", average peak area of the molecular ion per nanogram of original steroid
[d] average percent reconstructed ion current for the molecular ion

Figure 4-6: Analysis of a mixture of underivatized steroids on (a) a short (4 m) column and (b) a long (30 m) column under optimized GC/MS conditions. Mass chromatograms show the four compounds (1: nortestosterone, 2: testosterone, 3: methyltestosterone, and 4: dehydrotestosterone) least resolved chromatographically.

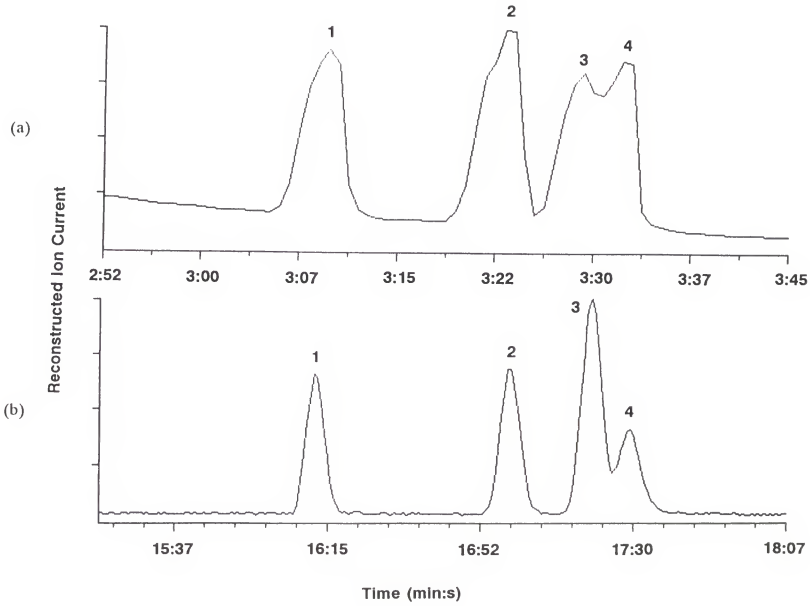
(a)
(b)
1
2
3
4
Reconstructed Ion Current
2:52
3:00
3:07
3:15
3:22
3:30
3:37
3:45
15:37
16:15
16:52
17:30
18:07
Time (min:s)

Figure 4-7: Mass spectra of the three compounds, (a) testosterone (peak 2), (b) methyltestosterone (peak 3), and (c) dehydrotestosterone (peak 4), least separated on the short column and run as part of a six-component mixture.

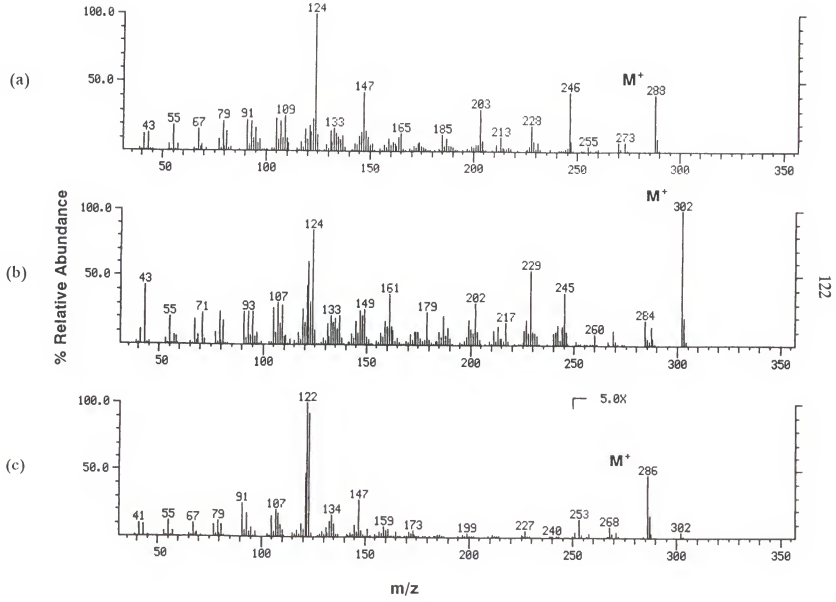
(a)
(b)
(c)
% Relative Abundance
m/z
100.0
50.0
M+
124
147
246
283
203
213
223
255
273
43
55
67
79
91
109
133
165
185
302
229
245
161
179
202
217
284
260
107
149
71
93
122
5.0X
286
41
134
159
173
199
227
240
253
268
50
100
150
200
250
300
350

Figure 4-8: Mass spectra of the three compounds, (a) testosterone, (b) methyltestosterone and (c) dehydrotestosterone, least separated on the short column and run as individual solutions.

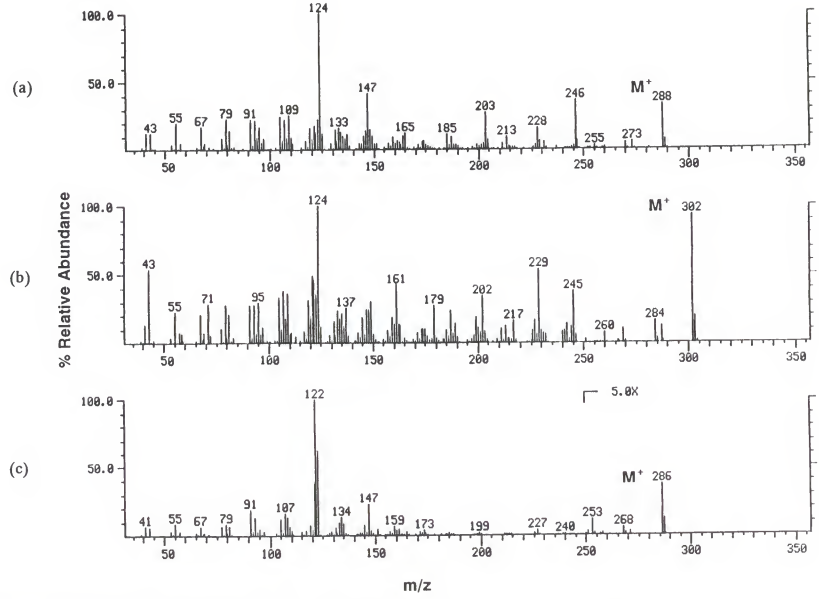
(a)
(b)
(c)
% Relative Abundance
m/z
100.0
50.0
124
M+ 288
M+ 302
122
M+ 286
5.0X
43 55 67 79 91 109 133 147 165 185 203 213 228 246 255 273
43 55 71 95 137 161 179 202 217 229 245 260 284
41 55 67 79 91 107 134 147 159 173 199 227 240 253 268
50 100 150 200 250 300 350
124

range is different than that of methyltestosterone (as seen in the mass spectra of the individually analyzed steroids in Figure 4-8).

An estimate of the improvement in sensitivity can be determined by comparing the response factors for the underivatized steroid before (Table 4-4) and after (Table 4-5) optimization. An average improvement in sensitivity of approximately 4 times was gained by optimization of the GC/MS parameters.

Precision and limit of detection. The reproducibility of the short-column GC/MS method was determined by making ten replicate injections of the individual steroids and ten injections of a mixture of all six steroids. Table 4-5 shows the results obtained at the helium inlet pressures determined both for optimum sensitivity, 2 psi, and for maximum chromatographic selectivity, 6 psi. It is evident from these data that injection reproducibilities (%relative standard deviation, %RSD) range from approximately 3% to 30% without an internal standard and generally are poorer for compounds with longer elution times (compounds listed in order of elution in Table 4-5). Also tabulated are average response factors, expressed as the average peak area of the $M^{+\cdot}$ ion per nanogram of steroid injected, and average % RIC corresponding to the $M^{+\cdot}$ ion. The higher sensitivity at the lower column inlet pressure is reflected in the higher absolute response factors for all steroids at 2 psi. The degree of fragmentation of the compounds, as reflected in the % RIC carried by the molecular ion, is relatively unaffected by the column inlet

pressure or the presence of other steroids in the mixture; however, the sensitivity is directly affected by these factors.

A calibration curve for methyltestosterone by short-column GC/MS with full scan mass spectra obtained at a column inlet pressure of 2 psi and using temperature programming is shown in Figure 4-9. A linear dynamic range of approximately two and a half orders of magnitude was obtained. Deviation from linearity at higher concentrations was due to the steroid undergoing self-CI (m/z 302 becomes m/z 303 for methyltestosterone). An estimate of the limit of detection, LOD, based on the average GC peak area of the $M^{+\cdot}$ ion using triplicate injections, is in the low-nanogram range, with a signal-to-noise ratio of approximately 5:1. Literature LODs using full scan mass spectra also report low nanogram detection limits for the steroid stanozolol (99). A lower LOD would be expected if selected ion monitoring were employed rather than full scan; better precision and accuracy could be obtained by use of an internal standard.

Conclusions

Considering only sensitivity, optimum conditions are achieved at low column inlet pressures using temperature programming and splitless injection with a splitless period of approximately 0.5 minutes. Maximum sensitivity could be obtained by using subambient inlet pressures and 40 eV electron ionization. The best chromatographic resolution is obtained at a column inlet pressure of 6 psi using a

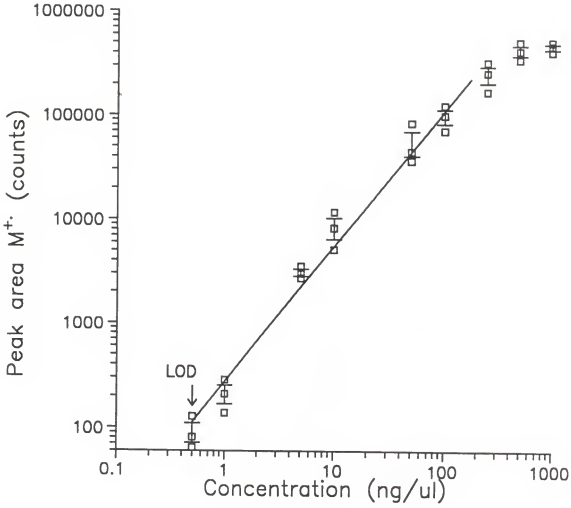

Figure 4-9: Calibration curve for methyltestosterone by short-column GC/MS (full scan). The slope of the log-log plot is equal to 1.24, not including the curvature at high concentrations where the steroid undergoes self-chemical ionization (m/z 302 going to m/z 303).

temperature program and splitless injection. Under these conditions there is minimal solvent tailing and the sharpest peaks are produced. The shortest retention times, when considering speed of analysis, were achieved at a column inlet pressure of 6-10 psi operating the column isothermally at 205 °C. Based on the above statements, it is evident that optimum conditions for all the criteria (sensitivity, chromatographic integrity, and speed of analysis) cannot be obtained under the same short-column GC/MS conditions. Therefore, it is clear that certain compromises must be made depending on which of the criteria are most important to an analysis.

These studies have also shown that the direct determination of underivatized anabolic steroids by short-column GC/MS is a potential alternative to derivatization GC/MS methods and other MS (FAB, LD, LC) methods that are used to determine underivatized steroids directly. The elimination of the derivatization procedure shortens the analysis time significantly, as does the rapid analysis times that are achievable using short-columns as compared to conventional-length columns. The recommended experimental conditions for the determination of underivatized steroids by short-column GC/MS were summarized in Table 4-1. These results indicate the need to optimize conditions to maximize sensitivity, selectivity, and speed of analysis of short-column GC/MS methods.

The major limitation found in short-column GC/MS is the limited chromatographic resolution, making the separation of complex mixtures more difficult. Chapter 5 will focus on developing short-column GC strategies in conjunction with tandem mass spectrometry (MS/MS) to compensate for the loss in

chromatographic selectivity inherent in short-column techniques. To increase the sensitivity and selectivity of the method and to simplify the resulting mass spectra, GC/MS/MS strategies involving chemical ionization will be presented in more detail. The feasibility and potential of short-column GC/MS/MS strategies for the screening of anabolic steroids in biological matrices will be presented in Chapter 6.

CHAPTER 5

OPTIMIZATION OF A GC/MS/MS METHOD BASED ON SELECTIVITY AND SENSITIVITY FOR THE DETERMINATION OF UNDERIVATIZED ANABOLIC STEROIDS

Introduction

Tandem mass spectrometric (MS/MS) methods for the determination of steroids have been reported previously in the literature (100-105). These include LC/MS/MS methods for the determination of several anabolic and estrogen steroids, metabolites, and conjugates (100-102) and the determination of other steroid conjugates by FAB/MS/MS (103,104). Trace analysis of oestradiol by GC/MS/MS using a tert-butyldimethylsilyl ether derivative has also been reported (105). The common feature of these reports is the use of tandem mass spectrometry to increase the selectivity of the analysis and to increase the structural information. These reports also indicate sub-nanogram quantitation capabilities and the potential for rapid screening of steroids in complex biological samples. Another key feature of the reported LC and FAB methods is the ability to analyze steroid conjugates directly, thereby reducing sample preparation time.

In this chapter, a complementary screening/confirmation method is described based upon short-column GC/MS/MS for the determination of underivatized anabolic steroids. The ability to handle steroids underivatized with short GC columns was demonstrated in Chapter 4. Short-column GC/MS, however, suffers from limited selectivity necessitating the use of MS/MS detection. Therefore, to develop a screening and/or confirmation method for the determination of underivatized anabolic steroids by short-column GC/MS/MS, ionization and collisionally activated dissociation (CAD) conditions for each of the steroids must be characterized and optimized. For trace analysis of mixtures, the production of a minimum number of ions by the ionization method is desired. In addition, it also is desirable that the CAD process produce abundant characteristic daughter ions. Under optimized conditions, the feasibility of short-column GC/MS/MS as a rapid, sensitive, and selective screening method can then be evaluated.

Experimental

Steroids and Reagents

The anabolic steroids 19-nortestosterone, dehydrotestosterone, testosterone, methyltestosterone, stanozolol, and oxymetholone were all purchased from Fisher Scientific; their structures were shown previously in Figure 4-1. Reagent grade methylene chloride (Fisher Scientific) was used as the solvent for the GC samples. Commercial grade helium (Liquid Air Corp.) was used as the GC carrier gas. High

purity methane (Matheson) was used as the chemical ionization reagent gas. Commercial grade nitrogen (Liquid Air Corp.) and argon (Matheson) were used as collision gases in the MS/MS experiments.

Sample Introduction

Optimization of tandem mass spectrometric parameters was performed on individual steroid samples introduced within capped aluminum vials using a solids probe. The solids probe was programmed to and then maintained at 150 °C; at this temperature a constant rate of sample vaporization was produced for several minutes. Gas chromatographic introduction was carried out on a J&W Scientific DB-5 capillary column (4 m, 0.25 mm i.d., 0.25 μm film thickness). A temperature program was used starting at an initial column temperature of 150 °C and then programming to a final temperature of 250 °C at a rate of 20 °C/minute. The GC injection port, interface and transfer line temperatures were all 250 °C. Typically, injections were made in the splitless injection mode using a column inlet pressure of 2 psi.

Mass Spectrometry

All experiments were performed on a Finnigan MAT TSQ45 gas chromatograph/triple quadrupole mass spectrometer. Mass spectrometric conditions were ionizer temperature of 190 °C (EI) or 150 °C (CI), electron energy of 70 eV (EI) or 100 eV (CI), emission current of 0.3 mA, and preamp gain of 10^8 V/A. The

chemical ionization reagent gas pressure was optimized by varying the methane pressure over the range of 0.1 to 2 torr. Full scan mass spectra were acquired from 41 to 375 u in 0.55 s for EI and 60 to 375 u in 0.55 s for CI. Selected ion monitoring experiments were set-up by monitoring 3 ions per compound, scanning each ion over a 1 u window at a rate of 0.10 s per ion per scan.

In the MS/MS experiments, collision gas pressure and collision energy were optimized for each of the six anabolic steroids. Nitrogen, for CAD of M^+ parent ions formed by EI, and argon, for $(M+H)^+$ and $(M-H)^-$ parent ions formed by CI, collision gas pressures were optimized over the pressure range of 0 to 4 mtorr at constant collision energies for M^+ ions of 26.9 eV (met and dehyt), 22.0 eV (stan), 29.0 (oxym), and 24.8 (test and nort), and for $(M+H)^+$ ions of 14.6 eV (nort, dehyt, test, and met) and 27.8 (stan and oxym), and for $(M-H)^-$ ions of 27.2 eV (all steroids). The collision energy was optimized over the range of 0 to 30 eV at a constant nitrogen collision gas pressure of 1.0 mtorr for M^+ ions, and at argon collision gas pressures of 2.5 mtorr for $(M+H)^+$ ions and 4.0 mtorr for $(M-H)^-$ ions; note that the highest collision energy possible on the TSQ45 is 30 eV. Full sca daughter spectra for all the compounds were acquired over the mass range 33 - 351 u for M^+ ions and 59 - 376 u for $(M+H)^+$ and $(M-H)^-$ ions. Selected reaction monitoring experiments were set-up on the basis of retention time for each of the six steroids of interest. Three ions per compound (the parent ion and the two most abundant daughter ions) were monitored by scanning each ion over a 1 u window at

a scan rate of 0.10 s per ion per scan. Tables 5-1 and 5-2 list the selected fragment and daughter ions monitored by SIM and SRM for the studies comparing EI and CI sensitivities.

Results and Discussion

High sensitivity and selectivity are essential to trace analytical schemes, as are rapid analysis capabilities when numerous samples must be analyzed. These factors can be optimized in GC/MS/MS strategies by maximizing the chromatographic separation, the intensity of the selected parent ion (typically the molecular ion), and the efficiency of the CAD process for the selected reaction. Optimization of the chromatographic separation was discussed in Chapter 4; these conditions will be used in the remaining experiments. The intensity of the molecular ion and the extent of fragmentation will be characterized for three different ionization methods, electron ionization (EI), positive ion chemical ionization (PCI), and negative ion chemical ionization (NCI). In addition, determination of the efficiency of the CAD process for each of the molecular ions was performed. Optimization of MS/MS conditions can result in improved sensitivity and selectivity and the potential for rapid screening or confirmation capabilities.

Table 5-1: Ions monitored by SIM

	molecular ions			selected fragment ions		
	M^+	$(M+H)^+$	$(M-H)^-$			
steroid	EI	PCI	NCI	EI	PCI	NCI
nortestosterone	274*	275*	273*	110,215	257,303	235,274
dehydrotestosterone	286	287*	285*	122*,123	269,273	216,286
testosterone	288*	289*	287*	124,246	271,317	235,288
methyltestosterone	302*	303*	301*	124,229	285,331	127,302
stanozolol	328*	329*	327*	96,270	311,357	127,328
oxymetholone	332*	333*	331	174,216	315,361	314*,332

* indicates ions employed for quantitation

Table 5-2: Ions monitored by SRM

	molecular ions			selected daughter ions		
	M^+	$(M+H)^+$	$(M-H)^-$			
steroid	EI	PCI	NCI	EI	PCI	NCI
nortestosterone	274	275	273	110,215*	109*,257	215,271*
dehydrotestosterone	286	287	285	107,122*	121*,135	229*,269
testosterone	288	289	287	109,124*	97,109*	229,285*
methyltestosterone	302	303	301	124,229*	97,109*	285*,299
stanozolol	328	329	327	96*,270	95,121*	309,311*
oxymetholone	332	333	331	174*,216	99*,107	315,316*

* indicates ion employed for quantitation

Selection of Ionization Method

The selection of an appropriate ionization method depends on the type of analysis desired: for structural information electron ionization is used due to the abundance of fragment ions produced. For trace and quantitative analyses, in contrast, chemical ionization generally is preferred since it produces a minimum number of more abundant ions per compound. Most commonly, methane, isobutane, or ammonia is used as the chemical ionization reagent gas. For chemical ionization studies of the six anabolic steroids, methane was used as the CI reagent gas. Although not studied, it should be noted that additional selectivity and/or sensitivity may be gained by use of a different reagent gas. The use of ammonia (with a relatively high proton affinity, 207 kcal/mole, as compared to 127 kcal/mole for methane) (98), for example, can be used to selectively ionize nitrogen-containing compounds (also with high proton affinities), and may have been a better choice for steroids such as stanozolol.

Reagent gas pressure study. Both PCI and NCI methods were studied for each of the six anabolic steroids shown in Figure 4-1. With a constant amount of steroid being introduced into the ion source from a capped aluminum vial on the solids probe, reagent gas pressure was varied and its effect on the intensity of the analyte ions of interest was determined. As shown in Figure 5-1a, the intensity of each of the protonated molecules, $(M+H)^+$, increased from the lowest pressure studied (0.1 torr) and maximized between 0.2 and 0.4 torr. As the reagent gas

Figure 5-1: Reagent gas pressure optimization studies using methane as the reagent gas for (a) positive ion chemical ionization and (b) negative ion chemical ionization. Note that absolute intensities among the different steroids cannot be compared as different quantities of steroid were used and rates of sample volatilization were not the same.

(a)

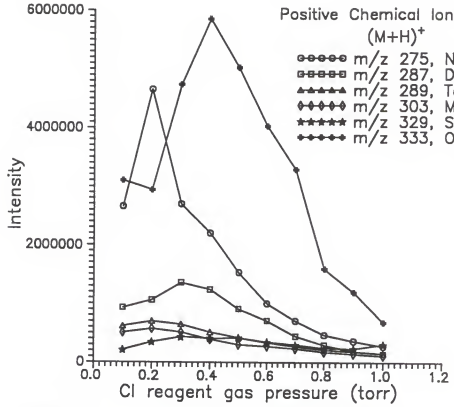
Positive Chemical Ionization
(M+H)+
m/z 275, Nort
m/z 287, Dehyt
m/z 289, Test
m/z 303, Met
m/z 329, Stan
m/z 333, Oxym
Intensity
6000000
4000000
2000000
0
0.0
0.2
0.4
0.6
0.8
1.0
1.2
CI reagent gas pressure (torr)

(b)

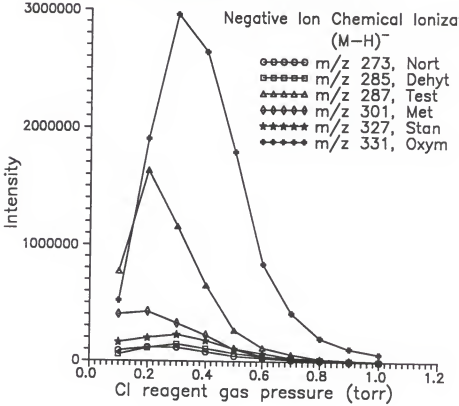
Negative Ion Chemical Ionization
(M−H)−
m/z 273, Nort
m/z 285, Dehyt
m/z 287, Test
m/z 301, Met
m/z 327, Stan
m/z 331, Oxym
Intensity
3000000
2000000
1000000
0
0.0
0.2
0.4
0.6
0.8
1.0
1.2
CI reagent gas pressure (torr)

pressure was increased further, a decrease in the intensity of the protonated molecular ions was observed. This is probably due to decreased transmission efficiency through the ion optics and first quadrupole as a function of increasing pressure. For the analysis of a mixture of steroids, a compromise in reagent gas pressure (approximately 0.25 torr) was chosen and used in subsequent PCI studies. As seen in Figure 5-1b, a similar behavior was observed for the $(M-H)^-$ ions produced by NCI for each of the steroids. For NCI, maximum intensities were between 0.2 and 0.3 torr and a compromise of 0.25 torr was chosen for subsequent mixture analysis studies. Although these pressures are lower than those typically suggested, the optimum pressures coincide with the maximum production (at 0.2 torr) of the methane reagent gas ion at m/z 17.

Extent of fragmentation. The extent of fragmentation, as estimated by the intensity of the molecular-type ions, affects the sensitivity and selectivity of an analysis; this can be estimated by comparing the percentage of the reconstructed ion current (% RIC) carried by the molecular-type ions for each of the ionization methods. The % RIC for the M^+, $(M+H)^+$, and $(M-H)^-$ ions for EI, PCI, and NCI, respectively, are summarized in Table 5-3; note that EI, PCI, and NCI spectra for each of these compounds are presented in the Appendix. From these data, it is evident that the extent of fragmentation is much greater for EI than for either PCI or NCI, as anticipated. Electron ionization results in extensive fragmentation for these compounds resulting in a peak at every mass in the mass spectra. The PCI

Table 5-3: Comparison of the extent of fragmentation as a function of ionization method

ionization method	% RIC molecular ion[a]					
	Nort	Dehyt	Test	Met	Stan	Oxym
EI[b]	6	1	3	5	5	2
PCI[c]	40	32	43	40	32	44
NCI[c]	88	41	71	55	59	30

[a] for normal Q1 MS
[b] data from GC/MS runs of individual steroids samples
[c] data from solids probe runs of individual steroid samples

mass spectra are much simpler having only an ion corresponding to the loss of water $(M+H - H_2O)^+$ and adduct ions (common to methane PCI) corresponding to $(M+29)^+$ and $(M+41)^+$ for the majority of the steroids studied. The NCI mass spectra typically showed one highly abundant characteristic ion corresponding to the abstraction of a proton, $(M-H)^-$. For stanozolol, methyltestosterone, and dehydrotestosterone, the % RIC $(M-H)^-$ was slightly lower than for nortestosterone and testosterone due to the presence of a few low abundance fragment ions. For oxymetholone, a second ion corresponding to $(M-2H)^-$ and an abundant fragment ion corresponding to loss of an OH group was present resulting in the much lower %RIC for the $(M-H)^-$ ion for this compound as compared to the other steroids.

The production of only one or two characteristic ions per compound by chemical ionization is advantageous for two reasons. Firstly, an increase in sensitivity can be achieved when monitoring a single characteristic molecular ion. Secondly, since the number of fragment ions produced by the compound or from other components in the matrix is reduced under CI conditions, the possibility of spectral interference is reduced and the selectivity may therefore be increased. These two figures of merit, sensitivity and selectivity, will be discussed further in a later section.

Optimization of MS/MS Conditions

The overall efficiency of the MS/MS process can be evaluated by determining the individual fragmentation, collection and CAD efficiencies. These efficiencies can be calculated using the following equations (106):

$$E_f = \Sigma D_i / (P + \Sigma D_i) \quad (5\text{-}1)$$

$$E_c = (P + \Sigma D_i) / P_0 \quad (5\text{-}2)$$

$$E_{CAD} = \Sigma D_i / P_0 \quad (5\text{-}3)$$

where, E_f is the fragmentation efficiency, E_c is the collection efficiency, E_{CAD} is the overall CAD efficiency, and D_i, P, and P_0 are the intensities of the daughter ions resulting from CAD, the parent ion remaining after CAD, and the parent ion prior to CAD, respectively.

The fragmentation efficiency is used to determine the fraction of ions present after CAD which are daughter ions. The fraction of the initial parent ion that remains following CAD and is collected as either intact parent or daughter ions determines the collection efficiency. The overall CAD efficiency is the fraction of the original parent ion that is converted into daughter ions and is equal to $E_f \times E_c$. These efficiencies are used to monitor the processes of fragmentation and scattering as they ultimately determine the level of sensitivity obtainable by MS/MS.

Collision gas pressure and collision energy are the two most commonly used parameters for maximizing the CAD efficiency for a particular parent ion. As collision gas pressure and collision energy increase, fragmentation efficiency also increases; this results in a reduction in the relative abundance of the parent ion and an increase in the abundance of the daughter ions. While fragmentation efficiency increases with increasing collision gas pressure and energy, collection efficiency

begins to decrease due to an increase in scattering losses. In general, for most compounds, a decrease in overall CAD efficiency will be observed at higher collision gas pressures and energies. Since MS/MS efficiencies are affected by both collision energy and collision gas pressure, each of these parameters will be optimized to maximize the CAD efficiency for a particular parent ion to form all daughter ions (full scan MS/MS) and to form a selected daughter ion (selected reaction monitoring). In addition, MS/MS efficiencies were determined for each of the molecular-type ions and steroids of interest.

Collision gas pressure studies. Both nitrogen and argon were used in the collision gas pressure studies. Nitrogen was used with electron ionization since the M^+ ions of these steroids were fragmented easily. Initially, nitrogen was used also as the collision gas for CI. However, with nitrogen little fragmentation was observed for the $(M+H)^+$ or $(M-H)^-$ ions, even at high collision gas pressures (e.g. 3 mtorr). Subsequently, argon was used with CI since the molecular ions produced by CI were more difficult to fragment. In the case of argon, the greater mass of the argon gas molecules, compared to nitrogen, increases the energy deposited into the parent ion and increases the fragmentation as a result. With increasing collision gas pressures, fragmentation efficiency also increases since the number of collisions an ion experiences will be greater.

MS/MS efficiencies for each of the steroids and molecular-type ions are tabulated in Table 5-4 as a function of collision gas pressure. Figure 5-2 depicts typical efficiency and pressure-resolved breakdown curves for PCI-CAD of the compound methyltestosterone. These efficiencies have been calculated with respect to all daughter ions (selected reaction monitoring efficiencies will be discussed in a later section). For all six steroids as shown in Table 5-4, CAD of M^+ ions resulted in the highest fragmentation, collection, and overall CAD efficiencies and the most structural information. Optimum nitrogen collision gas pressures ranged from 1 to 3 mtorr and resulted in CAD efficiencies from 35 to 100% for the M^+ ions. Note that in some cases, collection efficiencies of $\geq$ 100% were observed , presumably due to a "buffer gas" effect. In contrast to EI-CAD, fewer daughter ions were produced by PCI-CAD or NCI-CAD, suggesting the greater stability of the CI molecular-type ions under the conditions studied. As can be seen in Figure 5-2a, even at the highest collision gas pressures studied, the efficiency of fragmentation for PCI-CAD of methyltestosterone was still only around 75%. In the pressure-resolved breakdown curve, Figure 5-2b, this is evident in that the parent ion is still more abundant (higher %RIC) than the individual daughter ions. For PCI-CAD, optimum argon collision gas pressures ranged from 2 to 3 mtorr and produced CAD efficiencies of only 7 to 53%. Optimum argon pressures (1 to 3 mtorr) for NCI-CAD resulted in efficiencies of 4 to 29%. Overall, the $(M+H)^+$ and $(M-H)^-$ ions produced by methane CI are more stable towards CAD and are not as efficiently fragmented as are the M^+ ions produced by EI. In fact, NCI-CAD conditions were

Table 5-4: Optimization of MS/MS efficiencies as a function of collision gas pressure

efficiency/ *optimum	ionization method	parent ion	Nort	Dehyt	Test	Met	Stan	Oxym
E_f (%)	EI	M^+	100	98	100	83	100	100
E_c (%)			45	100	66	42	140	61
E_{CAD} (%)			45	98	66	35	140	61
CE (eV)			24.8	26.9	24.8	26.9	22.0	29.0
*N_2 (mtorr)			3	1	3	1	3	2.5
E_f (%)	PCI	$(M+H)^+$	62	93	64	72	30	81
E_c (%)			58	57	48	40	22	16
E_{CAD} (%)			36	53	31	29	7	13
CE (eV)			14.6	14.6	14.6	14.6	27.8	27.8
*Ar (mtorr)			2	2	2	3	3	2
E_f (%)	NCI	$(M-H)^-$	60	92	61	40	19	21
E_c (%)			28	32	28	22	65	21
E_{CAD} (%)			17	29	17	9	12	4
CE (eV)			27.2	27.2	27.2	27.2	27.2	27.2
*Ar (mtorr)			3	3	3	3	3	1

Figure 5-2: PCI-CAD curves for the $(M+H)^+$ ion of methyltestosterone depicting (a) fragmentation, collection, and CAD efficiencies and (b) pressure-resolved breakdown of the parent and selected daughter ions as a function of argon collision gas pressure at a constant collision energy of 14.6 eV.

(a)

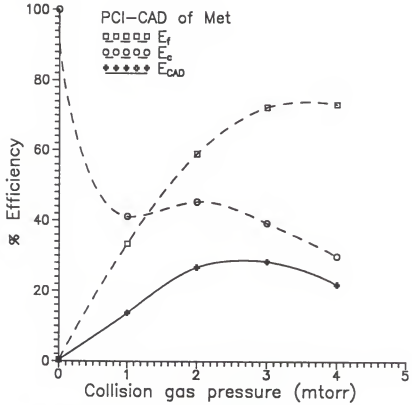
PCI–CAD of Met
E_f
E_o
E_{CAD}
% Efficiency
Collision gas pressure (mtorr)

(b)

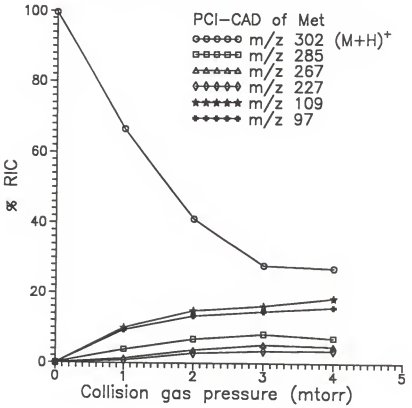
PCI–CAD of Met
m/z 302 $(M+H)^+$
m/z 285
m/z 267
m/z 227
m/z 109
m/z 97
% RIC
Collision gas pressure (mtorr)

the harshest and still produced the lowest fragmentation and overall CAD efficiencies for the majority of the steroids studied.

Collision energy studies. Collision energy is another parameter that can be used to maximize the CAD efficiency for a particular parent ion where increasing collision energies result in more energetic collisions and increasing fragmentation efficiency. Optimization of collision energy for each of the steroids and molecular-type ions is shown in Table 5-5. Figure 5-3 depicts efficiency and energy-resolved breakdown curves for methyltestosterone as a function of collision energy under PCI-CAD conditions. For methyltestosterone, approximately 100% fragmentation efficiency was achieved for the $(M+H)^+$ ion at collision energies > 20 eV, as shown in Figure 5-3a. In Figure 5-3b, it is evident that at these higher collision energies, the parent ion is almost totally replaced by the two most abundant daughter ions. For the majority of the steroids shown in Table 5-5, electron ionization, however, again resulted in the highest fragmentation, collection, and CAD efficiencies. Optimum collision energies ranged from 9 to 29 eV (EI), 14 to 27 eV (PCI), and 17 to 24 eV (NCI). CAD efficiencies ranged from 26 to 94% (EI), 10 to 40% (PCI), and 2 to 15% (NCI). Based on these data, EI-CAD would appear to be the best analytical method for screening of these steroids as it is the most efficient at CAD and yields the most structural information. Other factors, however, influence the choice of analytical method for anabolic steroid screening, as will be discussed further in the following sections.

Table 5-5: Optimization of MS/MS efficiencies as a function of collision energy

efficiency/ *optimum	ionization method	parent ion	Nort	Dehyt	Test	Met	Stan	Oxym
E_f (%)	EI	M^+	85	94	82	89	92	93
E_c (%)			31	100	61	43	100	49
E_{CAD} (%)			26	94	50	38	92	46
N_2 (mtorr)			1.0	1.0	1.0	1.0	1.0	1.0
*CE (eV)			29	9	17	24	29	24
E_f (%)	PCI	$(M+H)^+$	60	99	97	97	41	34
E_c (%)			18	40	27	27	36	30
E_{CAD} (%)			11	40	26	26	15	10
Ar (mtorr)			2.5	2.5	2.5	2.5	2.5	2.5
*CE (eV)			17	14	22	22	27	24
E_f (%)	NCI	$(M-H)^-$	32	72	43	25	14	21
E_c (%)			48	20	22	19	31	12
E_{CAD} (%)			15	14	9	5	4	2
Ar (mtorr)			4.0	4.0	4.0	4.0	4.0	4.0
*CE (eV)			22	19	19	19	17	24

Figure 5-3: PCI-CAD curves for the $(M+H)^+$ ion of methyltestosterone depicting (a) fragmentation, collection, and CAD efficiencies and (b) energy-resolved breakdown of the parent and selected daughter ions as a function of collision energy and at a constant argon collision gas pressure of 2.5 mtorr.

(a)

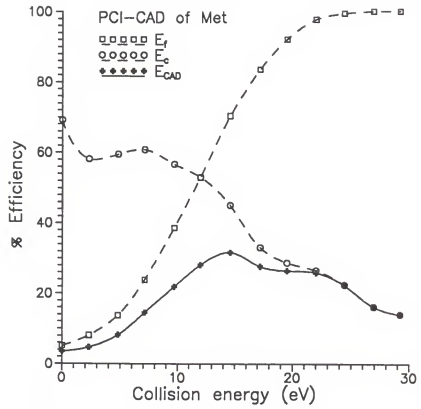
PCI–CAD of Met
E_f
E_c
E_{CAD}
% Efficiency
Collision energy (eV)

(b)

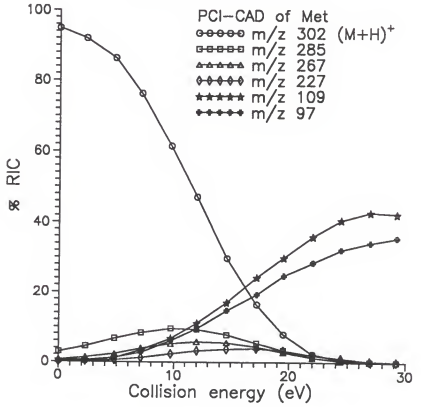
PCI–CAD of Met
m/z 302 $(M+H)^+$
m/z 285
m/z 267
m/z 227
m/z 109
m/z 97
% RIC
Collision energy (eV)

Evaluation of daughter mass spectra. For screening purposes, common daughter ions and characteristic neutral losses can be used as an advantage. If the analytes of interest have common daughter ions, then these specific ions can be monitored using parent scans for identification purposes. In the parent scan mode, Q1 is scanned over a mass range including the parent ions of interest, while Q3 is set to transmit only the selected daughter ion produced in Q2. The fewer ions that are monitored, the better the analytical signal will be since the dwell time per ion is increased. In addition, if several of the analytes of interest lose a common functional group, neutral loss spectra can be utilized. In the neutral loss scan mode, both Q1 and Q3 are scanned with a specific mass difference between them corresponding to the characteristic neutral loss. In any case, common ions make screening of targeted classes of compounds more efficient. The most abundant daughters ions for full scan MS/MS of the six structurally-related anabolic steroids have been tabulated in Table 5-6 (EI), 5-7 (PCI), and 5-8 (NCI); mass spectra for these compounds can be examined in the Appendix. The common neutral loss for these compounds in the normal MS mode is water and/or a methyl group. These ions (indicated by $^{\circ}$ for loss of water and $^{+}$ for loss of a methyl group in Tables 5-5, 5-6, and 5-7) tend to be of relatively low abundance in the MS/MS scan mode, however, and would not be good choices for neutral loss monitoring due to poor sensitivity. Furthermore, these ions carry little structural information, since the loss of H_2O and CH_3 are fairly common.

Table 5-6: EI-CAD daughter ions

steroid	M^+	daughter ions[a]			
nortestosterone[b]	274 (5)	215 (67)	160 (15)	148 (21)	147 (14)
		146 (15)	133 (16)	131 (14)	110 (100)
		109 (59)	72 (18)		
dehydrotestosterone[c]	286 (.2)	147 (2)	134 (1)	122 (100)	121 (2)
		119 (1)	110 (1)	109 (1)	108 (1)
		107 (10)	105 (1)		
testosterone[b]	288 (1)	273 (2)[+]	246 (2)	147 (8)	146 (3)
		131 (2)	124 (100)	123 (6)	110 (7)
		109 (23)	96 (2)		
methyltestosterone[c]	302 (1)	229 (100)	161 (5)	135 (3)	124 (23)
		123 (3)	122 (7)	121 (5)	109 (6)
		97 (8)	95 (4)		
stanozolol[d]	328 (.5)	271 (3)	215 (3)	175 (6)	159 (4)
		148 (5)	147 (3)	146 (3)	135 (5)
		96 (100)	94 (25)		
oxymetholone[e]	332 (2)	216 (36)	176 (77)	175 (26)	174 (100)
		172 (61)	161 (49)	159 (52)	150 (45)
		100 (26)	85 (24)		

[a] ten most intense daughter ions with % relative abundance ( ) > 1%
[b] collision energy 24.8 eV, collision gas pressure 2.0 mtorr N_2
[c] collision energy 26.9 eV, collision gas pressure 2.0 mtorr N_2
[d] collision energy 22.0 eV, collision gas pressure 2.0 mtorr N_2
[e] collision energy 29.0 eV, collision gas pressure 2.0 mtorr N_2
[+] indicates the loss of a methyl group, $(M\text{-}CH_3)^+$

Table 5-7: PCI-CAD daughter ions

steroid	$(M+H)^+$	daughter ions[a]			
nortestosterone[b]	275 (100)	257 (35)*	239 (31)	199 (12)	187 (9)
		185 (7)	161 (6)	147 (7)	145 (11)
		135 (7)	109 (18)		
dehydrotestosterone[b]	287 (14)	269 (9)*	187 (4)	179 (5)	173 (22)
		161 (6)	159 (3)	149 (6)	147 (14)
		135 (55)	121 (100)		
testosterone[b]	289 (100)	271 (10)*	253 (15)	213 (3)	187 (2)
		175 (2)	159 (2)	147 (2)	123 (5)
		109 (74)	97 (80)		
methyltestosterone[b]	303 (100)	285 (30)*	267 (19)	245 (4)	227 (12)
		211 (5)	189 (13)	177 (9)	121 (5)
		109 (58)	97 (53)		
stanozolol[c]	329 (100)	149 (2)	147 (1)	135 (2)	133 (1)
		121 (6)	119 (1)	109 (3)	107 (4)
		95 (5)	81 (5)		
oxymetholone[c]	333 (100)	159 (14)	145 (12)	133 (12)	121 (14)
		119 (15)	109 (11)	107 (24)	105 (16)
		99 (41)	95 (11)		

[a] ten most intense daughter ions with % relative abundance ( ) > 1%
[b] collision energy 14.6 eV, collision gas pressure 3.0 mtorr Ar
[c] collision energy 27.8 eV, collision gas pressure 3.0 mtorr Ar
* indicates the loss of water, $(M+H - H_2O)^+$

Table 5-8: NCI-CAD daughters ions

steroid[a]	$(M-H)^-$	daughter ions[b]			
nortestosterone	273 (85)	271 (100)	269 (16)	215 (6)	213 (1)
dehydrotestosterone	285 (18)	283 (18) 267 (8)* 120 (8)	270 (8)$^+$ 255 (1)	269(100) 229 (26)	268 (2) 171 (2)
testosterone	287 (89)	285 (100) 259 (3) 123 (3)	283 (8) 257 (2)	271 (2) 231 (4)	269 (3)* 213 (1)
methyltestosterone	301 (100)	299 (6) 271 (1) 123 (1)	285 (35) 257 (1)	283 (4)* 231 (4)	273 (2) 229 (2)
stanozolol	327 (100)	311 (17)	309 (4)*	295 (1)	
oxymetholone	331 (100)	316 (44)$^+$	315 (3)		

[a] collision energy 27.2 eV, collision gas pressure 3.0 mtorr Ar
[b] ten most intense daughter ions with % relative abundance ( ) > 1%
* indicates the loss of water, $(M-H - H_2O)^-$
$^+$ indicates the loss of a methyl group, $(M-H - CH_3)^-$

For the EI-CAD data, common daughter ions include m/z 147 and m/z 109 or 110 for four of the six steroids and m/z 122 or 124 for three of the six steroids. Unfortunately, neither stanozolol or oxymetholone would be detected if only these ions were monitored due to their dissimilar structure. Common ions in PCI-CAD, in contrast, include m/z 95, m/z 97, m/z 109, m/z 121, and m/z 135. In this mode, all six steroids contain at least two of the above daughter ions. In most cases, these ions are also of high enough abundance not to limit sensitivity. For NCI-CAD, the least number of common ions were available. As in EI-CAD, stanozolol and oxymetholone would not be detected if the common ions at m/z 285, m/z 283, and m/z 269 were monitored for NCI-CAD.

Although not discussed in this chapter, parent scans using PCI-CAD may be an alternative method for screening of anabolic steroids in complex matrices. The limiting factor in this analytical scheme would be the varying relative intensities of the common daughter ions monitored for each of the different compounds. Even though the sensitivity may be adequate for certain compounds, it may limit the detection of others.

Selectivity and Sensitivity

A variety of methods can be used to increase selectivity and sensitivity for trace analytical work. A summary of these methods was given in Table 1-2. Sample cleanup and chromatographic separation were two of the methods listed for increasing selectivity and, potentially, sensitivity. Sample preparation schemes

attempt to remove contaminants prior to analysis and to preconcentrate the analyte(s) of interest. Selective derivatization can also be used to increase the stability, volatility, and detection sensitivity for certain biologically significant compounds. Chromatographic separation is used to separate the analyte(s) from the chemical background/matrix while serving as an introduction method for mass spectrometric detection. This maximizes the concentration of the analyte at the detector resulting in improved detection limits. Unfortunately, both these methods result in significantly increased analysis times.

As stated previously, CI methods can be used to enhance sensitivity and selectivity by the production of an intense molecular ion and by reducing the fragmentation of the molecule after ionization and the possibility of spectral interference. Tandem mass spectrometric methods also can be used to increase selectivity and improve the signal-to-noise ratio with rapid analysis capabilities. Separation of the analyte(s) and interferents is performed mass spectrometrically by selecting the analyte ion of interest with the first quadrupole, collisionally dissociating the parent ion in the second quadrupole to produce daughter ions, and mass analyzing the daughter ions in the third quadrupole. Thus, for a contaminant to interfere in this method, it must have the same parent ion as the analyte and must produce the same daughter ions after CAD. The MS/MS sensitivity can be increased by monitoring only selected daughter ions in Q3, thus maximizing the analytical signal. GC/MS/MS strategies using selected reaction monitoring are discussed below. A comparison of selectivity and sensitivity is given for full scan GC/MS, selected ion

monitoring GC/MS, and selected reaction monitoring GC/MS/MS for EI, PCI, and NCI ionization methods.

Full scan. Figures 5-4 and 5-5 show the sensitivity and selectivity that result from normal full scan GC/MS for the six underivatized anabolic steroids. In Figure 5-4, the peak areas of the molecular-type ions (EI M^+ ion, PCI $(M+H)^+$ ion, NCI $(M-H)^-$ ion) were used as an indication of sensitivity for each of the steroids, except for the EI data for dehydrotestosterone in which case m/z 122 was used and the NCI data for oxymetholone where m/z 330 was used. These ions, in all cases, were the base peak (100% relative abundance) in their respective mass spectra under the conditions used in this study. From this figure it is evident that the sensitivity of the analyte ions produced by PCI are greater than both the EI and NCI ions for the majority of the steroids studied. The sensitivity, estimated as the average peak area of analyte ion, for PCI is shown to be greater by a factor of approximately 4 to 40 times that of EI and NCI depending on the individual steroid. In the case of EI, the lower sensitivity may be the result of the ease of fragmentation of the M^+ ions under EI conditions. The lower sensitivity for NCI may be the result of poor production of negative ions from this class of compounds.

In Figure 5-5, the degree of selectivity for full scan GC/MS can be seen in the mass spectra for dehydrotestosterone. This compound was chosen as an example since it is separated on the short GC column with the least chromatographic resolution; e.g. it is chromatographically unresolved from methyltestosterone. This

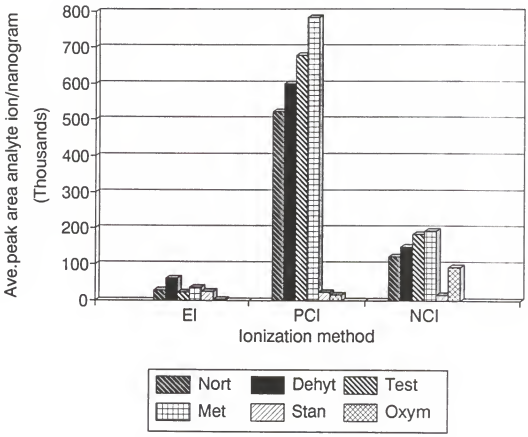

Figure 5-4: Determination of EI, PCI, and NCI sensitivities for full scan GC/MS for each of the six underivatized anabolic steroid molecular-type ions; note that the fragment ion at m/z 122 was used in place of M^+ ion for dehydrotestosterone and the fragment ion at m/z 330 was used in place of the $(M\text{-}H)^-$ ion for oxymetholone.

Figure 5-5: Mass spectra of dehydrotestosterone under (a) EI, (b) PCI, and (c) NCI full scan GC/MS conditions.

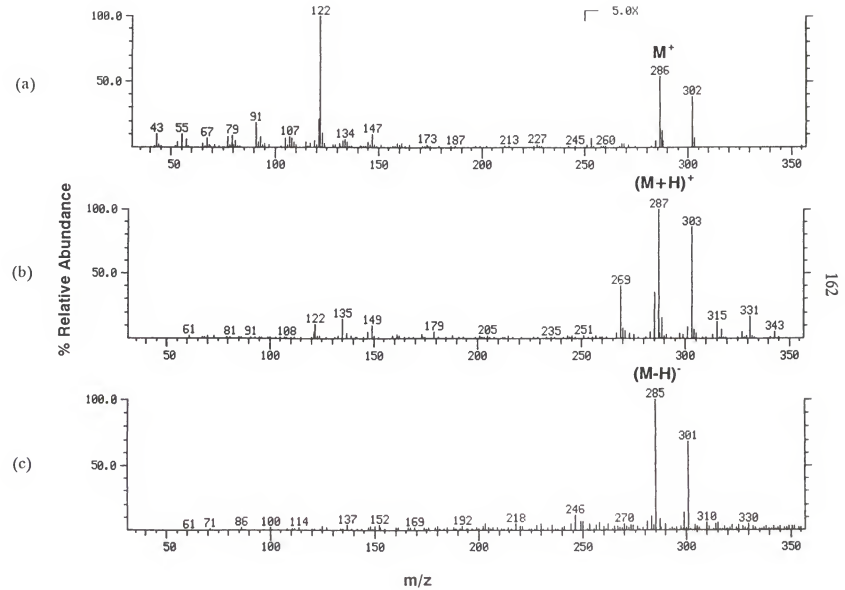
(a)
(b)
(c)
% Relative Abundance
m/z
M+
(M+H)+
(M-H)-
5.0X
122
286
302
287
303
269
285
301
246
162

is evident by the large molecular ion peak (m/z 302, EI) from the overlapping chromatographic peak for methyltestosterone. Identification of dehydrotestosterone, molecular ion at m/z 286 (EI), from these spectra could be difficult, especially if a library search routine were employed due to the presence of the higher molecular weight ion from methyltestosterone. The adduct ions in the PCI and NCI spectra also may interfere in the interpretation of the CI spectra if the $(M+29)^+$ or $(M+41)^+$ ions of one steroid coincided with the molecular ion of another coeluting steroid; this, however, was not a problem for the two compounds used in this example.

Selected ion monitoring. Selected ion monitoring is typically used for routine screening of anabolic steroids in complex matrices because of its high sensitivity. Since fewer ions are monitored, the signal-to-noise (S/N) ratio is improved for SIM compared to full scan MS. Figure 5-6 compares SIM sensitivities for each of the six steroids under EI, PCI, and NCI conditions; the ions that were monitored and quantitated on are indicated by an * in Table 5-1. In this figure, sensitivity was estimated as the peak areas for the molecular-type ions except for the EI data for dehydrotestosterone and the NCI data for oxymetholone. For these compounds, the fragment ions at m/z 122 (dehyt) and m/z 314 (oxym) were the most abundant peaks in the mass spectra and therefore were used for quantitation. As for normal full scan GC/MS, it is apparent that PCI is the most sensitive ionization method compared to EI and NCI. The relative sensitivity for PCI is, in some cases, 5 or more times greater than that for either EI or NCI. In comparison to full scan PCI

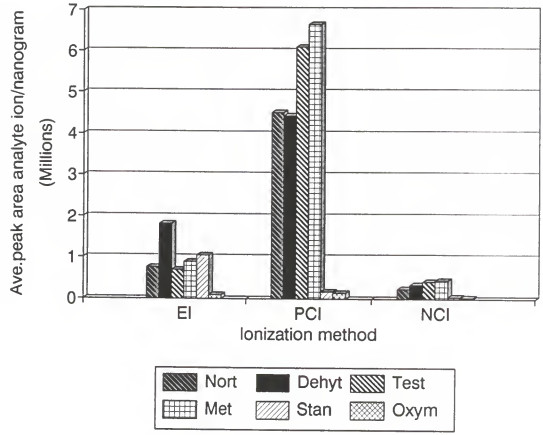

Figure 5-6: Determination of EI, PCI, and NCI sensitivities for SIM GC/MS for each of the six underivatized anabolic steroid molecular-type ions; note that the fragment ion at m/z 122 was used in place of the M^+ ion of dehydrotestosterone and the fragment ion at m/z 314 was used in place of the $(M-H)^-$ ion of oxymetholone.

sensitivities (Figure 5-4), PCI SIM sensitivities (Figure 5-6) are greater by at least 10 times. Therefore, SIM would be a better choice for increasing the sensitivity (S/N ratio) for trace analysis.

The selectivity of SIM, however, was decreased as compared to full scan GC/MS. Selectivity is decreased in SIM as only selected ions of interest are monitored. In Figure 5-7, 3 ions per compound continuously were monitored during the chromatographic run. The spectra, however, again contain interfering ions from adjacent unresolved chromatographic peaks. The molecular ions for dehydrotestosterone and methyltestosterone are seen in all the mass spectra; notice that the EI mass spectrum was enlarged 2x to see the M^+ ion for dehydrotestosterone while the M^+ ion of methyltestosterone could be observed without an enlargement factor. In addition, selected fragment and adduct ions can be seen in the mass spectra corresponding to some of the other steroids; notice the low abundant ions at m/z 96, 110, 174, 215, 229, 246, and 270 in the EI mass spectrum. In a real biological sample such spectral interference could make positive identification of the steroid more difficult. This experiment should have been set up on the basis of retention time of the compound of interest. This presumably would have helped minimize the spectral interference from other sample components. Although sensitivity for SIM is extremely high, a method of increasing selectivity is still necessary.

Figure 5-7: Mass spectra for dehydrotestosterone under (a) EI, (b) PCI, and (c) NCI SIM GC/MS conditions.

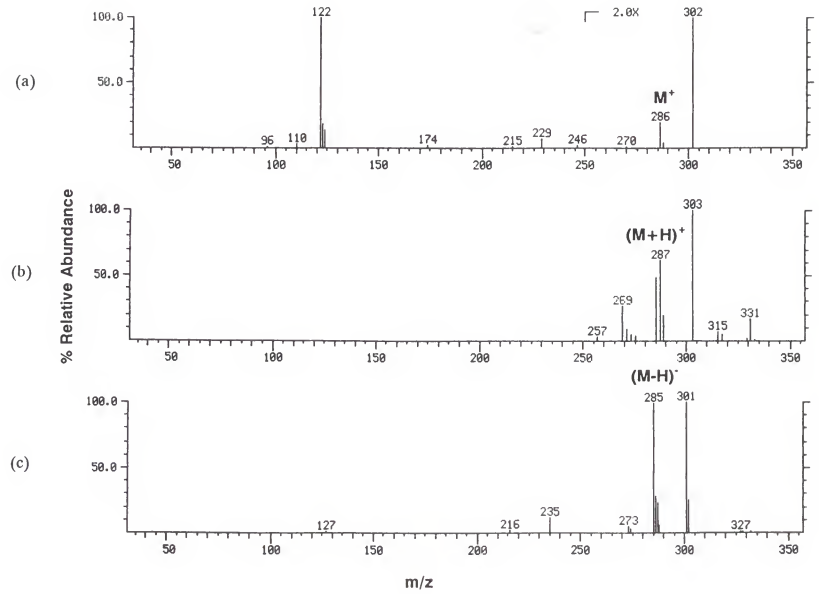
(a)
100.0
50.0
122
2.0X
302
M+
286
96
110
174
215
229
246
270
50
100
150
200
250
300
350
(b)
% Relative Abundance
100.0
50.0
303
(M+H)+
287
269
257
315
331
(M-H)-
285
301
127
216
235
273
327
m/z

Selected reaction monitoring. Tandem mass spectrometric strategies can be used to achieve the selectivity required for trace analysis. In addition, MS/MS using selected reaction monitoring can result in improved detection limits. Selectivity is achieved through the CAD process and improved detection limits achieved by increasing the S/N ratio. In Figure 5-8, the sensitivity was estimated as the peak area of the most intense daughter ion for each of the steroids; note that quantitation was performed on only one daughter ion although two daughter ions and the remaining parent ion were monitored for each compound. Table 5-2 lists the reactions and ions that were monitored and quantitated on (indicated by an *) for this experiment. As in the case of full scan and SIM GC/MS, SRM PCI sensitivities were much greater than either EI or NCI. The overall sensitivity for PCI SRM, however, was reduced compared to that of PCI SIM by a factor of ten or more. The reduction in sensitivity for SRM compared to SIM is a function of the CAD efficiencies for the parent ions of each of the compounds.

Figures 5-9, 5-10, and 5-11 show the SRM CAD efficiencies for EI, PCI, and NCI, respectively, as a function of both collision gas pressure and energy. Collisionally activated dissociation efficiencies were calculated by taking the fraction of the most intense daughter ion produced over the original parent ion. This yields the CAD efficiency for that selected daughter ion, in contrast to the data presented in Tables 5-3 and 5-4. It is evident in these figures that SRM CAD efficiencies were the greatest for EI, followed by PCI, then NCI. This is in agreement with the full scan CAD efficiencies.

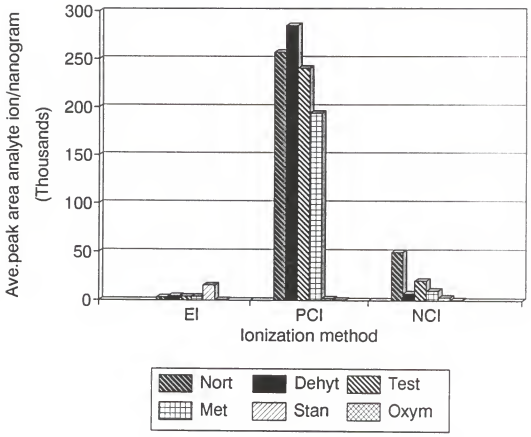

Figure 5-8: Determination of EI, PCI, and NCI sensitivities for SRM GC/MS/MS for each of the six underivatized anabolic steroids. Refer to Table 5-2 for a list of the reactions that were monitored and the ions that were employed for quantitation.

Figure 5-9: SRM EI-CAD efficiencies of the M^+ ions as a function of (a) collision gas pressure and (b) collision energy.

(a)

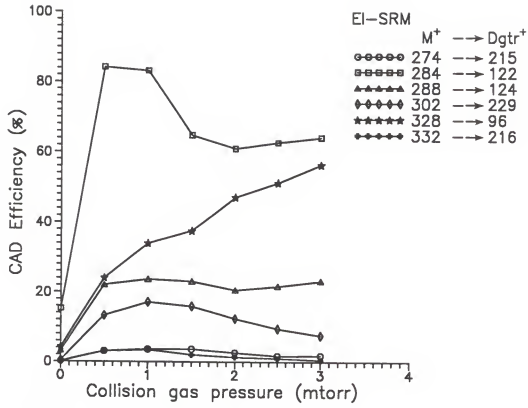
EI–SRM
M+ → Dgtr+
274 → 215
284 → 122
288 → 124
302 → 229
328 → 96
332 → 216
CAD Efficiency (%)
Collision gas pressure (mtorr)

(b)

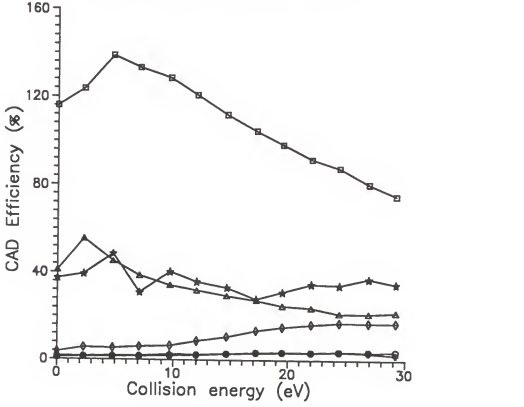
CAD Efficiency (%)
Collision energy (eV)

Figure 5-10: SRM PCI-CAD efficiencies of the $(M+H)^+$ ions as a function of (a) collision gas pressure and (b) collision energy

(a)

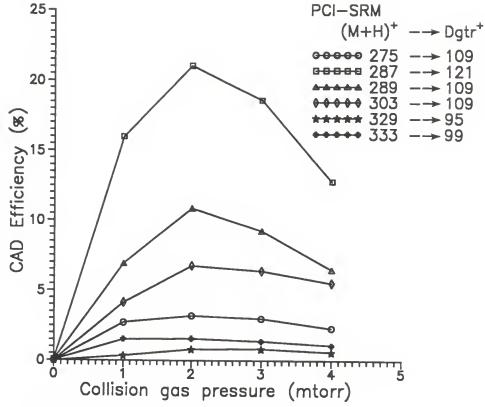
PCI–SRM
(M+H)+ → Dgtr+
275 → 109
287 → 121
289 → 109
303 → 109
329 → 95
333 → 99
CAD Efficiency (%)
Collision gas pressure (mtorr)

(b)

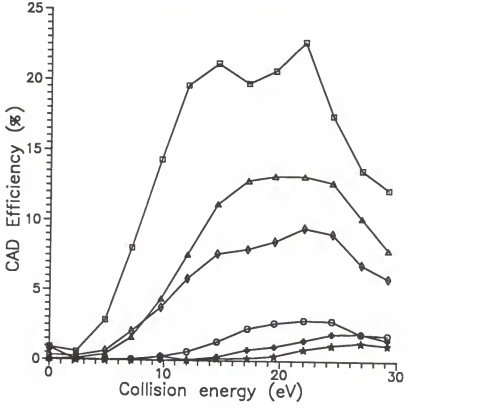
CAD Efficiency (%)
Collision energy (eV)

Figure 5-11: SRM NCI-CAD efficiencies of the $(M-H)^-$ ions as a function of (a) collision gas pressure and (b) collision energy

(a)

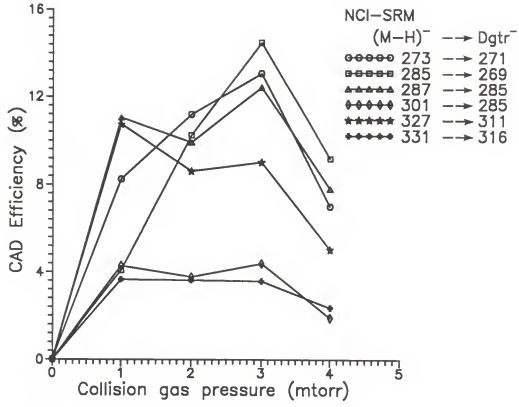
NCI–SRM
(M–H)⁻ → Dgtr⁻
273 → 271
285 → 269
287 → 285
301 → 285
327 → 311
331 → 316
CAD Efficiency (%)
Collision gas pressure (mtorr)

(b)

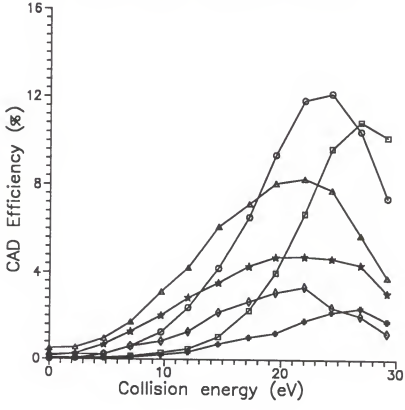
CAD Efficiency (%)
Collision energy (eV)

The increased selectivity of MS/MS methods can be seen by comparing Figure 5-12 to Figures 5-5 and 5-7. In the SRM spectra, it is evident that no interfering ions are present even though the two compounds, dehydrotestosterone and methyltestosterone, are still chromatographically unresolved. Positive identification of all the steroids can be made by this method even in complex mixtures. In choosing the best analytical method, the lower overall sensitivity for SRM compared to SIM must be weighed against the increase in selectivity. It should be noted, however, that although absolute sensitivities may be worse for SRM compared to SIM, detection limits for SRM may in fact be better, at least for compounds in real matrices. For limit of detection studies, the limiting factor is not sensitivity, but S/N ratio. Therefore, because of the increased selectivity of SRM (higher S/N ratio) compared to SIM, lower LODs may be obtained for SRM. This will be discussed further in Chapter 6.

Conclusions

The choice of analytical method is complicated by the necessity for high sensitivity, selectivity, CAD efficiency, and characteristic mass spectra. Electron and chemical ionization methods have been evaluated in conjunction with tandem mass spectrometric detection using selected reaction monitoring. Tandem mass spectrometric detection methods have also been compared to full scan and selected

Figure 5-12: Daughter mass spectra for the molecular-type ions of dehydrotestosterone under (a) EI, (b) PCI, and (c) NCI SRM GC/MS/MS conditions.

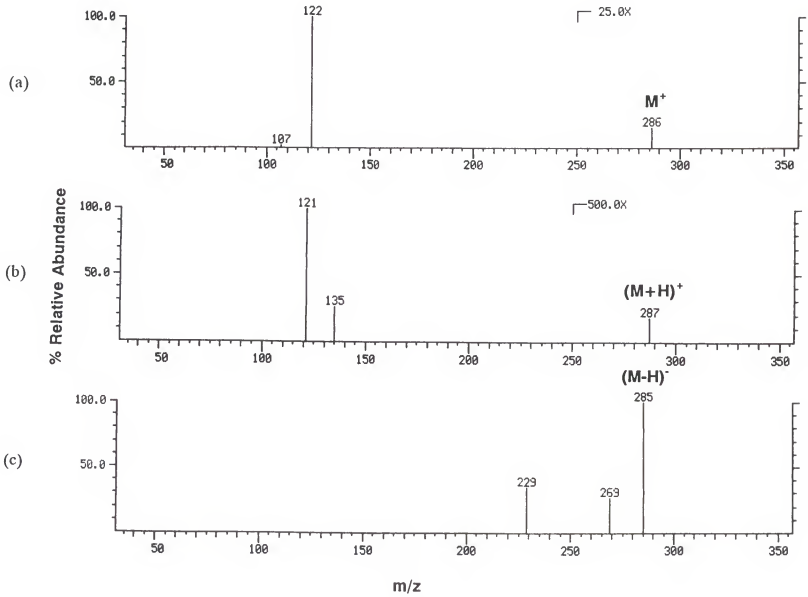
(a)
100.0
50.0
122
25.0X
M+
286
107
50
100
150
200
250
300
350
(b)
% Relative Abundance
100.0
50.0
121
500.0X
135
(M+H)+
287
50
100
150
200
250
300
350
(c)
100.0
50.0
(M-H)-
285
229
263
50
100
150
200
250
300
350
m/z

ion monitoring GC/MS methods. On the basis of sensitivity, selected ion monitoring using positive ion chemical ionization yields the highest values. In comparison to EI and NCI, as well as full scan and selected reaction monitoring, this method could allow much lower limits of detection to be obtained for trace analysis. Unfortunately, SIM has limited selectivity, since only selected ions are monitored. In addition, unresolved chromatographic peaks still present a problem in interpreting the resulting mass spectra.

The best selectivity is obtained using MS/MS. Full scan MS/MS strategies using electron ionization yield the most structural information. Full scan EI-CAD, however, suffers from limited sensitivity due to the low abundance of parent ion produced by EI. Selected reaction monitoring can be used to increase the sensitivity but at the expense of some selectivity. Even though CAD efficiencies (full scan and SRM) are better for EI than for PCI, the poor sensitivity for the EI molecular ions limits EI SRM as a useful analytical tool for steroid determination in biological samples. Therefore, it was concluded that PCI in combination with SRM was the most selective and sensitive method evaluated for the determination of underivatized anabolic steroids. In Chapter 6, the use of PCI SRM will be evaluated for screening of anabolic steroids in spiked urine samples.

CHAPTER 6

DEVELOPMENT OF AN ASSAY FOR TRACE ANALYSIS OF UNDERIVATIZED ANABOLIC STEROIDS BY SHORT-COLUMN GC/MS/MS

Introduction

Profiling of urinary steroids and steroid hormones has been reviewed extensively by Shackleton (107), including isolation procedures, profiling methods, media types, and various classes of steroids. In addition, it is stated in the review that the goal remains a single profile where all components of interest are determined in a non-discriminatory way (107). This, however, has yet to be achieved by any of the current profiling methods. The first step in developing such a method is the sample preparation steps (isolation procedures), extraction, hydrolysis, and derivatization. The extraction step involves separating the steroids of interest from the majority of the urinary matrix components. Extraction procedures can be performed either by solvent partitioning, requiring solvents of varying polarity, or by solid-phase extraction using adsorbents (108). Hydrolysis of the extract is required to liberate the free parent steroid, since many of these compounds are excreted as either glucuronide or sulfate conjugates. Typically, hydrolysis is performed with the enzyme β-glucuronidase/sulfatase from the bacteria *Helix pomatia*. Finally, selective

derivatization procedures can be employed to improve the chromatographic and mass spectrometric characteristics of the steroids. For example, derivatization decreases the polarity of the steroids, making them more amenable to gas chromatographic separation; further, the typically larger yield of derivatized M^+ ions increases mass spectrometric sensitivity which is preferable for quantitation using SIM.

The most commonly used profiling method involves conventional GC/MS of derivatized steroids. Derivatization of hydroxy and keto groups has been performed using a variety of reagents, including methoxime (MO), trimethylsilyl (TMS), and mixed MO-TMS reagents. If only TMS reagents are used, TMS ethers of hydroxyls are usually formed. Keto functions may also be derivatized into TMS enols depending on the reaction time, silylating strength, and steric hindrance (23). Advantages of the TMS enol formation are improved sensitivity and specificity; however, if enolization is incomplete, the sensitivity and quantitation precision of the assay are reduced. The major limitation inherent in GC/MS assays requiring derivatization is the potential for limited sensitivity and specificity for screening of a wide variety of anabolic steroids. Steric hindrance and odd functionalities, such as the pyrazole ring in stanozolol, necessitate the use of more selective derivatization reagents or different reaction times (25).

In this chapter, an assay for the determination of the six underivatized steroids will be evaluated based on the methodology developed in Chapters 4 and 5. Development of an analytical assay for the determination of underivatized steroids based on short-column GC/MS/MS would be designed to accomplish the following

goals: to reduce and simplify sample preparation procedures, to reduce analysis times, and to improve the sensitivity and selectivity of present screening methods. A comparison of full scan and selected ion monitoring GC/MS and selected reaction monitoring GC/MS/MS will be presented to illustrate the differences in sensitivity and selectivity of these methods for screening of steroids spiked into urine samples. In these studies, electron ionization was used since it is the most commonly used ionization method in conventional GC/MS screening strategies. These results will then be compared to similar studies using positive ion chemical ionization. Finally, detection limit studies will be presented for the analytical method of choice, selected reaction monitoring using positive ion chemical ionization, as developed in Chapter 5. These results will be compared to literature limits of detection (LODs) using conventional electron ionization and derivatization GC/MS strategies.

Experimental

Sample Preparation

Spiked urine samples were prepared according to standard literature procedures (23,25,108). Urine samples were prepared by spiking 5 mL of urine with 1 mL of a standard steroid solution (containing the six steroids previously studied) over the concentration range of 10 ng/mL to 5000 ng/mL. The spiked urine samples were extracted using C-18 Spice sep-pak cartridges (Analtech, Inc., Newark, DE) previously washed with 5 mL of methanol and 5 mL of water. The urine sample was

passed through the cartridge followed by 5 mL of water to wash away most of the urinary constituents. The steroids were eluted from the cartridge with 2 mL of methanol which was evaporated to dryness under a nitrogen stream. The residue was dissolved in 1 mL of 0.2 M acetate buffer (pH 5.2). The samples were then hydrolyzed by incubating with 100 μL of β-glucuronidase enzyme from *Helix pomatia* (Sigma Chemical Co.) at 60 °C for 3 hours. The hydrolysate was cooled to room temperature and 100 mg potassium carbonate was added. The sample was vortexed gently to mix and then extracted with 5 mL diethyl ether. The extract was dried over anhydrous sodium sulfate (1 g) and evaporated to dryness under a nitrogen stream. The dry residue was redissolved in 100 μL of methanol and 1 μL aliquots were analyzed. Urine samples and standard solutions were spiked prior to extraction or analysis, respectively, with 1 mL of a 50 to 100 ng/mL standard solution of 5α-androstan-17-one (Sigma Chemical Co.) as the internal standard.

Instrumental Conditions

Gas chromatography/mass spectrometry was performed on a Finnigan MAT TSQ45 gas chromatograph/triple quadrupole mass spectrometer. Additional studies were performed on a Finnigan MAT TSQ70 mass spectrometer for comparative purposes. Gas chromatographic sample introduction was carried out on a short J&W Scientific DB-5 capillary column (3.5 m long, 0.25 mm i.d., 0.25 μm film thickness). Injections were made in the splitless injection mode (0.5 min. splitless) with a column inlet pressure of approximately 2 psi using helium as the carrier gas. A temperature program was employed in which the column temperature was initially held at 150 °C

for 0.5 min., then increased at 20 °C/min. (15 °C/min. for the TSQ70 studies) to a final temperature of 250 °C. The injector temperature was 250 °C.

Conditions for the mass spectrometer were GC/MS interface and transfer line temperatures of 250 °C and ionizer temperatures of 190 °C for EI and 150 °C for CI. The conditions varied between the two instruments and were different for EI and CI experiments, as detailed in Tables 6-1 (EI) and 6-2 (CI). For CI studies, methane was used as the reagent gas at an indicated pressure of 0.2 torr (TSQ45) and 1.5 torr (TSQ70). Note that these reagent gas pressures corresponded to the maximum production of the methane reagent gas ion at m/z 17. For the MS/MS experiments, nitrogen was used as the collision gas at a pressure of 2.5 mtorr for EI experiments and argon was used for CI studies at a pressure of 2.5 mtorr (TSQ45) and 1.5 mtorr (TSQ70). For quantitative studies, peak areas from mass chromatograms of selected ions were calculated by integrating the ion current over the peak profile after visually choosing the baseline for each GC peak.

Results and Discussion

Initial Assay Development

The short-column GC/MS and MS/MS methodologies developed in Chapters 4 and 5 were tested on spiked urine samples. Aliquots of standard steroid solutions were spiked into 5 mL of urine, extracted, hydrolyzed, and analyzed without derivatization by short-column GC/MS and GC/MS/MS. Preliminary studies were

Table 6-1: Mass spectrometric conditions for electron ionization studies

steroid	scan range	TSQ45[a] scan rate	electron energy	multiplier
		full scan		
all	50 to 400 u	0.5s	40 eV	900 V
		SIM		
Nort	274, 215, 110	0.1s	40 eV	900 V
Test	288, 246, 124			
Met	302, 229, 124			
Dehyt	286, 123, 122			
Oxym	332, 216, 174			
Stan	328, 270, 96			
		SRM[b]		
Nort	274 → 215, 110	0.1s	40 eV	1500 V
Test	288 → 124, 109			
Met	302 → 229, 124			
Dehyt	286 → 122, 107			
Oxym	332 → 216, 174			
Stan	328 → 270, 96			

[a] conditions for EI-CAD of spiked urine samples
[b] collision energy of 20 eV

Table 6-2: Mass spectrometric conditions for chemical ionization studies

steroid	scan range	scan rate	electron energy	multiplier	collision energy
		TSQ45[a]			
		SIM			
Nort	275*, 303, 256	0.1s	100 eV	1150 V	
Test	289*, 317, 271				
Met	303*, 331, 285				
Dehyt	287*, 315, 269				
Oxym	333*, 361, 315				
Stan	329*, 357, 311				
		SRM			
Nort	275 → 257, 109*	0.05s	100 eV	1800 V	17 eV
Test	289 → 109*, 97				22 eV
Met	303 → 109*, 97				22 eV
Dehyt	287 → 135, 121*				14 eV
Oxym	333 → 107, 99*				24 eV
Stan	329 → 121, 95*				27 eV
		TSQ70[b]			
		full scan			
all	60 to 500 u	0.5s	100 eV	1250 V	
		SIM			
Nort	275, 303, 256	0.05s	100 eV	1800 V	
Test	289, 317, 271				
Met	303, 331, 285				
Dehyt	287, 315, 269				
Oxym	333, 361, 315				
Stan	329, 357, 311				
		SRM+			
Nort	275 → 257, 109	0.05s	100 eV	1800 V	17 eV
Test	289 → 109, 97				22 eV
Met	303 → 109, 97				22 eV
Dehyt	287 → 135, 121				14 eV
Oxym	333 → 107, 99				24 eV
Stan	329 → 121, 95				27 eV

[a] conditions for PCI-CAD LOD study of standard steroid solutions

[b] conditions for PCI-CAD LOD study of testosterone and stanozolol and spiked urine samples

*(+) indicates ions (sum of ions) that were quantitated on

performed using electron ionization to compare results to conventional methods. Final method development was performed using positive ion chemical ionization.

Full scan EI GC/MS. Figure 6-1 shows full scan EI GC/MS chromatograms (background-enhanced by the INCOS data system) for the reconstructed ion current of a blank urine sample, a spiked urine sample (2000 ng/mL or 50 ng injected of each steroid), and a standard solution (100 ng injected of each steroid) of the six steroids of interest. It is evident from the blank urine trace (Figure 6-1a) that several urinary steroids are present, including androsterone and etiocholanolone, the two major metabolites of testosterone (labelled with * in the mass chromatogram). Note that these two steroids were positively identified based on comparison of sample and library spectra. Other possible urinary constituents include endogenous testosterone (identified based upon the correct retention time), epitestosterone, 11β-OH-androsterone, and 11β-OH-etiocholanolone (labelled with + in the mass chromatogram). Positive identification of these compounds based on comparison of sample and library spectra was not possible, however, due to high column background and poor analyte signal. The other peaks present in the mass chromatograms are either unidentified urinary components or due to siloxanes from stationary phase contamination. Compared to Figure 6-1c for the standard solution, coeluting urinary components in the spiked urine sample in Figure 6-1b limit the chromatographic resolution in the RIC trace, making the separation of the spiked and endogenous urinary steroids difficult, although all of the steroids can be mass chromatographically resolved as shown in Figure 6-2. In addition, it should be noted

Figure 6-1: Full scan EI GC/MS reconstructed ion chromatograms for (a) blank urine sample, (b) spiked urine sample, and (c) a standard solution of the six anabolic steroids of interest. The peaks can be identified as number 1: nortestosterone, 2: testosterone, 3: methyltestosterone, 4: dehydrotestosterone, 5: oxymetholone, 6: stanozolol, IS: internal standard, *: androsterone and etiocholanolone, and +: other possible endogenous urinary steroids.

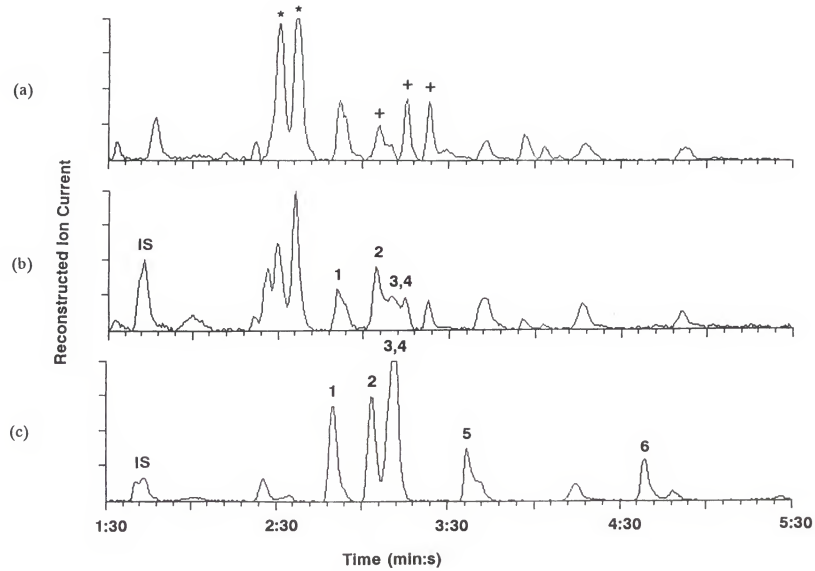
(a)
(b)
(c)
Reconstructed Ion Current
IS
1
2
3,4
5
6
*
+
1:30
2:30
3:30
4:30
5:30
Time (min:s)

Figure 6-2: Full scan EI GC/MS mass chromatograms for a spiked urine sample containing the six anabolic steroids of interest. The peaks can be identified as (a) 1: nortestosterone, (b) 4: dehydrotestosterone, (c) 2: testosterone, (d) *: endogenous testosterone metabolites, (e) 3: methyltestosterone, and (f) the RIC (not background-enhanced); note that stanozolol and oxymetholone were not detected in this sample.

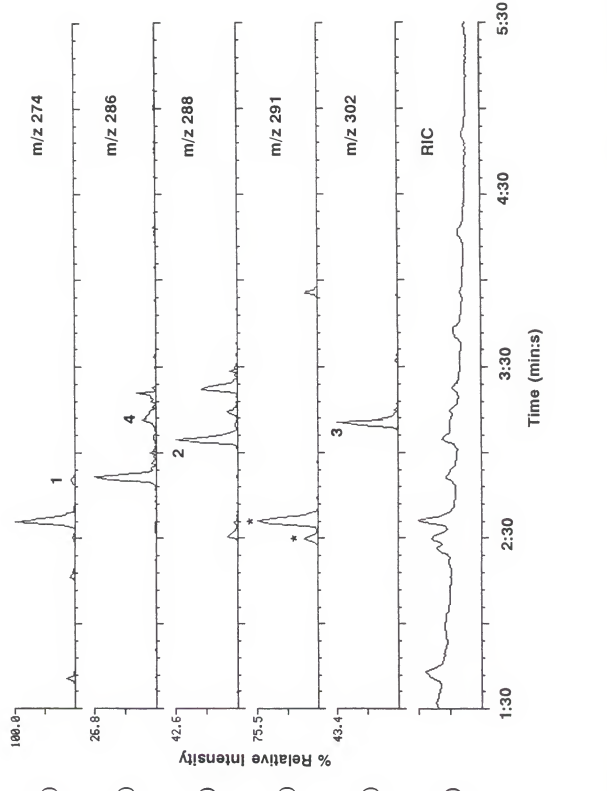
(a)
(b)
(c)
(d)
(e)
(f)
100.0
26.8
42.6
75.5
43.4
% Relative Intensity
m/z 274
m/z 286
m/z 288
m/z 291
m/z 302
RIC
1
2
3
4
*
*
1:30
2:30
3:30
4:30
5:30
Time (min:s)

that stanozolol and oxymetholone, although spiked into the urine sample were not detected in this sample. This was probably a result of being below their detection limits or due to the loss of these steroids during the sample preparation procedures.

SIM EI GC/MS. Selected ion monitoring is typically the method used in conventional GC/MS procedures. Discrete groups of ions are monitored on the basis of retention time; generally 2 to 3 ions per compound are required for positive identification. In Figure 6-3, 3 ions per compound were monitored for the six anabolic steroids for a blank urine sample, a spiked urine sample (2000 ng/mL or 50 ng injected of each steroid), and a standard solution (100 ng injected of each steroid). The ions that were monitored are listed in Table 6-1 for SIM. From Figure 6-3a, it is evident that some of the analyte ions monitored were present in the urine blank from the endogenous steroids. Even though the complexity of the reconstructed ion chromatograms is somewhat less (due to decreased chemical background for SIM compared to the RIC trace in Figure 6-1), additional selectivity is required to make up for the limited chromatographic resolution. In addition, although not directly evident in Figures 6-1, 6-2, and 6-3, the S/N ratio is much better for SIM (note: the SIM RIC chromatogram was not background-enhanced) than for the full scan RIC or individual mass chromatograms resulting in improved sensitivity; note that for direct comparative purposes S/N ratios should be compared for individual (or summed) mass chromatograms, rather than reconstructed ion chromatograms. It also should be pointed out that the SIM experiment was not set

Figure 6-3: Selected ion monitoring EI GC/MS RIC chromatograms (for the sum of the 18 ions listed in Table 6-1) for a (a) blank urine sample, (b) spiked urine sample, and (c) a standard solution of the six anabolic steroids of interest. The peak numbers correspond to 1: nortestosterone, 2: testosterone, 3: methyltestosterone, 4: dehydrotestosterone, 5: oxymetholone, 6: stanozolol, IS: internal standard, and */+: endogenous urinary steroids, as noted in the text.

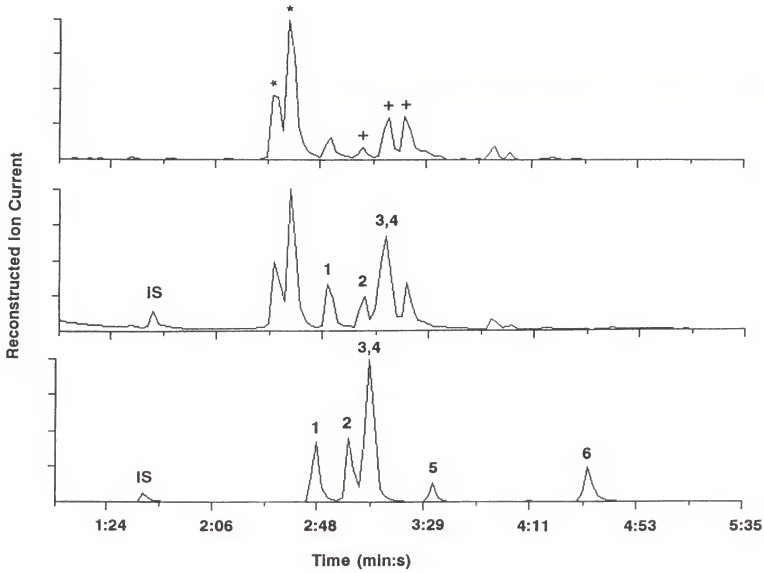
(a)
(b)
(c)
Reconstructed Ion Current
*
*
+
+ +
IS
1
2
3,4
IS
1
2
3,4
5
6
1:24
2:06
2:48
3:29
4:11
4:53
5:35
Time (min:s)

up on the basis of retention time. Therefore, 18 ions (3 ions for each of 6 compounds) were continuously being monitored over the entire chromatographic run, taking 1.8 s per scan. This resulted in a limited number of data points per GC peak and as a result poorly defined peak shapes compared to the full scan GC/MS data (0.5 s per scan). Ultimately, if this were the method of choice, the experiment would need to be set up on the basis of retention time, monitoring ions only at specific time intervals corresponding to the elution of the compounds of interest to obtain maximum sensitivity and quantitative precision.

SRM EI GC/MS/MS. The additional selectivity required to compensate for short GC columns was obtained by using tandem mass spectrometric detection. The mass chromatograms for the reactions listed in Table 6-1 (SRM) are shown as unsplit data files in Figure 6-4. The SRM chromatogram for the blank urine sample (Figure 6-4a) shows no peaks, unlike the chromatograms for full scan and SIM GC/MS (Figures 6-1a and 6-3a); this indicates that MS/MS provides the selectivity necessary to detect only the targeted steroids even with only short-column GC separation. The spiked urine sample (20 μg/mL or 500 ng injected of each steroid) and the standard solution (100 ng injected of each steroid) therefore, contain the same peaks, except for oxymetholone (peak #5) which does not show up in the spiked urine chromatogram. The jagged appearance of peaks 2-4 in Figure 6-4 is a result of the unsplit data file. To obtain quantitative data from these results the data files must be split according the multiexperiment; note in Table 6-1 that the SRM conditions

Figure 6-4: Selected reaction monitoring EI GC/MS/MS RIC chromatograms (for the 18 reactions listed in Table 6-1) for a (a) blank urine sample, (b) spiked urine sample, and (c) a standard solution of the six anabolic steroids of interest. Peaks are identified as 1: nortestosterone, 2: testosterone, 3: methyltestosterone, 4: dehydrotestosterone, 5: oxymetholone (missing), 6: stanozolol, and IS: internal standard.

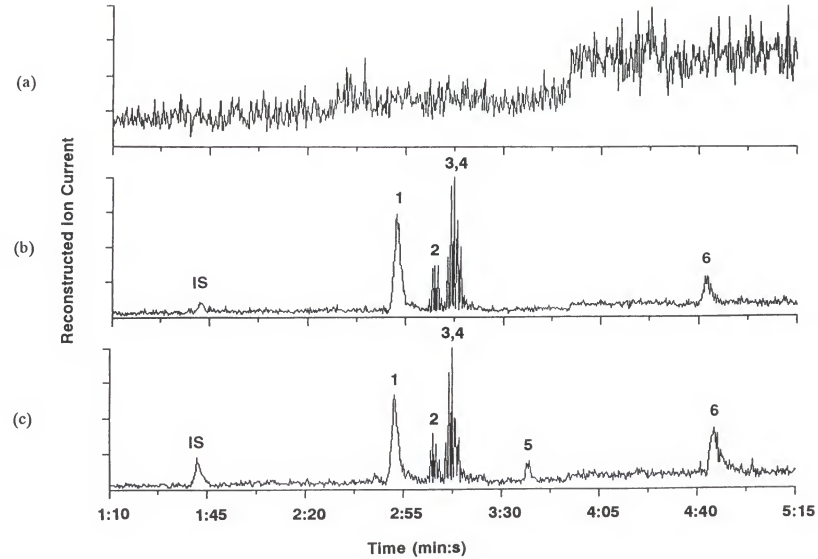
(a)
(b)
(c)
Reconstructed Ion Current
IS
1
2
3,4
5
6
1:10
1:45
2:20
2:55
3:30
4:05
4:40
5:15
Time (min:s)

correspond to the multiexperiment in question where each selected reaction is a separate experiment, except for the reactions for test, met, and dehyt which together compose the second of the four experiments. The splitting of the data file is accomplished by the INCOS data system. The split data are shown in Figure 6-5; note that in the process of splitting the data files the time base information becomes inconsistent with that for the SRM unsplit trace and must be corrrected according to the individual experiments (i.e. compounds are not shown in the correct elution order). As in the SIM data, it is apparent in Figure 6-5 that rapid scanning is critical to obtain an adequate number of data points per GC peak.

Based on the data presented in Chapter 5, however, electron ionization was not the best method for obtaining adequate sensitivity for these compounds. Positive ion chemical ionization, therefore, was used for the remaining method development studies.

PCI GC/MS and GC/MS/MS. As in the EI studies, full scan, selected ion monitoring and selected reaction monitoring studies were performed on the TSQ70 using positive ion chemical ionization. Figure 6-6 shows the results for full scan PCI GC/MS of a 5000 ng/mL spiked urine sample (or 50 ng injected of each steroid). The mass chromatograms for the $(M+H)^+$ ions of nortestosterone (m/z 275), dehydrotestosterone (m/z 287), testosterone (m/z 289), methyltestosterone (m/z 303), and the endogenous testosterone metabolites at m/z 291 (identification based upon comparison to the EI data and retention time information), as well as the RIC are

Figure 6-5: Selected reaction monitoring split data files for (a) 1: nortestosterone, (b) 4: dehydrotestosterone, (c) 2: testosterone, (d) 3: methyltestosterone, (e) 5: oxymetholone, and (f) 6: stanozolol.

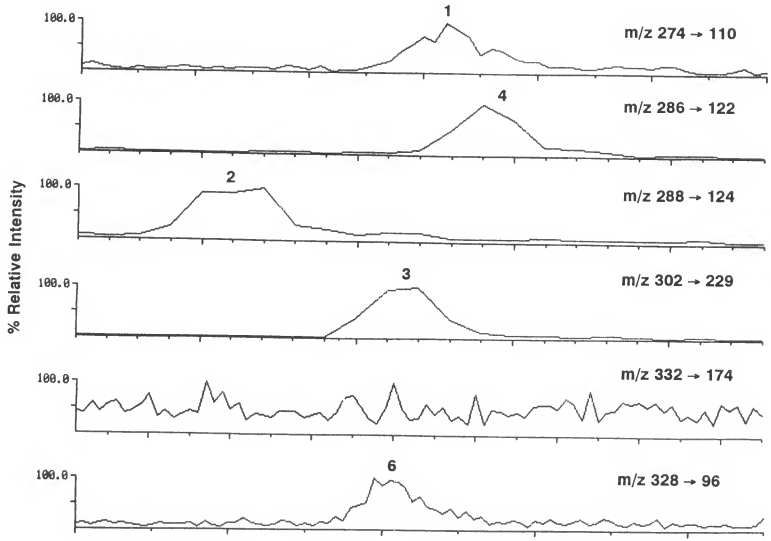
(a)
(b)
(c)
(d)
(e)
(f)
100.0
1
m/z 274 → 110
4
m/z 286 → 122
2
m/z 288 → 124
3
m/z 302 → 229
m/z 332 → 174
6
m/z 328 → 96
% Relative Intensity

Figure 6-6: Full scan PCI GC/MS mass chromatograms for the $(M+H)^+$ ions of (a) 1: nortestosterone, (b) 4: dehydrotestosterone, (c) 2: testosterone, (d) *: suspected testosterone metabolite, (e) 3: methyltestosterone, and (f) the reconstructed ion current.

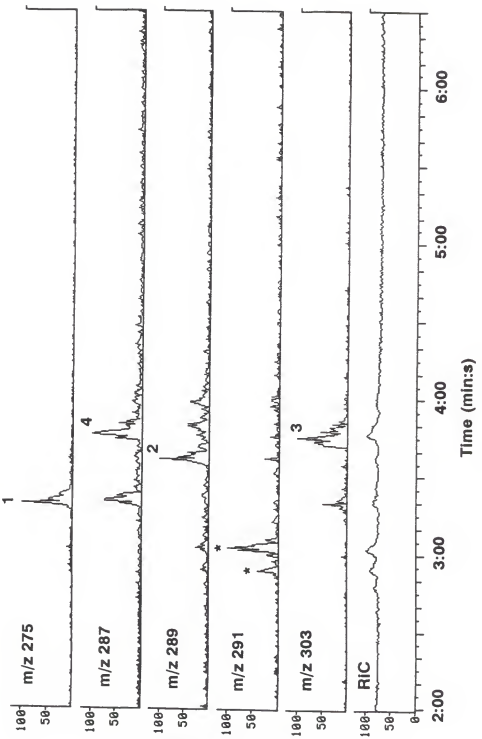
(a)
(b)
(c)
(d)
(e)
(f)
% Relative Intensity
100
50
0
m/z 275
m/z 287
m/z 289
m/z 291
m/z 303
RIC
1
2
3
4
*
*
2:00
3:00
4:00
5:00
6:00
Time (min:s)

shown. It should be noted that stanozolol and oxymetholone were not shown as they were not detected in the spiked urine sample at this concentration. It is apparent in the RIC trace (Figure 6-6f) that a high chemical background was present in the PCI experiment. This high background was a result of hydrocarbon contamination in the methane chemical ionization reagent gas lines and the presence of ions from an unknown source (instrumental contaminants). As evident in these data, positive identification and detection of trace levels of steroids by full scan GC/MS using PCI can be difficult due to chemical contaminants and high backgrounds.

In Figure 6-7, mass chromatograms for the sum of selected ions are shown for a 5000 ng/mL spiked urine sample (or 50 ng injected of each steroid). Three ions per compound were monitored during specified time intervals based upon the retention times of the steroids, as listed in Table 6-2 (SIM TSQ70). As in the full scan data, oxymetholone and stanozolol were not detected. It is also evident for these data that the S/N ratio for SIM (Figure 6-7) is better than for full scan (Figure 6-6); note that this was also true for the EI data, but not as apparent. In addition, for testosterone three peaks were detected; note that the first peak corresponds to the correct retention time for testosterone. It is speculated that the second and third peaks are a result of either endogenous steroids or urinary constituents that contain at least one of the three ions being monitored for testosterone. These additional peaks also were observed in the full scan data. In addition, the elevated background for testosterone and dehydrotestosterone was a result of an instrumental contaminant (m/z 287) which contained a ^{37}Cl isotope peak (m/z 289).

Figure 6-7: Selected ion monitoring PCI GC/MS mass chromatograms for the sum of selected ions for (a) 1: nortestosterone, (b) 4: dehydrotestosterone, (c) 2: testosterone, (d) 3: methyltestosterone, and (e) the reconstructed ion current.

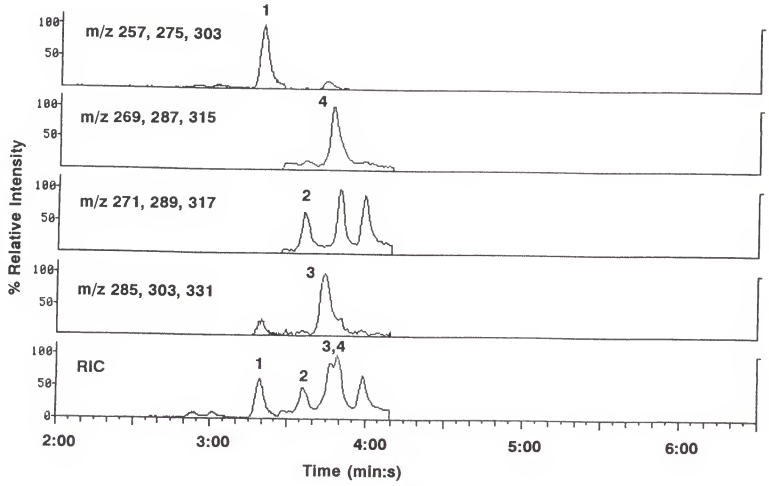
(a)
(b)
(c)
(d)
(e)
m/z 257, 275, 303
m/z 269, 287, 315
m/z 271, 289, 317
m/z 285, 303, 331
RIC
1
4
2
3
1
2
3,4
100
50
0
% Relative Intensity
2:00
3:00
4:00
5:00
6:00
Time (min:s)

Based on the above data, it is apparent that MS/MS detection is necessary to achieve the selectivity required for positive identification of the steroids of interest given the limited selectivity of short-column GC separation. Selected reactions for the steroids of interest were set up on the basis of retention time, as shown in Table 6-2 (SRM TSQ70). In this experiment, testosterone, nortestosterone, methyltestosterone, and dehydrotestosterone were the only spiked steroids detected in the 5000 ng/mL urine sample (or 50 ng injected of each steroid). The compounds oxymetholone and stanozolol were not detected. The mass chromatograms for the sum of the daughter ions monitored and the remaining parent ion for the four compounds and the RIC are shown in Figure 6-8. Note that for SRM, only one peak was produced for testosterone at the correct retention time, in contrast to the three peaks by SIM. For methyltestosterone, however, an additional peak was present in the SRM data (Figure 6-8b) that was not apparent in the full scan or SIM data at m/z 303. The first peak for methyltestosterone is unexpected, as the second peak corresponds to the correct retention time for this compound. It is speculated that the first peak may be due to testosterone, since it elutes at the same retention time. The normal PCI mass spectrum of testosterone contains an adduct ion, $(M+15)^+$, at m/z 303 which could produce daughter ions at m/z 109 and 97 by CAD. A daughter spectrum of this adduct ion was not obtained, however, to see if it fragmented to produce ions at m/z 109 and/or 97. From these data, it is apparent that SRM using positive ion chemical ionization was the most sensitive and selective

Figure 6-8: Selected reaction monitoring PCI GC/MS/MS mass chromatograms for the sum of selected daughter ions and remaining parent ion for (a) 4: dehydrotestosterone, (b) 3: methyltestosterone, (c) 2: testosterone, (d) 1: nortestosterone, and (e) the reconstructed ion current; note that the jagged appearance of the RIC is a result of monitoring three different parent ions over the same time interval and the data not being split.

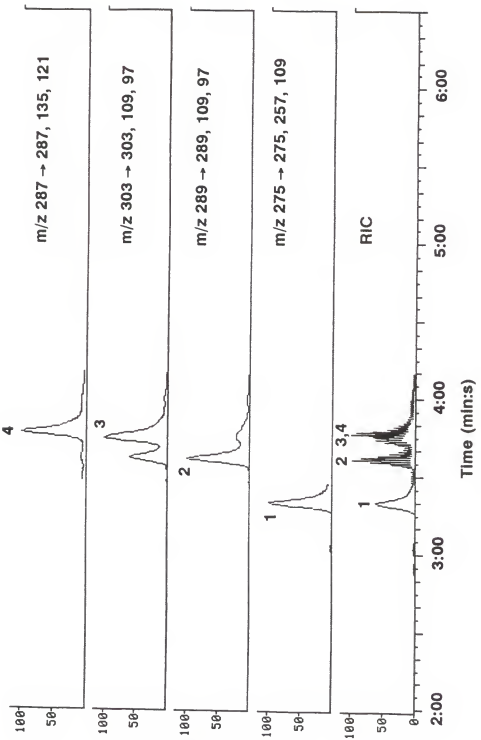
(a)
(b)
(c)
(d)
(e)
% Relative Intensity
100
50
0
m/z 287 → 287, 135, 121
m/z 303 → 303, 109, 97
m/z 289 → 289, 109, 97
m/z 275 → 275, 257, 109
RIC
4
3
2
1
1
2 3,4
2:00
3:00
4:00
5:00
6:00
Time (min:s)

method evaluated; calibration curve studies were therefore performed to determine the limit of detection of this method for anabolic steroid screening.

SIM and SRM Detection Limit Studies

Based on the data shown in Figures 6-4 and 6-8, it is evident that for maximum selectivity, MS/MS detection is the method of choice when used in conjunction with short GC columns. For conventional (derivatization) GC/MS on a 30 m column, selected ion monitoring is adequate, since ample selectivity is achieved by the chromatographic separation. Although conventional methods still rely on electron ionization, it was shown in Chapter 5 that increased sensitivity for the majority of the steroids studied can be gained by using positive ion chemical ionization. Therefore, it can be concluded from the work presented that PCI SRM has the most potential for the determination of underivatized steroids in real biological samples using short-column strategies. To test the analytical capabilities of this method, PCI SRM detection limit studies were performed and compared to PCI SIM detection limits. For this method to be useful for screening purposes, detection limits of < 10 ng/mL need to be achieved (23).

Calculations of limits of detection. Discussion of quantitative results can sometimes be confusing based on the varied definitions of terms such as limit of detection, limit of guarantee of purity, sensitivity, analytical signal, and analytical noise. Several reviews have been written on this subject defining certain concepts

relating to trace analysis (109-111) and discussing the LOD concept in chromatography (112,113). To avoid confusion, this section will discuss how the limits of detection were determined in this chapter.

The limit of detection describes the lowest concentration (or amount) of analyte that can be statistically differentiated from the analytical blank (111). Limits of detection were estimated using three different methods for comparative purposes. In the first method, the lower limit was determined as the analytical signal that produced a peak apparent at the correct retention time upon visual inspection of the mass chromatogram. This has been termed previously as the decision limit and defined as the lowest signal that can be distinguished from the background (114). This estimate of the detection limit is very conservative and probably will be the highest value compared to the other methods of determining detection limits.

The next two methods of estimating the LOD involve the use of the IUPAC definition shown in equation 6-1 (111),

$$X_L = \bar{X}_B + ks_B \qquad (6\text{-}1)$$

where X_L is the smallest detectable signal, $\bar{X}_B$ is the average blank signal, s_B is the standard deviation of the blank signal, and k is a numerical factor chosen in accordance with the confidence level desired. Typically, a k of 3 is used (111). The IUPAC LOD, X_L, can then be used to estimate the detection limit by converting the smallest detectable signal into concentration units. The first method calculates the

smallest detectable concentration , C_L, based on equation 6-2 (115),

$$C_L = (X_L - \bar{X}_B)/m = ks_B/m \qquad (6\text{-}2)$$

where m is the calibration sensitivity (slope of the calibration curve at the concentration of interest). In the second method, C_L is read directly from a calibration curve (signal versus concentration or amount) using the value of X_L.

PCI LODs for standard solutions. Standard solutions in the concentration range of 100 pg/μL to 500 ng/μL were prepared; 1 μL aliquots were analyzed by PCI SIM and PCI SRM monitoring the ions listed in Table 6-2 for the TSQ45. The results for these studies are shown in Table 6-3. Preliminary work investigating the use of selected ion monitoring for standard solutions showed promising detection limits of approximately 500 pg injected for nortestosterone, dehydrotestosterone, and testosterone and approximately 300 pg for methyltestosterone. Detection limits for stanozolol and oxymetholone were worse by a factor of ten (approximately 5 ng injected). These results are, on the average, slightly higher than reported literature values (50-500 pg injected) for conventional-length column GC/MS using SIM and derivatized steroids (99,116-119). Detection limits for PCI SRM were around 2 ng for most of the steroids as determined from a calibration curve and the IUPAC definition of LOD. Selected reaction monitoring detection limits were slightly worse than those for SIM; note that LODs for stanozolol and oxymetholone again were significantly worse than for the other steroids. The higher LODs for SRM as

Table 6-3: PCI SIM and SRM LODs for standard solutions of six underivatized anabolic steroids

limit of detection[b]	steroid[a] nort	dehyt	test	met	stan	oxym
SIM:						
visual[c]	0.53	0.57	0.50	0.28	5.0	5.3
SRM:						
visual[c]	5.3	5.7	5.0	5.5	50.0	26.5
IUPAC[d]	2	2	1	2	45	15
IUPAC[e]	0.9	0.6	0.2	0.7	24	8

[a] refer to Table 6-2 for the ions that were used for quantitation
[b] detection limits reported as nanograms of steroid injected on the column
[c] LOD based seeing a distinguishable peak in the mass chromatogram
[d] LOD determined from calibration curve ($X_L = \overline{X}_B + 3s_B$, for triplicate blank injections)
[e] LOD calculated as a function of the sensitivity of a 125 ng calibration standard

compared to SIM result from the less than 100% efficiency of CAD, and the transmission losses through a second mass filter. It should be noted that, for standard solutions, the added selectivity of MS/MS is of little use in improving the LOD. In addition, for both SIM and SRM experiments, the detection limits for stanozolol and oxymetholone were significantly worse than the testosterone analogs. This may be a result of the lower overall CAD efficiencies and poor chemical ionization efficiency (sensitivity), as shown in Chapter 5, for these two compounds.

Because these detection limits were not as good as anticipated, a comparative study was performed on the TSQ70 to rule out any instrumental considerations. It should be noted that these two instruments are quite similar, the major differences being a newer GC and an octapole collision cell on the TSQ70. Testosterone and stanozolol were used as test compounds as they had the best and worst detection limits, respectively, on the TSQ45. Standard solutions were prepared in the concentration range of 50 ng/μL to 250 ng/μL. On the TSQ70, selected reaction monitoring detection limits for testosterone and stanozolol were improved over the data acquired on the TSQ45. The limit of detection for testosterone was decreased by approximately an order of magnitude, from 1 ng to 100 pg injected, and for stanozolol was decreased from 45 ng to 15 ng injected. Since the limits of detection were better on the TSQ70, detection limits for spiked urine samples were determined on this instrument. The lower LODs obtained on the TSQ70 may be due to the decreased instrumental noise and the better GC of this instrument compared to the TSQ45.

PCI LODs for spiked urine samples. Spiked urine samples in the concentration range of 50 ng/mL to 5000 ng/mL were analyzed by selected reaction monitoring using positive ion chemical ionization. Table 6-4 shows the results for limits of detection and precision studies for four of the six steroids. Oxymetholone and stanozolol were not detected and may have been lost in the sample preparation procedures. Limits of detection for selected reaction monitoring of these compounds have not been reported in the literature, however, the IUPAC LODs (determined from a calibration curve) obtained in this study (2 to 40 ng/mL) are comparable to the low end of suggested physiological levels (5 to 500 ng/mL) in urine. Injection precision for this method was also good at approximately 10% RSD for five replicate injections.

Figure 6-9 shows representative calibration data for the compound testosterone spiked into urine. In addition, calibration curves for testosterone in standard solutions and in spiked urine samples are shown in Figure 6-10. It is evident from the blank chromatogram that some endogenous testosterone is present in the sample; this is shown in the calibration curves at an arbitrary amount of 0.01 ng since an amount corresponding to 0 ng cannot be plotted on a log-log plot. This raises the IUPAC estimate of the LOD in the spiked sample (compared to the standard solution) because of the endogenous levels of testosterone in the "blank" urine sample. Note, in addition, that the slopes of the two calibration curves were different presumably due to the extraction efficiency of the spiked urine samples in comparison to the standards which were not extracted. The higher detection limits

Table 6-4: PCI SRM LODs for spiked urine samples

limit of detection[b]	steroid[a] nort	dehyt	test	met	stan	oxym
visual[c]	50	50	50	50	nd[d]	nd
IUPAC[e]	2 (0.02)	40 (0.4)	20 (0.2)	3 (0.03)	nd	nd
IUPAC[f]	0.3	55	30	2.5	nd	nd
%RSD[g]	11	12	11	12	nd	nd

[a] refer to Table 6-2 for reactions that were used for quantitation
[b] detection limits reported as nanograms of steroid per milliliter of urine
[c] LOD based seeing a distinguishable peak in the mass chromatogram
[d] nd refers to not determined
[e] LOD determined from calibration curve ($X_L = \bar{X}_B + 3s_B$, for five replicate blank injections); note ( ) indicate nanograms of steroid injected on the column
[f] LOD calculated as a function of the sensitivity of the 50 ng/mL sample
[g] percent relative standard deviation of five replicate injections

Figure 6-8: Calibration data for SRM GC/MS/MS using PCI for spiked urine samples at concentrations of (a) blank urine, (b) 50 ng/mL, (c) 500 ng/mL, and (d) 5000 ng/mL for the compound testosterone. Note that the reactions monitored and the ions summed for quantitation corresponded to m/z 288 → 288, 109, and 97.

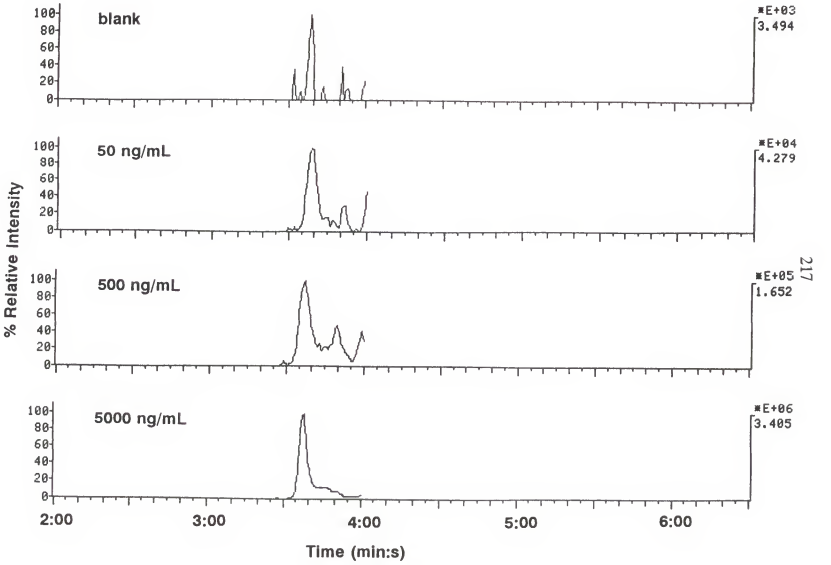
(a)
blank
100
80
60
40
20
0
E+03
3.494
(b)
50 ng/mL
E+04
4.279
(c)
500 ng/mL
E+05
1.652
(d)
5000 ng/mL
E+06
3.405
% Relative Intensity
2:00
3:00
4:00
5:00
6:00
Time (min:s)

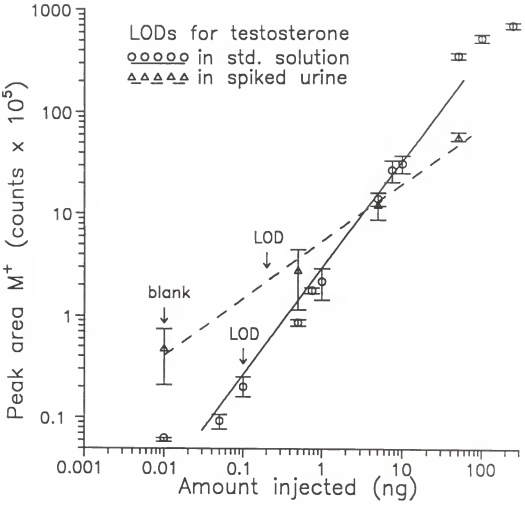

Figure 6-10: Calibration curves for testosterone in standard solution and in spiked urine samples. Note that blanks were plotted versus an arbitrary amount (0.01 ng) since 0 ng cannot be plotted on a log-log plot.

for dehydrotestosterone and testosterone, as compared to nortestosterone and methyltestosterone, also were a result of high chemical background. As stated previously, a contaminant ion at m/z 287 was present which was the same as the molecular ion of dehydrotestosterone and produced a daughter ion at m/z 107. Because this contaminant contained chlorine, the isotopic peak (m/z 289 producing a daughter ion at m/z 109) also interfered with the determination of testosterone. Compared to the SRM LODs (nanograms of steroid detected) for the standards (Table 6-3), the spiked urine LODs (nanograms injected in parenthesis in Table 6-4) were typically much better due to the added selectivity of MS/MS and the improved operating conditions on the TSQ70.

Conclusions

The method described here demonstrates the ability to analyze underivatized anabolic steroids in urine matrices. The short-column GC/MS/MS method using selected reaction monitoring and positive ion chemical ionization permits positive identification of the steroids based on retention time and production of characteristic daughter ions, as well as offering quantitative capabilities. Detection limits in spiked urine samples are promising for four of the six compounds studied. The main advantages of this method compared to conventional-length column GC/MS screening methods is its rapidity and selectivity, since positive identification of the

steroids studied can be performed with a short-column GC/MS/MS run of less than 6 minutes.

The main limitation of the method is the need to obtain adequate sensitivity for all the steroids of interest such that a single profile can be obtained in a non-discriminatory way. Although preconcentration is an accepted and commonly used method of increasing detection limits in biological samples, care must be taken since urinary constituents are preconcentrated as well. In the case of stanozolol and oxymetholone, however, preconcentration was not sufficient to obtain adequate detection limits for these two compounds in spiked samples.

CHAPTER 7

CONCLUSIONS AND FUTURE WORK

Conclusions

Analysis of underivatized anabolic steroids in biological samples using short-column GC/MS/MS strategies can be performed successfully if care is taken to optimize the analytical method based on sensitivity, selectivity, and speed of analysis. It was demonstrated that these criteria are essentially controlled by the analytical method and instrumental operating conditions. The steps that were investigated in developing an analytical method for the determination of underivatized steroids included sample preparation, sample introduction, ionization, and detection.

Sample preparation schemes for the determination of steroids in urine typically require extraction and hydrolysis procedures to eliminate unwanted urinary constituents and to free the conjugated steroids. Time-consuming derivatization procedures, however, have been shown here to be an unnecessary part of the sample preparation scheme. It was demonstrated that the analysis of underivatized steroids resulted in minimal loss of selectivity and sensitivity compared to conventional derivatization methods. In addition, both sample preparation and analysis times were decreased using short-column GC/MS strategies. The potential advantages of

derivatization, such as increased volatility, thermal stability, sensitivity, and selectivity, unfortunately, must be balanced against the lengthy preparation procedures. A more rapid derivatization technique that minimizes the time required for sample preparation, as discussed below, would therefore be an attractive alternative.

Sample introduction methods that have separation capabilities, such as gas chromatography, often eliminate the need for extensive sample cleanup due to the ability to separate the analyte and other components prior to ionization and mass spectrometric detection. Therefore, short-column GC was investigated as an alternative to conventional (30 m) GC introduction and compared to probe introduction to maximize sample transfer efficiency for the thermally-labile steroids. Initially, probe sensitivities were found to be much greater than short-column GC for the same amount of sample. Fundamental studies were performed to investigate the differences in these two introduction methods and to determine the sensitivity-limiting factors in short-column GC introduction methods. It was found that for maximum sample transfer efficiency/sensitivity, subambient column inlet pressures were required. The low carrier gas flows that were thus obtained allowed minimal disturbance of the ionization process. Under subambient inlet operation, short-column GC introduction offers several advantages over direct insertion probe methods, including lower limits of detection, minimal analysis times, a large linear dynamic range, and most importantly, separation capabilities.

In addition to reducing short-column GC/MS sensitivity, high carrier gas velocities were found to affect the input bandwidth for syringe injections such that

peak widths were greater than predicted theoretically. This was determined to be a result of extracolumn band-broadening from the injection method; therefore, development of an ideal injection for short-column GC that minimized the input bandwidth was investigated. Curie-point thermal desorption was shown to meet some of the requirements of an ideal injection method for use with short GC columns. For example, the effects of solvent overload in short column GC/MS was demonstrated, and the utility of a solventless injection method such as Curie-point thermal desorption to overcome these problems was shown. However, because the input bandwidth was not reduced to that predicted theoretically at high gas velocities, design changes in the Curie-point unit may be needed, as discussed below.

The choice of ionization and detection schemes was complicated by the necessity for high sensitivity, selectivity, and production of characteristic mass spectra. The major limitation found in the short-column GC/MS method was the limited chromatographic resolution, making the separation of complex mixtures more difficult. The use of tandem mass spectrometric detection, however, overcame this limitation, making short-column GC/MS/MS a rapid and selective analytical method. It was found that the best selectivity and sensitivity were obtained using positive ion chemical ionization and selected reaction monitoring as the detection method.

The use of short-column GC/MS/MS for screening of underivatized anabolic steroids was shown to be feasible, but somewhat less sensitive (higher LODs) than derivatization GC/MS screening methods; for two of the steroids studied, stanozolol and oxymetholone, the LODs were particularly poor. Despite this limitation,

increased speeds of analysis and enhanced selectivity were demonstrated and suggest that further work in this area be carried out. To increase the analytical utility of this method, future work would entail developing methods to improve detection limits, especially for stanozolol and oxymetholone. One possibility involves the use of electron capture agents in positive ion chemical ionization methods. It has been shown that the addition of electron capture agents increases sensitivity by increasing the ionic residence times in the ion source, thereby increasing the extent of ion/molecule reactions (120-122). The use of electron capture reagents in ammonia CI studies has been shown to increase the sample positive ion current by as much as 20 times (122). Ammonia CI would be beneficial, as well, for use with nitrogen containing steroids such as stanozolol due to the similarity of proton affinities. The study of alternative CI reagent gases such as ammonia is another area that could be investigated to improve detection limits and to increase selectivity.

Since most anabolic steroids are excreted largely as metabolites, rather than as free parent molecules, current analytical methods focus on screening for the metabolites of interest. Further study in the area of steroid analysis by short-column GC/MS/MS, therefore, would require characterizing the MS/MS behavior of the steroid metabolites to determine optimum operating parameters (collision energy and collision gas pressures) and to determine the most abundant daughter ions for screening purposes. Typically, steroid metabolites are oxidized/reduced analogs of the parent molecule such that structural differences are minor. Therefore, it is possible that the major daughter ions observed for the free steroid and its

metabolite(s) may be the same. Furthermore, it would be necessary to ascertain whether the metabolites, potentially more polar than the parent drug, would be amenable to GC separation without derivatization.

Suggestions for Future Work

Alternative Strategies for the Analysis of Thermally-Labile Compounds

New drug testing methods continuously are being developed as the need for more rapid, sensitive, and selective screening methods as a deterrent for drug abuse increases. Novel synthetic drug design and the simultaneous use of chemicals that mask the detection of the analyte of interest continue to challenge the development of useful analytical methods. A potential alternative to conventional GC/MS methods includes the development of capillary supercritical fluid chromatography/mass spectrometry (SFC/MS). Like LC/MS and short-column GC/MS, SFC/MS holds the potential for analysis of underivatized anabolic steroids, thereby minimizing sample preparation and retaining chromatographic separation capabilities. Another alternative to current methods, is on-wire derivatization Curie-point thermal desorption GC/MS. In this method, the advantages of derivatization are utilized, but sample preparation and handling is minimized.

Capillary SFC/MS. Supercritical fluid chromatography allows high resolution or high speed analysis of less volatile and thermally-labile compounds that may not

be amenable to GC/MS. The physical properties (viscosity and diffusion rate) of supercritical fluids combined with variable solvent properties are the basis for the advantages of SFC (123). For the analysis of more polar analytes, such as the anabolic steroids, polar supercritical fluids or polar modifiers can be used to enhance the solvating power or to change chromatographic selectivity. Analysis of anabolic steroids by SFC/MS has been reported in the literature (124,125). One report discusses how steroids epimers not resolved by GC/MS can be baseline resolved by capillary SFC/MS (125). This was possible because the SFC analysis was performed at low enough temperatures to prevent epimerization. The use of capillary SFC/MS for real world samples (urine) also has been demonstrated (125). Enhanced solvating power, low column temperatures, temperature or pressure programming capabilities, and chromatographic selectivity are just a few of the advantages of SFC/MS that warrants further study of this technique as a potential screening method for anabolic steroids.

On-wire derivatization. An alternative to conventional derivatization techniques based on Curie-point pyrolysis/thermal desorption was developed for profiling microorganisms (126,127). In this technique, the sample is applied directly to the Curie-point filament followed by the application of a drop of derivatizing reagent. Under the Curie-point pyrolysis conditions, the on-wire derivatization process goes to completion within a fraction of a second (126). Preliminary investigations into on-wire derivatization Curie-point thermal desorption of anabolic

steroids showed promising results. Chromatograms were produced showing a mixture of derivatized and underivatized steroids. These results suggest that on-wire derivatization may be a potential alternative to conventional solution-phase derivatization methods, allowing for improved chromatographic performance for the derivatized compounds with no additional sample preparation time. Although a potentially attractive alternative, further work needs to be done to characterize the on-wire derivatization reaction, to determine the best derivatization reagent, and to optimize the Curie-point thermal desorption process.

If, however, further work is to be done with the present Curie-point unit, design changes will need to be made. These include the design of a more powerful rf supply, incorporation of the Curie-point unit inside a normal injection port to modify heat and flow characteristics, and to minimize the dead volume. A new power supply needs to be built that would produce an rf output in the 1 to 2 kW range. In effect, this should decrease the temperature rise time, TRT, of the wire and allow for faster temperature time profiles, TTP, (sharper GC peaks). Other significant problems with the present design include the large dead volume and poor heat and carrier gas flow characteristics. If the unit could be incorporated into a normal GC injection port, these problems potentially could be overcome. Essentially, the top portion of the Curie-point unit (containing the rf coil) would be mounted directly on the conventional GC injection port. The Curie-point unit base and external heating unit would not be used. The GC column would be mounted in the injection port as for normal syringe operation. A pulsed flow gas valve could

then be used to pulse carrier gas through the glass reaction tube (which is placed within the Curie-point unit) while the wire is being heated. After the total heating time, THT, has ended, the pulse valve could be closed and helium carrier gas allowed to enter the injection port through the normal GC carrier gas lines. The use of the conventional GC carrier gas lines would be advantageous since the column, split and sweep flow paths are well characterized. This should thus overcome the problem of not being able to operate the Curie-point unit under subambient inlet conditions. In addition, the dead volume of the Curie-point unit should be decreased or at least comparable to that for normal syringe injection methods. Lastly, no external heating elements would be required since the conventional injection port is heated and maintained at a constant temperature more easily.

APPENDIX

FULL SCAN MS AND MS/MS (EI, PCI, AND NCI) MASS SPECTRA OF SIX STRUCTURALLY-RELATED ANABOLIC STEROIDS AND INTERPRETATION OF EXAMPLE MASS SPECTRA

In general, steroid structures are quite diverse and interpretation of their mass spectra can be extremely complicated. A list of the general features of steroid mass spectra has been published (128,129) and a few of these include the following:

(a) The complexity of steroid mass spectra is largely due to the fact that multiple bond breaking is required to produce fragment ions from the alicyclic (aliphatic cyclic) ring system.

(b) Hydrogen rearrangements can be random or stereospecific and are typically ubiquitous.

(c) Stereochemical influences will generally be reflected by variations in mass intensities.

(d) The fragmentation process and resulting mass spectra may be altered by the addition of a double bond or other functional group to a given molecule.

(e) The most commonly encountered thermal and catalytic decomposition processes for steroids include the loss of H_2O from hydroxy steroids, of acetic acid from acetates, of hydrogen from species that readily aromatize, and of CO_2 from free carboxylic acids.

In this appendix the EI, PCI, and NCI mass spectra for full scan (normal) MS and for full scan (daughter) MS/MS of each of the six anabolic steroids are shown. The structure of each steroid and a table of conditions under which each of the mass spectra were acquired are given on the page preceding the corresponding spectra. In addition, as structure elucidation by mass spectrometry is an important issue, the EI fragmentation pattern of an example compound will be interpreted. In this example, the compound testosterone will be used and fragmentation pathways will be suggested for the main fragment ions (MS) and the most abundant daughter ions (MS/MS). Note that fragmentation pathways are only suggested; for confirmation of fragment structures, detailed deuterium labeling and high-resolution mass spectrometric techniques are generally required (128).

Based on interpretation guidelines found in the literature (128-131), possible fragmentation pathways and suggested fragment ion assignments were made. In addition, an example mechanism for the formation of the base peak ion of testosterone, m/z 124, is shown in Figure A-1 (129). Note in the structure below the correct assignment of ring letters and carbon numbers (23).

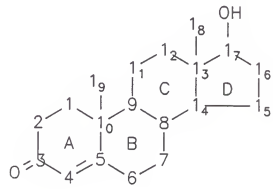

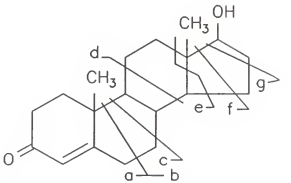

Table A-1: Interpretation of the normal full scan EI mass spectrum of testosterone (129,131)

fragment ion assignment	EI m/z	fragment ion assignment	EI m/z
M^+	288	b - OH	147
$(M - CH_3)^+$	273	c	133
$(M - H_2O)^+$	270	a	124
$(M - CH_3 - H_2O)^+$	255	a - CH_3	109
g	246	C_7H_7	91
f	228	C_6H_7	79
f - CH_3	213	C_5H_7	67
e	203	CH_2=CHCHCH_3	55
e - H_2O	185	CH_2=$CHCH_2$	41
d	165		

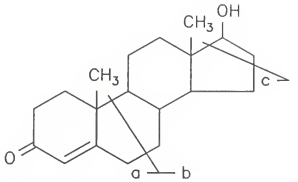

Table A-2: Interpretation of the full scan EI daughter mass spectrum of testosterone

fragment ion assignment	EI m/z
M^+	288
$(M - CH_3)^+$	273
c	246
b - OH	147
a	124
a - CH_3	109

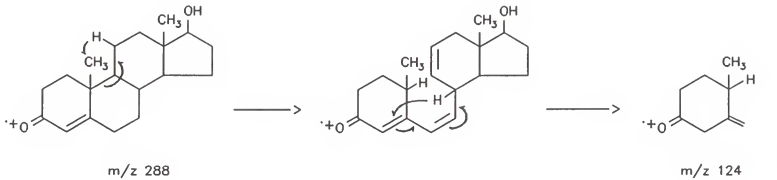

Figure A-1: Mechanism for the formation of the fragment ion at m/z 124 for the anabolic steroid testosterone.

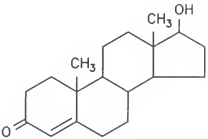

Table A-3: Conditions for the MS and MS/MS mass spectra of testosterone

normal full scan MS

ionization method	electron energy eV	ionizer temperature °C	reagent gas[a] pressure torr	scan range u	scan rate s	introduction method
EI	40	190	----	33-500	0.75	GC[b]
PCI	100	150	0.21	58-350	1.04	SP[c]
NCI	100	150	0.19	58-350	1.04	SP[c]

full scan daughter MS/MS[d]

ionization method	collision energy eV	collision gas pressure mtorr	reagent gas[a] pressure torr	scan range u	scan rate s	introduction method
EI	24.8	1.5 N_2	----	33-350	1.04	SP[c]
PCI	24.4	2.3 Ar	0.25	59-375	1.04	SP[c]
NCI	27.2	3.0 Ar	0.25	59-375	1.04	SP[c]

[a] using methane as the reagent gas

[b] short-column GC introduction using a temperature program from 150 to 250 °C at 25 °C/min., splitless injection, and a column inlet pressure of 2 psi

[c] solids probe introduction using an isothermal temperature of 150 °C

[d] using the same electron energy and ionizer temperature as for normal MS

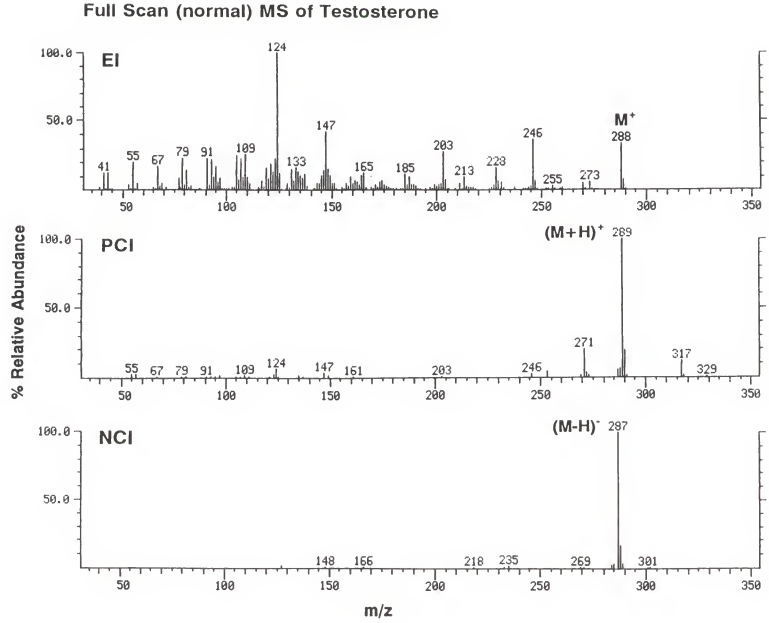
Full Scan (normal) MS of Testosterone
EI
PCI
NCI
% Relative Abundance
m/z
M+
288
(M+H)+ 289
(M-H)- 287

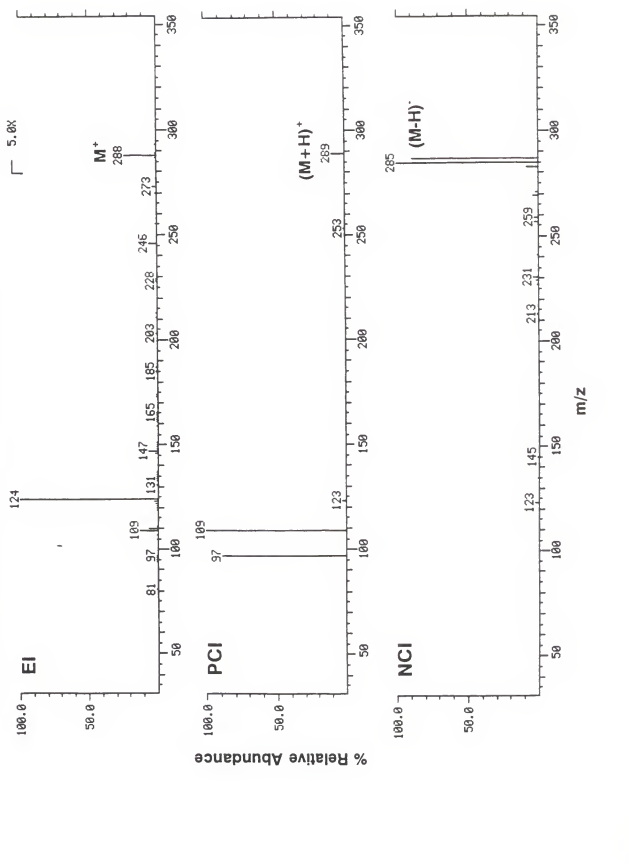
Full Scan (daughter) MS/MS of Testosterone
EI
PCI
NCI
5.0K
M+
(M+H)+
(M-H)-
% Relative Abundance
m/z

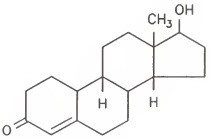

Table A-4: Conditions for the MS and MS/MS mass spectra of nortestosterone

normal full scan MS

ionization method	electron energy eV	ionizer temperature °C	reagent gas[a] pressure torr	scan range u	scan rate s	introduction method
EI	40	190	----	33-500	0.75	GC[b]
PCI	100	150	0.21	58-350	1.04	SP[c]
NCI	100	150	0.20	58-350	1.04	SP[c]

full scan daughter MS/MS[d]

ionization method	collision energy eV	collision gas pressure mtorr	reagent gas[a] pressure torr	scan range u	scan rate s	introduction method
EI	24.8	1.5 N_2	----	33-350	1.04	SP[c]
PCI	24.4	2.3 Ar	0.25	59-375	1.04	SP[c]
NCI	27.2	3.0 Ar	0.25	59-375	1.04	Sp[c]

[a] using methane as the reagent gas
[b] short-column GC introduction using a temperature program from 150 to 250 °C at 25 °C/min., splitless injection, and a column inlet pressure of 2 psi
[c] solids probe introduction using an isothermal temperature of 150 °C
[d] using the same electron energy and ionizer temperature as for normal MS

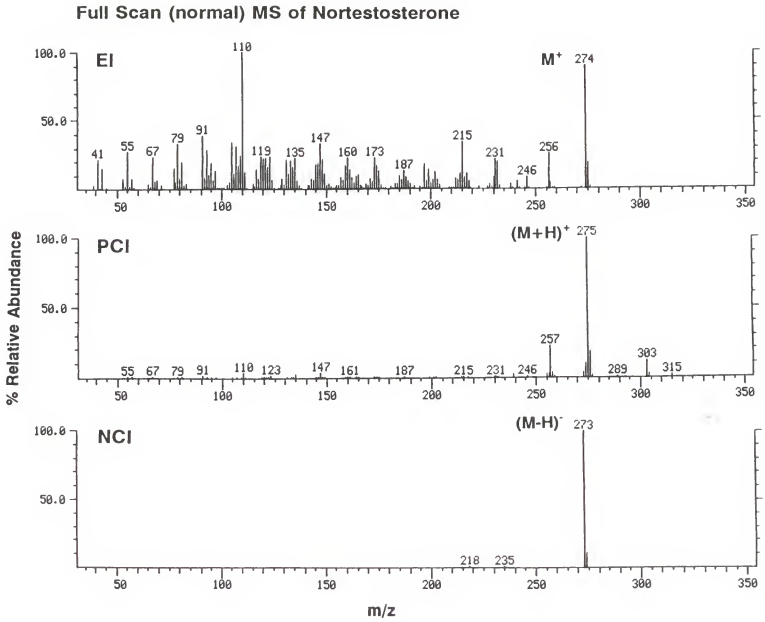
Full Scan (normal) MS of Nortestosterone
EI
PCI
NCI
M+ 274
(M+H)+ 275
(M-H)- 273
% Relative Abundance
m/z

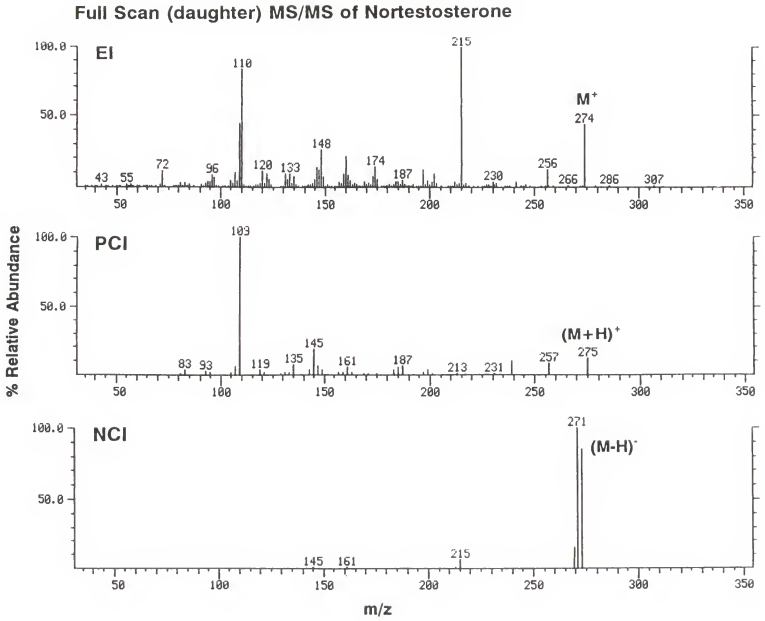
Full Scan (daughter) MS/MS of Nortestosterone
EI
PCI
NCI
% Relative Abundance
m/z
M+
274
(M+H)+
(M-H)-
100.0
50.0
50
100
150
200
250
300
350

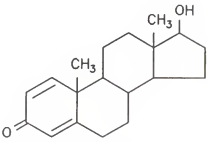

Table A-5: Conditions for the MS and MS/MS mass spectra of dehydrotestosterone

			normal full scan MS			
ionization method	electron energy eV	ionizer temperature °C	reagent gas[a] pressure torr	scan range u	scan rate s	introduction method
EI	40	190	----	33-500	0.75	GC[b]
PCI	100	150	0.19	58-350	1.04	SP[c]
NCI	100	150	0.19	58-350	1.04	SP[c]

			full scan daughter MS/MS[d]			
ionization method	collision energy eV	collision gas pressure mtorr	reagent gas[a] pressure torr	scan range u	scan rate s	introduction method
EI	26.9	1.0 N_2	----	33-350	1.04	SP[c]
PCI	14.6	2.2 Ar	0.25	59-375	1.04	SP[c]
NCI	27.2	3.0 Ar	0.25	59-375	1.04	Sp[c]

[a] using methane as the reagent gas

[b] short-column GC introduction using a temperature program from 150 to 250 °C at 25 °C/min., splitless injection, and a column inlet pressure of 2 psi

[c] solids probe introduction using an isothermal temperature of 150 °C

[d] using the same electron energy and ionizer temperature as for normal MS

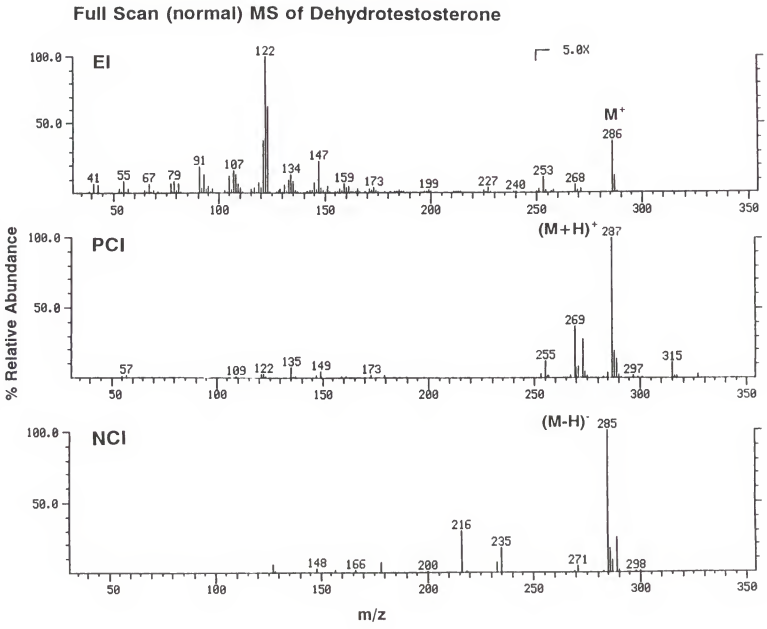
Full Scan (normal) MS of Dehydrotestosterone
EI
5.0X
M+
286
PCI
(M+H)+
287
NCI
(M-H)-
285
% Relative Abundance
m/z

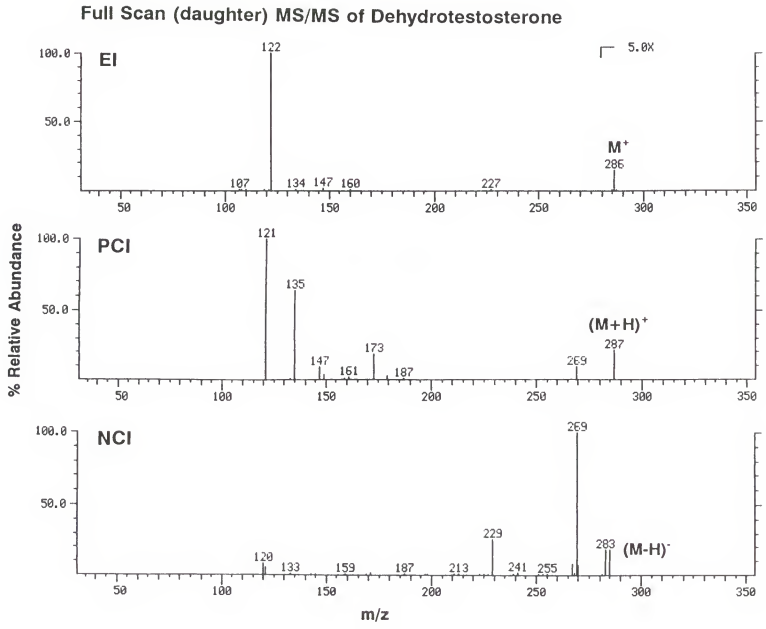
Full Scan (daughter) MS/MS of Dehydrotestosterone
EI
PCI
NCI
5.0X
M+
286
(M+H)+
287
(M-H)-
283
% Relative Abundance
m/z
100.0
50.0
122
107
134
147
160
227
121
135
147
161
173
187
269
229
120
133
159
187
213
241
255
50
100
150
200
250
300
350

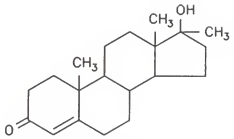

Table A-6: Conditions for the MS and MS/MS mass spectra of methyltestosterone

normal full scan MS

ionization method	electron energy eV	ionizer temperature °C	reagent gas[a] pressure torr	scan range u	scan rate s	introduction method
EI	40	190	----	33-500	0.75	GC[b]
PCI	100	150	0.22	58-350	1.04	SP[c]
NCI	100	150	0.20	58-350	1.04	SP[c]

full scan daughter MS/MS[d]

ionization method	collision energy eV	collision gas pressure mtorr	reagent gas[a] pressure torr	scan range u	scan rate s	introduction method
EI	26.9	1.5 N_2	----	33-350	1.04	SP[c]
PCI	22.0	2.2 Ar	0.25	59-375	1.04	SP[c]
NCI	26.7	3.0 Ar	0.25	59-375	1.04	Sp[c]

[a] using methane as the reagent gas

[b] short-column GC introduction using a temperature program from 150 to 250 °C at 25 °C/min., splitless injection, and a column inlet pressure of 2 psi

[c] solids probe introduction using an isothermal temperature of 150 °C

[d] using the same electron energy and ionizer temperature as for normal MS

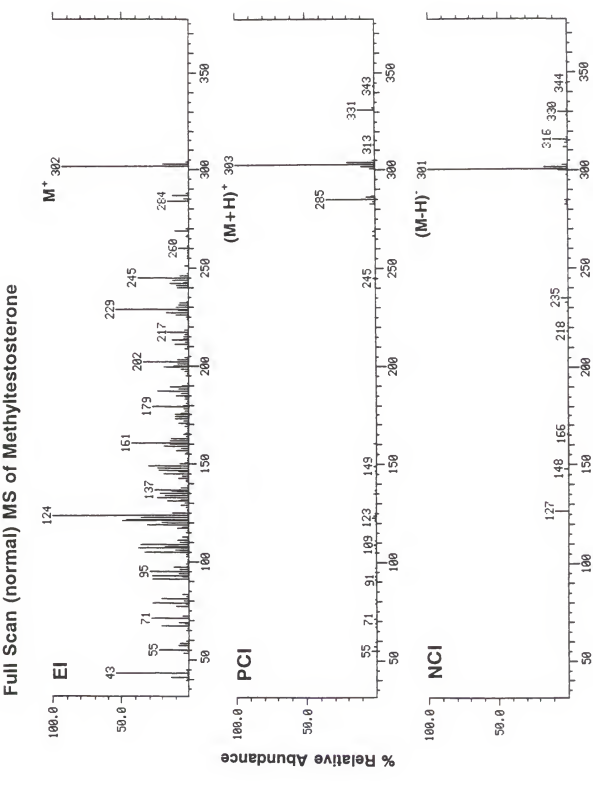
Full Scan (normal) MS of Methyltestosterone
EI
PCI
NCI
M+
(M+H)+
(M-H)-
% Relative Abundance
m/z

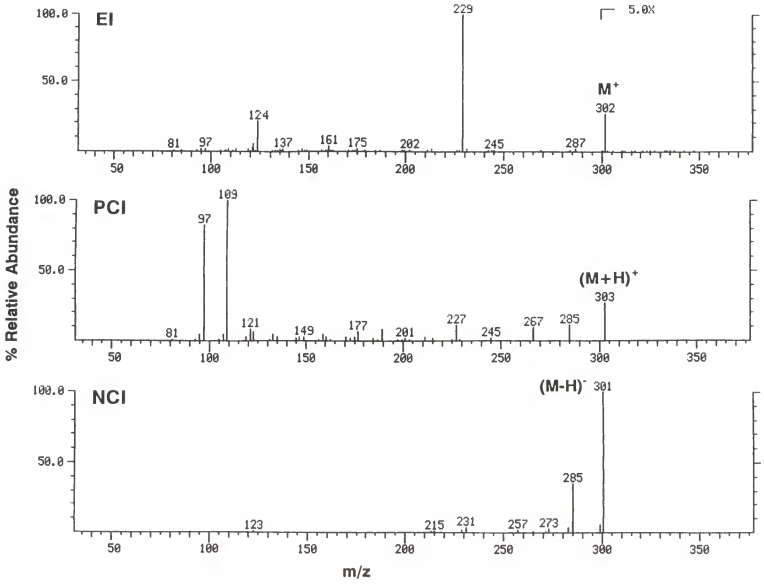
Full Scan (daughter) MS/MS of Methyltestosterone
EI
PCI
NCI
5.0X
M+
302
(M+H)+
303
(M-H)-
301
% Relative Abundance
m/z

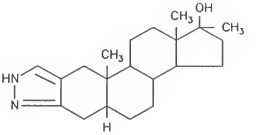

Table A-7: Conditions for the MS and MS/MS mass spectra of stanozolol

			normal full scan MS			
ionization method	electron energy eV	ionizer temperature °C	reagent gas[a] pressure torr	scan range u	scan rate s	introduction method
EI	40	190	----	33-500	0.75	GC[b]
PCI	100	150	0.30	58-350	1.04	SP[c]
NCI	100	150	0.29	58-350	1.04	SP[c]

			full scan daughter MS/MS[d]			
ionization method	collision energy eV	collision gas pressure mtorr	reagent gas[a] pressure torr	scan range u	scan rate s	introduction method
EI	22.0	1.5 N_2	----	33-350	1.04	SP[e]
PCI	26.9	2.5 Ar	0.25	59-375	1.04	SP[e]
NCI	27.2	3.0 Ar	0.25	59-375	1.04	Sp[e]

[a] using methane as the reagent gas
[b] short-column GC introduction using a temperature program from 150 to 250 °C at 25 °C/min., splitless injection, and a column inlet pressure of 2 psi
[c] solids probe introduction using an isothermal temperature of 200 °C
[d] using the same electron energy and ionizer temperature as for normal MS
[e] solids probe introduction using an isothermal temperature of 150 °C

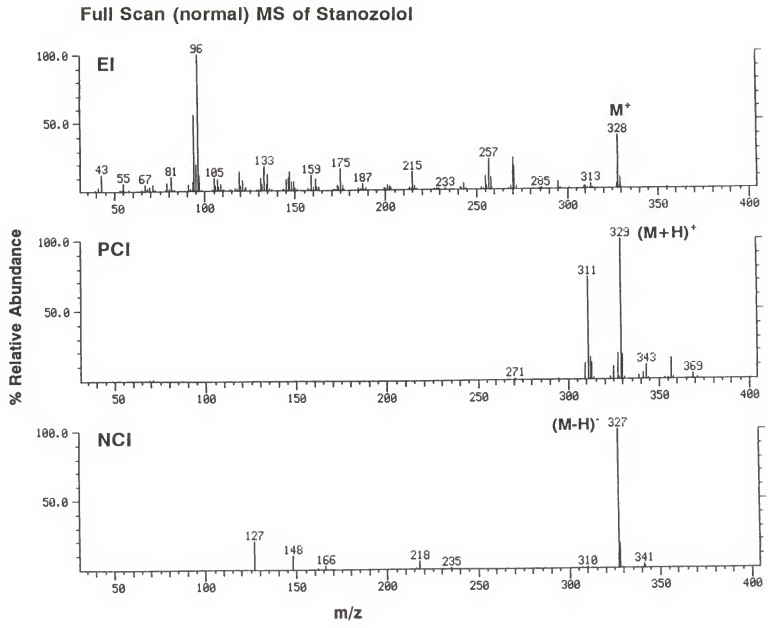
Full Scan (normal) MS of Stanozolol
EI
PCI
NCI
% Relative Abundance
m/z
M+
328
(M+H)+
329
311
271
343
369
(M-H)-
327
96
43
55
67
81
105
133
159
175
187
215
233
257
285
313
127
148
166
218
235
310
341
100.0
50.0
50
100
150
200
250
300
350
400

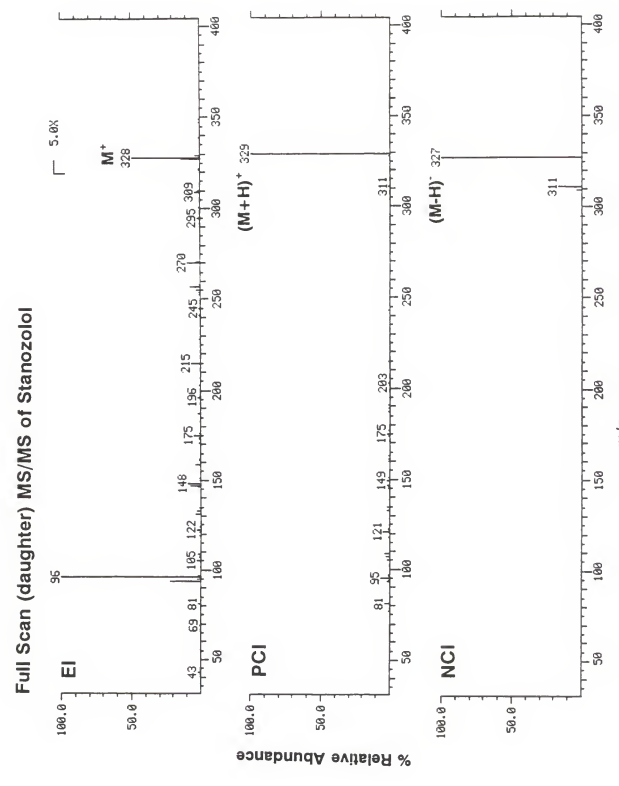
Full Scan (daughter) MS/MS of Stanozolol
EI
PCI
NCI
5.0X
M+
328
(M+H)+
329
(M-H)-
327
96
105
122
148
175
195
215
245
270
295
309
95
121
149
175
203
311
311
100.0
50.0
% Relative Abundance
50
100
150
200
250
300
350
400
m/z

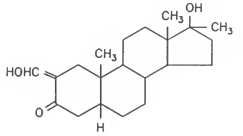

Table A-8: Conditions for the MS and MS/MS mass spectra of oxymetholone

normal full scan MS

ionization method	electron energy eV	ionizer temperature °C	reagent gas[a] pressure torr	scan range u	scan rate s	introduction method
EI	40	190	----	33-500	0.75	GC[b]
PCI	100	150	0.42	58-350	1.04	SP[c]
NCI	100	150	0.30	58-350	1.04	SP[c]

full scan daughter MS/MS[d]

ionization method	collision energy eV	collision gas pressure mtorr	reagent gas[a] pressure torr	scan range u	scan rate s	introduction method
EI	29.0	1.5 N_2	----	33-350	1.04	SP[e]
PCI	29.2	2.3 Ar	0.25	59-375	1.04	SP[e]
NCI	27.2	3.0 Ar	0.25	59-375	1.04	Sp[e]

[a] using methane as the reagent gas
[b] short-column GC introduction using a temperature program from 150 to 250 °C at 25 °C/min., splitless injection, and a column inlet pressure of 2 psi
[c] solids probe introduction using an isothermal temperature of 200 °C
[d] using the same electron energy and ionizer temperature as for normal MS
[e] solids probe introduction using an isothermal temperature of 150 °C

Full Scan (normal) MS of Oxymetholone

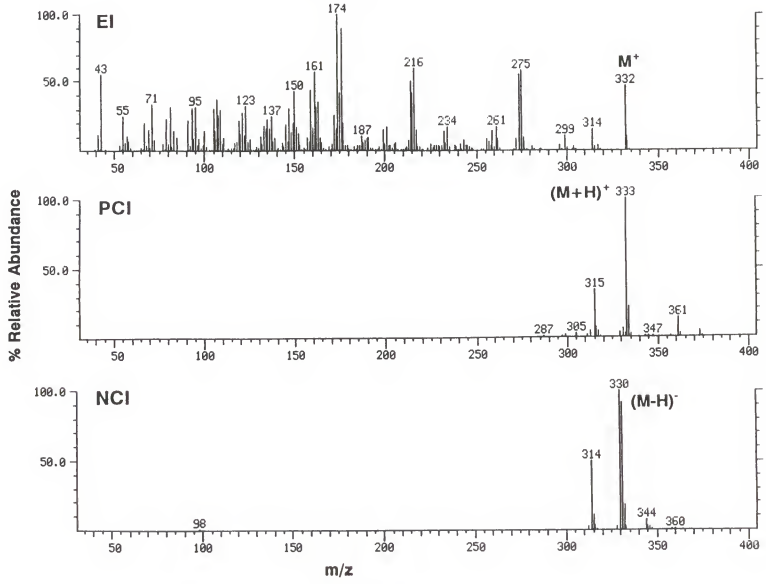

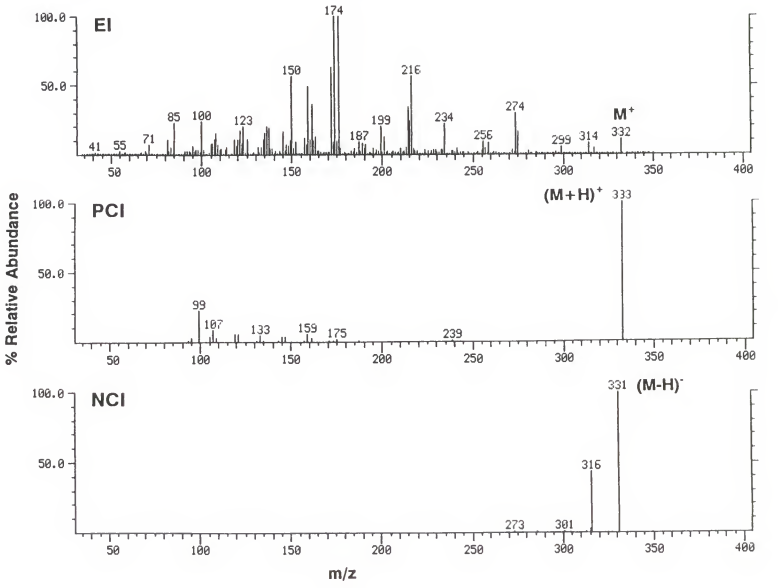
Full Scan (daughter) MS/MS of Oxymetholone
EI
PCI
NCI
% Relative Abundance
m/z
M+
(M+H)+
(M-H)-
100.0
50.0
50
100
150
200
250
300
350
400
41
55
71
85
100
123
150
174
187
199
216
234
256
274
299
314
332
99
107
133
159
175
239
333
273
301
316
331

LITERATURE CITED

1. Moss, M.S.; Cowan, D.A. "Clarke's Isolation and Identification of Drugs"; The Pharmaceutical Press: London, 1986, p.87-100.

2. Zurer, P.S. C&E News, 1984, **April 30**, 69-78.

3. Catlin, D.H.; Kammerer, R.C.; Hatton, C.K.; Sekera, M.H.; Merdink, J.L.Clin. Chem. 1987, **33**, 319-327.

4. Narducci, W.A.; Wagner, J.C.; Hendrickson, T.P; Jeffrey, T.P. Clin. Toxic., 1990, **28**, 287-310.

5. Strauss, R.H. Clinics in Sports Medicine 1984, **3**, 743-748.

6. Haupt, H.A.; Rovere, G.D. Am. J. Sports Med. 1984, **12**, 469-484.

7. Crist, D.M.; Stackpole, P.J.; Peake, G.T. J. Appl. Physiol. 1983, **54**, 366-370.

8. Fahey, T.D.; Brown, C.H.; Med. Sci. Sports 1973, **5**, 272-276.

9. Shepard, R.J.; Killinger, D.; Fried, T. Br. J. Sports Med. 1977, **11**, 170-173.

10. Johnson, L.C.; O'Shea, J.P. Science 1969, **164**, 957-959.

11. Johnson, L.C.; Roundy, E.S.; Allsen, D.E.; Fisher, A.G.; Silvester, L.J. Med. Sci. Sports 1975, **7**, 287-289.

12. Lamb, D.R. Med. Sci. Sports 1975, **7**, 1-5.

13. Loughton, S.J.; Ruhling, R.O. J. Sports Med. Phys. Fitness 1977, **17**, 285-296.

14. Murad, F.; Haynes, R.C. "Goodman and Gilman's the Pharmacological Basis of Therapeutics"; Macmillan Press: New York, 1985, p.1440-1458.

15. Freed, D.L.J.; Banks, A.J.; Longson, D. Br. J. Sports Med. 1975, **2**, 471-473.

16. Lamb, D.R. Am. J. Sports Med. 1984, **12**, 31-38.

17. Ariel, G.; Saville, W. Med. Sci. Sports 1972, **4**, 124-126.

18. Johnson, F.L. Med. Sci. Sports 1975, **7**, 284-286.

19. Wynn, V. Br. J. Sports Med. 1975, **9**, 60-64.

20. Hickson, R.C.; Ball, K.L.; Falduto, M.T. Med. Toxicol. Adverse Drug Exp. 1989, **4**, 254-271.

21. Kibble, M.W.; Ross, M.B. Clin. Pharmacol. 1987, **6**, 686-692.

22. Wilson, J.D. Endocrin. Rev. 1988, **9**, 181-199.

23. Sample, R.H.B.; Baenziger, J.C. "Analytical Aspects of Drug Testing"; Wiley: New York, 1989, ch. 10.

24. Kirk, D.N. Nat. Prod. Reports 1986, **3**, 505-513.

25. Masse, R.; Ayotte, C.; Dugal, R. J. Chromatogr. 1989, **489**, 23-50.

26. Axelson, M.; Sahlberg, B.-L.; Sjovall, J. J. Chromatogr. 1981, **224**, 355-370.

27. Setchell, K.D.R.; Axelson, M.; Sjovall, J. J. Steroid Biochem. 1976, **7**, 615-629.

28. Brooks, R.V.; Jeremiah, G.; Webb, W.A.; Wheeler, M. J. Steroid Biochem. 1979, **11**, 913-917.

29. Hampl, R.; Starka, L. J. Steroid Biochem. 1979, **11**, 933-936.

30. Mann, V.; Benko, A.B.; Kocsar, L.T. Steroids, 1981, **37**, 593-600.

31. Bjorkhem, I.; Ek, H. J. Steroid Biochem. 1983, **18**, 481-487.

32. Frischkorn, C.G.B.; Frischkorn, H.E. J. Chromatogr. 1978, **151**, 331-338.

33. Jansen, E.J.H.M.; Van Blitterswijk, H.; Zoontjes, P.W.; Both-Miedema, R.; Stephany, R.W. J. Chromatogr. 1985, **347**, 375-378.

34. Carignan, G.; Lodge, B.A. J. Chromatogr. 1979, **179**, 184-186.

35. Rhys Williams, A.T.; Winfield, S.A. J. Chromatogr. 1982, **240**, 224-229.

36. Van Den Berg, R.H.; Jansen, E.H.J.M.; Zomer, G.; Enkelaar-Willemsen, C.; Both-Miedema, R.; Stephany, R.W. J. Chromatogr. 1986, **360**, 449-451.

37. Shackleton, C.H.; Chai, W. Endocrine Reviews, 1985, **6**, 441-486.

38. Singh, A.K.; Gordon, B.; Hewetson, D.; Granley, K.; Ashraf, M.; Mishra, U.; Dombrovskis, D. J.Chromatogr. 1989, **479**, 233-242.

39. Lin, Y.Y; Smith, L.L. Mass Spectrom. Reviews 1984, **3**, 319-355.

40. Fung, E.T.; Wilkins, C.L. Biomed. Environ. Mass Spectrom. 1988, **15**, 609-613.

41. Sanghvi, A.; Wight, C.; Serenko, A.; Balachandran, R. Clin. Chim. Acta 1974, **56**, 49-57.

42. Chen, Y.; Chen, N.; Li, H.; Zhao, F.; Chen, N. Biomed. Environ. Mass Spectrom. 1987, **14**, 9-15.

43. Liehr, J.G.; Beckner, C.F.; Ballatore, A.M.; Caprioli, R.M. Steroids 1982, **39**, 599-605.

44. Shackleton, C.H.L. Clin. Chem. 1983, **29**, 246-249.

45. Yost, R.A.; Fetterolf, D.D.; Hass, J.R.; Harvan, D.J.; Weston, A.F.; Skotnicki, P.A.; Simon, N.M. Anal. Chem. 1984, **56**, 2228-2233.

46. Trehy, M.L.; Yost, R.A.; McCreary, J.J. Anal. Chem. 1984, **56**, 1281-1285.

47. Johnson, J.V.; Yost, R.A.; Faull, K.F. Anal. Chem. 1984, **56**, 1655-1661.

48. McClennen, W.H.; Richards, J.M.; Meuzelaar, H.L.C. Proc. 36th Ann. Conf. Mass Spectrom. Allied Topics, San Francisco, 1988, 403-404.

49. Richards, J.M.; McClennan, W.H.; Bunger, J.A.; Meuzelaar, H.L.C. Proc. 36th Ann. Conf. Mass Spectrom. Allied Topics, San Francisco, 1988, 547-548.

50. Trehy, M.L.; Yost, R.A.; Dorsey, J.G. Anal. Chem. 1986, **58**, 14-19.

51. Hail, M.E.; Yost, R.A. Anal. Chem. 1989, **61**, 2402-2410.

52. Leclerq, P.A.; Cramers, C.A. J. High Resol.Chromatogr. & Chromatogr. Commun. 1987, **10**, 269-272.

53. Giddings, J.C. Anal. Chem. 1962, **34**, 314-319.

54. Cramer, C.A.; Scherpenzeel, G.J.; Leclerq, P.A. J. Chromatogr. 1981, **203**, 207-216.

55. Leclerq, P.A.; Scherpenzeel, G.J.; Vermeer, E.A.; Cramers, C.A. J. Chromatogr. 1982, **241**, 61-71.

56. Leclerq, P.A.; Cramers, C.A. J. High Resol. Chromatogr. & Chromatogr. Commun. 1985, **8**, 764-771.

57. Hail, M.E.; Yost, R.A. Anal. Chem. 1989, **61**, 2410-2416.

58. Hail, M.E.; Berberich, D.W.; Yost, R.A. Anal. Chem. 1989, **61**, 1874-1879.

59. Hyver, K.J.; Phillips, R.J. J. Chromatogr. 1987, **399**, 33-46.

60. Gaspar, G.; Annino, R.; Vidal-Madjar, C.; Guiochon, G. Anal. Chem. 1978, **50**, 1512-1518.

61. Schutjes, C.P.M.; Vermeer, E.A.; Rijks, J.A.; Cramers, C.A. J. Chromatogr. 1982, **253**, 1-16.

62. Karger, B.L.; Martin, M.; Guiochon, G. Anal. Chem. 1974, **46**, 1640-1647.

63. Hatch, F.W.; Parrish, M.E. Anal. Chem. 1978, **50**, 1164-1168.

64. Golay, M.J.E. Nature 1958, **182**, 1146-1147.

65. Cramers, C.A.; Leclerq, P.A. CRC Critical Reviews 1988, **20**, 117-147.

66. van Es, A.; Bally, R.; Cramers, C.; Rijks, J. J. High Resol. Chromatogr. & Chromatogr. Commun. 1987, **10**, 273-279.

67. Meuzelaar, H.L.C.; McClennan, W.H.; Yun, Y. Proc. 35th Ann. Conf. Mass Spectrom. Allied Topics, Denver, 1987, 1142-1143.

68. Kruger, T.L.; Litton, J.F.; Kondrat, R.W.; Cooks, R.G. Anal. Chem. 1976, 48, 2113-2119.

69. Kondrat, R.W.; Cooks, R.G. Anal. Chem. 1978, **50**, 82A-92A.

70. McLafferty, F.W.; Bockhoff, F.M. Anal. Chem. 1978, **50**, 69-76.

71. Yost, R.A.; Enke, C.G. Anal. Chem. 1979, **51**, 1251A-1264A.

72. Glish, G.L.; Shaddock, V.M.; Harmon, K.; Cooks, R.G. Anal. Chem. 1980, **52**, 165-167.

73. Brotherton, H.O.; Yost, R.A. Anal. Chem. 1983, **55**, 549-553.

74. Johnson, J.V.; Yost, R.A. Anal. Chem. 1985, **57**, 758A-768A.

75. Cooks, R.G.; Glish, G.L. C&E News 1981, **Nov. 30**, 40-52.

76. McLafferty, F.W. Biomed. Mass Spectrom. 1981, **8**, 446-448.

77. Gaskell, S.J. "Mass Spectrometry in Biomedical Research"; Wiley: New York, 1986, ch. 18.

78. Grob, K. "Classical Split and Splitless Injection in Capillary GC"; Dr. Alfred Huethig Verlag: Heidelberg, 1986, ch.4.

79. James, A.T.; Martin, A.J.P. Biochem. J. 1952, **50**, 679-690.

80. Giddings, J.C.; Seagle, S.P.; Stucki, L.R.; Stewart, G.H. Anal. Chem. 1960, **32**, 867-870.

81. Berberich, D.W.; Hail, M.E.; Johnson, J.V.; Yost, R.A. Int. J. Mass Spectrom. Ion Phys. 1989, **94**, 115-147.

82. Rosenstock, H.M.; Draxl, K.; Steiner, B.W.; Herron, J.T. J. Phys. Chem. Ref. Data Suppl., 1977, **6**, 1.

83. Harrison, A.G. "Chemical Ionization Mass Spectrometry"; CRC: Boca Raton, 1983, ch.2.

84. Levin, R.; Lias, S.G. "Ionization Potential and Appearance Potential Measurements, 1971-1981"; Nat. Stand. Ref. Data Ser., Nat. Bur. Stand. (U.S.), 1982, **71**.

85. Wacks, M.E.; J. Chem. Phys. 1964, **41**, 1661-1666.

86. Dawson,P.H. "Quadrupole Mass Spectrometry and its Applications"; Elsevier Scientific Publishing Co.: Amsterdam, 1976, ch.2.

87. Levy, R.L.; Fanter, D.L.; Wolf, C.J. Anal. Chem. 1972, **44**, 38-42.

88. Buhler, C.; Simon, W. J. Chromatogr. Sci. 1970, **8**, 323-329.

89. Foley, J.P.; Dorsey, J.G. Anal. Chem. 1983, **55**, 730-737.

90. Drucker, D.B. "Microbiological Applications of GC"; Cambridge University Press: New York, 1981, p.365-380.

91. Irwin, W.J. J. Anal. Appl. Pyrol. 1979, **1**, 3-25.

92. May R.W. "Pyrolysis Gas Chromatography"; Chemical Society: London, 1977, p.23-52.

93. Windig, W.; Kistemaker, P.G.; Haverkamp, J. J. Anal. Appl. Pyrol. 1979, 1, 39-52.

94. Farre-Ruis, F.; Guiochon, G. Anal. Chem. 1968, **40**, 998-1000.

95. Levy, R.L. J. Gas Chromatogr. 1967, **5**, 107-113.

96. Zaretski Z.V.I.; Curtis, J.M.; Ghosh D.; Brenton, A.G. Int. J. Mass Spectrom. Ion Proc. 1988, **86**, 121-136.

97. Knapp, D.R. "Handbook of Derivatization Reactions" Wiley: New York, 1979, ch. 11.

98. Watson, J.T. "Introduction to Mass Spectrometry"; Raven Press: New York, 1985, ch. 6.

99. Masse, R.; Ayotte, C.; Bi, H.; Dugal, R.; J. Chromatogr. 1989, **497**, 17-37.

100. Cairns, T.; Siegmund, E.G.; Savage, T.S. Pharm. Res. 1988, **5**, 31-35.

101. Weidolf, L.O.G.; Lee, E.D.; Henion, J.D. Biomed. Environ. Mass Spectrom. 1988, **15**, 283-289.

102. Edlund, P.O.; Bowers, L.; Henion, J.D. J. Chromatogr. 1989, **487**, 341-356.

103. Gaskell, S.J.; Biomed. Environ. Mass Spectrom. 1988, **15**, 99-104.

104. Tomer, K.B.; Gross, M.L. Biomed. Environ. Mass Spectrom. 1988, **15**, 89-98.

105. Gaskell, S.J.; Porter, C.J.; Green, B.N. Biomed. Environ. Mass Spectrom. 1985, **12**, 139-141.

106. Yost, R.A.; Enke, C.G.; McGilvery, D.C.; Smith, D.; Morrison, J.D. Int. J. Mass Spectrom. Ion Proc. 1979, **30**, 127-136.

107. Shackleton, C.H.L. J. Chromatogr. 1986, **379**, 91-156.

108. Shackleton C.H.L.; Whitney, J.O. Clin. Chim. Acta 1980, **107**, 231-243.

109. Kaiser, H. Pure Appl. Chem. 1973, **34**, 35-61.

110. Boumans, P.W.J.M. Spectrochim. Acta 1978, **33B**, 625-634.

111. Long, G.L.; Winefordner, J.D. Anal. Chem. 1983, **55**, 712A-724A.

112. Foley, J.P.; Dorsey, J.G. Chromatographia 1984, **18**, 503-511.

113. Knoll, J.E. J. Chrom. Sci. 1985, **23**, 422-424.

114. Hubaux, A.; Vos, G. Anal. Chem. 1970, **42**, 849-855.

115. Skoog, D.A. "Principles of Instrumental Analysis"; CBS College Publishing: Philadelphia, 1985, ch.1.

116. Goudreault, D.; Masse, R. J. Steroid Biochem. Molec. Biol. 1990, **37**, 137-154.

117. Masse, R.; Laliberte, C.; Tremblay, L.; Dugal, R. Biomed. Mass Spectrom. 1985, **12**, 115-121.

118. Masse, R.; Bi, H.; Ayotte, C.; Dugal, R. Biomed. Environ. Mass Spectrom. 1989, **18**, 429-438.

119. Schanzer, W.; Opfermann, G.; Donike, M. J. Steroid Biochem. 1990, **36**, 153-174.

120. Rudewicz, P.; Feng, T.; Blom, K.; Munson, B. Anal. Chem. 1984, **56**, 2610-2611.

121. Johnson, J.V.; Yost, R.A. Proc. 34th Ann. Conf. Mass Spectrom. Allied Topics, Cincinnati, 1986, 521-522.

122. Rudewicz, P.; Munson, B. Proc. 32nd Ann. Conf. Mass Spectrom. Allied Topics, San Antonio, 1984, 178-179.

123. Kalinoski, H.T.; Udseth, H.R.; Chess, E.K.; Smith, R.D. J. Chromatogr. 1987, **394**, 3-14.

124. Andersen, M.R.; Porter, N.E.; Swanson, J.T.; Richter, B.E. reprint Am. Clin. Lab. 1989.

125. Later, D.W.; Richter, B.E.; Knowles, D.E.; Andersen, M.R. J. Chromatogr. Sci. 1986, **24**, 249-253.

126. Dworzanski, J.; Meuzelaar, H.L.C. Proc. 36th Ann. Conf. Mass Spectrom. Allied Topics, San Francisco, 1988, 401-402.

127. Dworzanski, J.; Meuzelaar, H.L.C. Proc. 38th Ann. Conf. Mass Spectrom. Allied Topics, Tucson, 1990, 1401-1402.

128. McCloskey, J.A. "Methods in Enzymology, vol. XIV"; Academic Press: New York, 1969, p.382-434.

129. Budzikiewicz, H. "Biochemical Applications of Mass Spectrometry"; Wiley Interscience: New York, 1972, ch. 10.

130. Tokes, L.; Jones, G.; Djerassi, C. J. Am. Chem. Soc. 1968, **90**, 5465-5477.

131. Gonzalez, M.; Burton, G. Biomed. Mass Spectrom. 1985, **12**, 405-408.

BIOGRAPHICAL SKETCH

Stacy-Ann Rossi was born in Lynn, Massachusetts, on January 23, 1965. She grew up in Topsfield, Massachusetts, where she attended Masconomet Regional High School. After completing high school in 1983 as an honors student, she entered Ripon College in Wisconsin, earning a Distinguished Honors Scholarship. During her four years at Ripon, she majored in chemistry and graduated cum laude with a B.A. degree in 1987. In August of 1987, she began her graduate studies at the University of Florida. The second semester of her first year she joined the analytical division under the direction of Dr. Richard A. Yost. After completing her doctoral studies in December, 1991, she will be accepting a position at Oak Ridge National Laboratories in Tennessee.

I certify that I have read this study and that in my opinion it conforms to acceptable standards of scholarly presentation and is fully adequate, in scope and quality, as a dissertation for the degree of Doctor of Philosophy.

Richard A. Yost, Chairman
Professor of Chemistry

I certify that I have read this study and that in my opinion it conforms to acceptable standards of scholarly presentation and is fully adequate, in scope and quality, as a dissertation for the degree of Doctor of Philosophy.

Willard W. Harrison
Professor of Chemistry

I certify that I have read this study and that in my opinion it conforms to acceptable standards of scholarly presentation and is fully adequate, in scope and quality, as a dissertation for the degree of Doctor of Philosophy.

James D. Winefordner
Graduate Research Professor of Chemistry

I certify that I have read this study and that in my opinion it conforms to acceptable standards of scholarly presentation and is fully adequate, in scope and quality, as a dissertation for the degree of Doctor of Philosophy.

David A. Micha
Professor of Chemistry

I certify that I have read this study and that in my opinion it conforms to acceptable standards of scholarly presentation and is fully adequate, in scope and quality, as a dissertation for the degree of Doctor of Philosophy.

Charles W. Thomas
Professor of Sociology

This dissertation was presented to the Graduate Faculty of the Department of Chemistry in the College of Liberal Arts and Sciences and to the Graduate School and was accepted as partial fulfillment of the requirements for the degree of Doctor of Philosophy.

December 1991

_____
Dean, Graduate School